ISSN 2730-2695

THAI GEOSCIENCE JOURNAL

Vol. 3 No. 3 January 2022

Sustainability For The Future

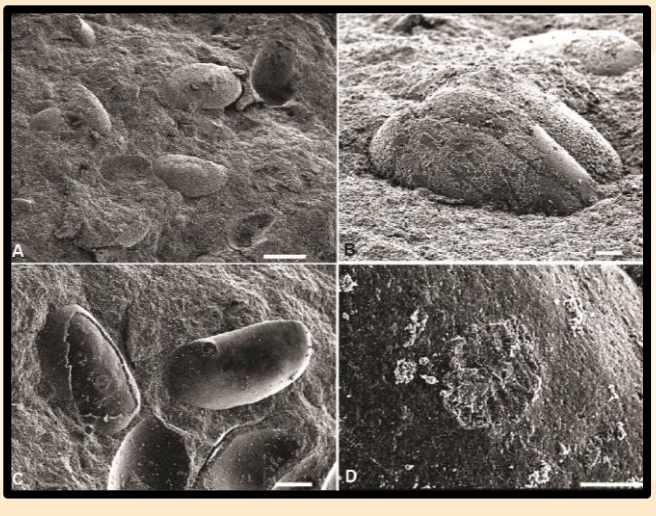

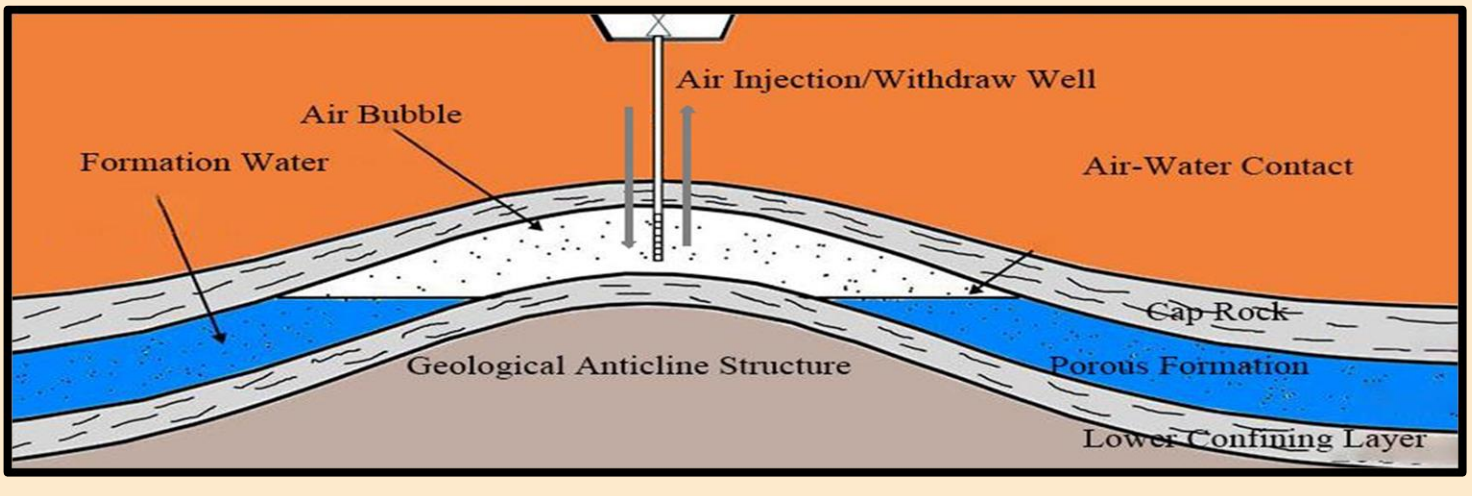

Published by
Department of Mineral Resources
Geological Society of Thailand
Coordinating Committee for Geoscience Programmes in East and Southeast Asia (CCOP)

Editorial Committee

On the cover

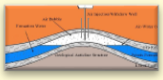

1) Conceptual model for Pittsfield CAESA model *(Lichao Yang et al. p.52, fig. 2)*

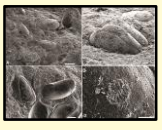

2) Pictures from scanning electron microscope showing ostracods embedded in calcareous mudstone in the lower part of the section with associated to stromatolite deposit: A, carapaces and valves partly exposed from the matrix, scale bar = 0.5 mm.; B, carapace partly exposed from the matrix, scale bar = 0.1 mm.; C, carapaces, cast sand mold with imprinted central muscle scar, scale bar = 0.2 mm.; D, central muscle scar, scale bar = 0.1 mm. *(Anisong Chitnarin et al. , p.40, fig. 7)*

THAI GEOSCIENCE JOURNAL

Vol. 3 No. 3
January 2022

Published By
Department of Mineral Resources • Geological Society of Thailand
Coordinating Committee for Geoscience Programmes in East and Southeast Asia (CCOP)

Thai Geoscience Journal website at http://www.dmr.go.th/tgjdmr

Preface

The publication of the Thai Geoscience Journal, Volume 3 Number 3, online in January 2022, continues with five papers on an excellent variety of academic and applied subjects. We will continue our journal with several geological and geoscience objectives and with an increased distribution. We need more co-operation with global geoscience organizations. Last year, we welcomed the Coordinating Committee for Geoscience Programmes in East and Southeast Asia (CCOP) as co-organizers of the TGJ and welcome Dr. Young Joo Lee, Director of CCOP as our Honorary Editor.

The theme of this TGJ issue is *Sustainability for the Future*. As geoscientists we play a critical role in our earth's future; in making our earth resources sustainable, in providing an unpolluted environment and providing clean water to an expanding world population. Geoscientists play many important roles in helping to keep the global temperature increase below 1.5^0C as agreed to at the United Nations Climate Change Conference (COP26) in Glasgow, Scotland in November 2021. Geoscientists play a critical role in assessing past climate changes and sea levels and predicting their future. In our schools, universities and museums, we play an important role in educating the public to past and future climate and environmental change. Around the world, there are already signs of harmful changes; from increased storm and cyclone activity, to glacier melting, heatwaves, bushfires, and sea level rise. Our capital city Krung Thep Maha Nakhon (Bangkok) is particularly at-risk to sea level rise and all of our country is vulnerable to increased cyclone severity, flooding and droughts. Geoscientists can make very significant contributions, for example, by accelerating the introduction of geothermal energy, by helping to drought-proof the country, by considering CO_2 sequestration, and by finding new mineral deposits to help build alternative energy sources and electric vehicles to meet the eventual goal of a sustainable future.

The COVID-19 pandemic situation in early 2022 continues to change the life and behavior of everyone around the world, most of us continue to work from home (WFH) along with masks and social distancing and field work and in-person meetings have been severely curtailed. Our 'New Normal' geological life means that it has been difficult and dangerous to go in the field. In this situation, we will probably do more research about data management instead and write articles from our stored data and unfinished manuscripts and then hopefully send the results to TGJ. There are hopeful signs that the pandemic will be over this year and that we may soon go back to the field, have face to face meetings again and possibly even resume international travel and welcome overseas colleagues to Thailand. Finally, we are pleased to invite all geologists, scientists and researchers to publish in our TGJ.

Thank you very much.

(Mr. Pongboon Pongtong)
Director-General of the Department of Mineral Resources

From the editor

Welcome to the Thai Geoscience Journal Volume 3 Number 3. This is our third year of publication since the first TGJ issue in July 2020. We have connected our TGJ with the Coordinating Committee for Geoscience Programmes in East and Southeast Asia (CCOP) and we have been working together on this and subsequent journal issues. We very much appreciate the kind cooperation of Dr. Young Joo Lee, Director of CCOP, and Dr. Dhiti Tulyatid, Regional Expert, CCOP. This issue contains interesting applied papers on groundwater studies in Brunei, compressed air storage in aquifers and boosting geosite interest through digital platforms in Malaysia.

These important practical studies on two of the most important current geoscience directions – aquifers and geo-tourism, are followed by reports on important discoveries of Cambrian to Ordovician tuffs in western Thailand and Triassic lacustrine stromatolites and ostracods in north east Thailand. The close cooperation with CCOP and this issue's diversity reflect the hoped for international flavour of TGJ with authors working in government organizations, industry and universities in Thailand and in eight other countries.

We would like to express our appreciation to all of our TGJ Volume 3 Number 3's authors for publishing their valuable articles in TGJ. As the TGJ editor in chief, I would like to express my thanks to TGJ's honorary, advisory, associate editors, and reviewers for their kind support. Special thanks are due to the editorial secretary team who have worked very hard on every TGJ issue. We continue to strive to make TGJ a high standard international journal and welcome all researchers to be TGJ members and to be part of our geoscience community.

Thank you very much.

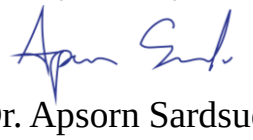

(Dr. Apsorn Sardsud)
Editor in Chief
Thai Geoscience Journal

Thai Geoscience Journal
Vol. 3 No. 3
January 2022
ISSN 2730-2695

LIST OF CONTENTS

Thai Geoscience Journal website at http://www.dmr.go.th/tgjdmr
Printed: 2twin Printing tel +66 2 185 9953, January 2022

Thai Geoscience Journal 3(3), 2022, p. 1-9

ISSN-2730-2695; DOI-10.14456/tgj.2022.1

Groundwater Exploration through 2D Electrical Resistivity Tomography in Labi Agricultural Site, Belait District, Brunei Darussalam

Siti Lieyana Azffri[1, 3*], Stefan Herwig Gödeke[1], Aziz Soffre Ali Ahmad[2], Mohammad Faizan Ibrahim[2], Amalina Abdul Khalid[3], James Jasmir Murphy[3]

[1]Universiti Brunei Darussalam, Bandar Seri Begawan, Brunei Darussalam
[2]Department of Agriculture and Agrifood, Bandar Seri Begawan, Brunei Darussalam
[3]Preston GeoCEM (B) Sdn Bhd, Bandar Seri Begawan, Brunei Darussalam
**Corresponding Author: lieyana.azffri@gmail.com*
Received 17 March 2021; Accepted 6 July 2021.

Abstract

Over the years, Brunei has relied on surface water as the primary water source for domestic, industrial and agricultural use. Increasing population and demands for water, especially in its growing agriculture sector, has led to groundwater exploration at the Labi agricultural site for irrigation purposes driven by the Brunei Government. Electrical Resistivity Tomography (ERT) has been used extensively to delineate subsurface structures and groundwater prospects. The technique was employed in the study area using the pole-dipole array configuration with a survey line of 300 m and a target investigation depth of 100 m from the surface. The 2D resistivity model revealed groundwater zone with resistivity values ranging from 5 to 100 ohm-m. A borehole was drilled through this zone to a maximum depth of 80 m from the surface. A borehole drilling encountered multiple saturated layers of sand between depths of 4 to 78 m. Pumping test showed the groundwater was able to be produced at a steady rate of 288 m^3/day. Aquifer transmissivity estimated using the unsteady Cooper Jacob analysis was 109 m^2/day indicated moderate potential for groundwater usage in the study area for irrigation purposes. The resistivity survey, combined with borehole drilling and testing, provided insights into groundwater hydrology at the Labi agricultural site. The present study helped decision-makers take suitable measures to place future irrigation wells and achieve significant groundwater exploration results in the study area and other regions with similar geological settings.

Keywords: Agricultural Site, Electrical Resistivity Tomography, Groundwater

1. Introduction

Brunei Darussalam, or simply known as Brunei, is located on the north coast of Borneo Island in Southeast Asia. The country has a total land area of 5,765 km^2 with an estimated population of 459,500 in 2019 (DEPS, 2019). Brunei is divided into four main districts: Brunei-Muara, Tutong, Belait and Temburong. The location map of Brunei and the study area are shown in Fig. 1.

The majority of the water supply in Brunei comes from surface water resources. Surface water accounts for 99.5 per cent of the total water supply used for domestic, industrial and agricultural, while the remaining 0.5 percent comes from groundwater resources. Groundwater abstraction is currently limited to the local bottled water industry found in the Liang area (FAO, 2011). Previous study in Brunei revealed groundwater flow system of shallow coastal aquifer in the Berakas area, Brunei-Muara District (Azhar, Abdul Latiff, Lim & Gödeke, 2019).

The Brunei Government emphasises developing agriculture and agri-food to ensure food supply security and enhance economic contribution to its GDP. Brunei's Department of Agriculture and Agrifood is currently improving irrigation, especially in relative water-scarce agricultural areas. The use of groundwater for irrigation purposes in Brunei has not been investigated before.

This study conducted groundwater exploration at the Labi agricultural site, Belait District, Brunei, for irrigation purposes.

Geophysical method using electrical resistivity tomography was first employed to investigate the subsurface lithological formations, geological structures and resistivity variations in the study area (Ashraf, Yusoh & Abidin 2018; Riwayat, Ahmad Nazri & Zainul, 2018; Kumar, Rajesh, Mondal, Warsi & Rangarajan, 2020). Resistivity results used to delineate groundwater zones and locate a suitable site for borehole drilling. A borehole lithology log was constructed and used to correlate with the study area's 2D resistivity inversion model. A pumping test of the newly drilled borehole provided a transmissivity estimate of the local aquifer.

2. Study Area

The Labi agricultural site is about 30 km inland from Seria town in Kampong Rampayoh, Mukim Labi, Belait District. The site has two separate lots, Lot A and Lot B. Groundwater exploration was conducted at Lot A, which covers about 45 ha of cultivable land. Groundwater exploration in the study area aims to improve the irrigation system, especially during the dry season. The area's climate is typical of equatorial tropics characterised by high rainfall and temperatures throughout the year, with total average annual precipitation of 2909 mm. There are two periods of rainy season i.e., from October to January and May to July. Two periods of dry season are from February to March and June to August (BDMD, 2021).

The study area is generally flat, with no significant geological structure outcrop and features seen on the surface. Topographical elevation in the study area ranges from 7 to 30 m above mean sea level. Drainage systems are controlled by streams flowing approximately from east-southeast to west-northwest directions. Previous borehole studies conducted by Brunei's Department of Agriculture & Agrifood revealed brown and greyish soil consisting of peat, clay, and silty clay up to 15 m below the ground surface (DAA, 2018). No further information on the deeper geological strata was available in the study area.

3. Regional Geological Setting

Brunei is located on the north coast of Borneo Island. The island's regional geology has resulted from a series of complex regional tectonic events since the Cenozoic period (Hall & Nichols, 2002; Baillie, Darman & Fraser, 2004). According to Baillie et al. (2004), the island's evolution resulted from two major tectonic events; the South China Sea opening and the Australian plate's northward movement. Consequently, overall compressional tectonics have formed deformation zones of mountainous terrain extending through the island's central part. High weathering and erosion rates of the mountainous terrain contributed to developing many known delta systems around the island.

The study area lies within the Champion delta system. The delta developed during the Middle Miocene to Early Pliocene formed at the eastern onshore and offshore Brunei areas. Rock strata in the area are consisted of thick sand-shale sequences deposited during delta development (Torres, Gartrell & Hoggmascal, 2011; Lambiase & Cullen, 2013). Quaternary deposits possibly overlie older bedrocks of the Miri and Lambir Formations in the study area (Fig. 2; Sandal, 1996). The Quaternary deposits are mainly unconsolidated rocks made up of clay, sand, silt and in places overlain by peat. The underlying Miri Formation is of the Middle to Late Miocene age. The lower part of the formation is argillaceous, and sandstones dominate the upper part. The Lambir Formation of Early to Middle Miocene age underlies the Lambir Hills. The northeast-southwest trending Belait anticline passes near Kampong Labi and in the Bukit Teraja areas. The predominant rock types of the Lambir Formation are sandstone and shale with minor limestone and marl intercalations.

4. Regional Geological Setting

4.1 Electrical Resistivity Tomography

Electrical Resistivity Tomography (ERT) is a geophysical survey method widely used to obtain subsurface information. It is a non-destructive and susceptible method typically used for groundwater exploration (Saad, Nawawi

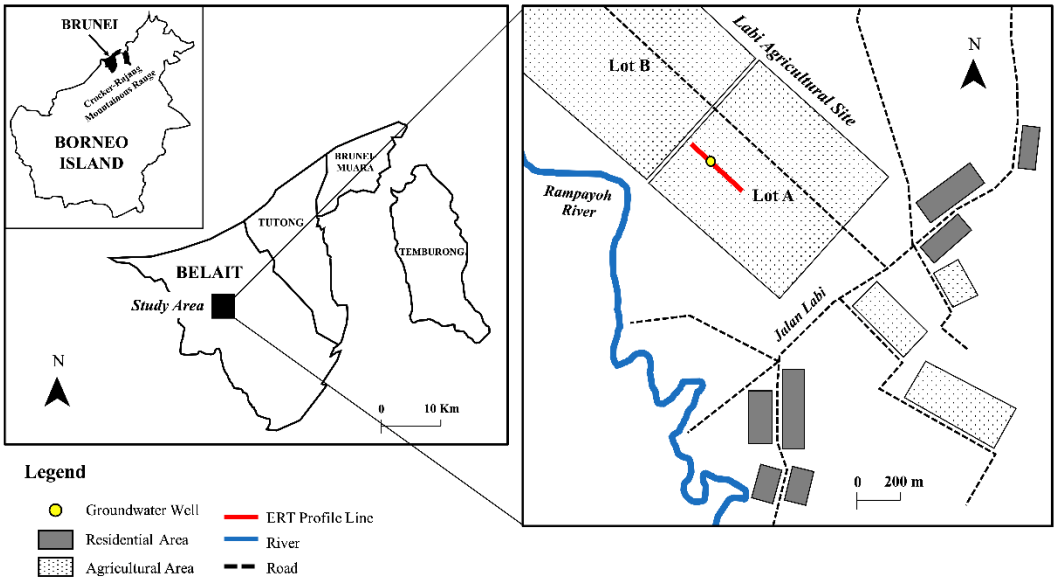

Fig. 1: Map of Brunei Darussalam showing the location of the study area.

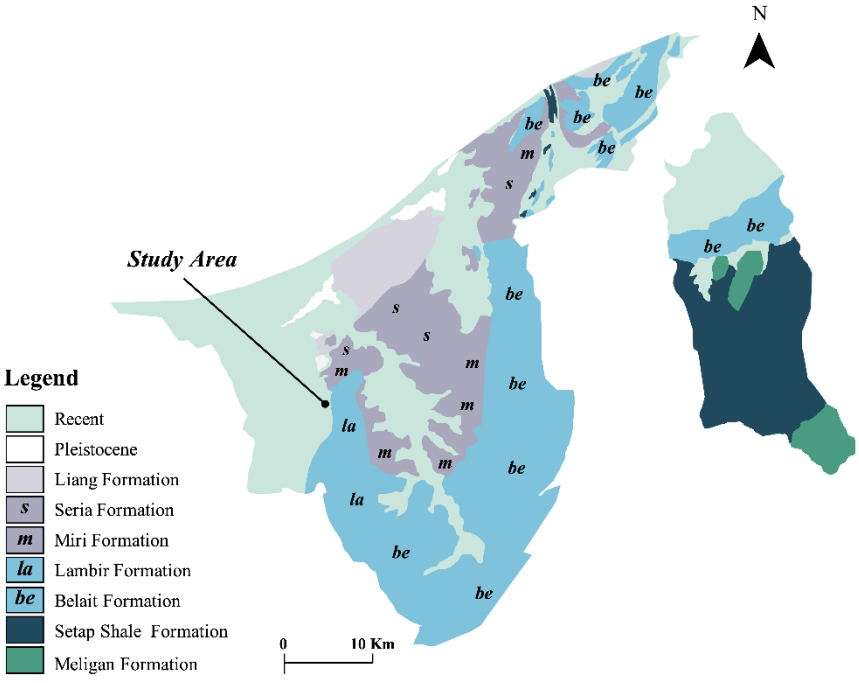

Fig. 2: Stratigraphic map of Brunei Darussalam showing the location of the study area (modified after Sandal, 1996).

& Mohamad, 2012; Annuar & Nordiana, 2018; Ashraf et al., 2018; Aziman et al., 2018; Riwayat et al., 2018; Kumar et al., 2020). Others used this method to solve geotechnical and environmental problems (Sudha, Israil, Mittal & Rai, 2009; Zawawi, Syafalni & Abustan, 2011; Galazoulas, Mertzanides, Petalas & Kargiotis 2015; Lech, Skutnik, Bajda & Markowsk-Lech, 2020).

Electrical resistivity method utilises the differences in electric potential to identify subsurface materials. The measurement of subsurface resistivity is performed by injecting electric current into the ground through two current electrodes (C1 and C2 in Fig. 3) and measuring the resulting voltage difference at two potential electrodes (P1 and P2). From the current (I), voltage difference (V) and a geometric factor (k), the apparent resistivity (ρ_a) is calculated using Eq.1:

$$\rho_a = \frac{kV}{I} \qquad (1)$$

The resistivity survey was carried out in this study by using the ABEM SAS4000 resistivity meter and ABEM ES10-64 multi-electrode system. The resistivity survey line covered a lateral distance of 300 m in the NW-SE direction in the study area. Sixty-one electrodes were deployed along the survey line with an interval 5 m and 10 m. The configuration of the resistivity survey used was the pole-dipole array (Fig. 3). The pole-dipole array offers a good horizontal data and depth coverage (Saad et al., 2012; Annuar & Nordiana, 2018; Ashraf et al., 2018; Kumar et al., 2020). The complete set of the observed apparent resistivity data were analysed to produce a two-dimensional (2D) resistivity model through an inversion process. The ZONDRES2D software was used for the 2D inversion.

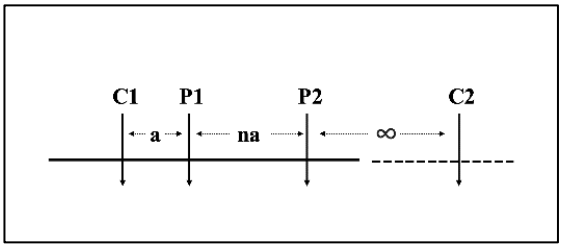

Fig. 3: The arrangement of electrodes for 2D electrical resistivity survey using the Pole-Dipole array configuration (Loke, 2012).

Resistivity values of some typical rocks, soil materials, saturated zones and water are shown in Table 1 and Table 2. Furthermore, overlapping resistivity values is dependent on several factors such as porosity, degree of water saturation and concentration of dissolved salts (Samouëlian, Cousin, Tabbagh, Bruand & Richard, 2005).

4.2 Borehole Drilling and Pumping Test

New borehole drilling accomplished at the study area was based on the interpretation of ERT data. A borehole was drilled using a mud rotary method to a depth of 80 m below the ground surface. The diameter of the drill bit is 10 inches. Materials drilled at the bottom of the borehole mixed with drilling fluid were sampled as they emerged at the top of the hole with a sampling interval of 3 m.

Borehole testing was performed immediately after the completion of the borehole drilling. 6-inch diameter UPVC casings up to 80 m and slotted screens with 1.5 mm openings were used to construct the groundwater pumping well. The slotted screens were installed at 18 to 28 m and 48 to 78 m depths below the ground surface. A gravel pack filter was installed between the aquifer and UPVC screens. The pumping test was carried out by installing a 1.5 HP submersible pump into the tube well at 45 m depth and continuously pumping water out from the well through a 2-inch riser pipe. The tube well responses in terms of water level change and water discharge rate were recorded. These were measured by using a water level meter installed inside the well and a volume meter connected at the outlet pipe on the surface. A constant rate pumping test was carried out for 24 hours with an initial water table of 21.4 m and final water table of 22.9 m below ground level, before allowing the well to recover naturally. The time-drawdown data in both trials were interpreted for aquifer transmissivity and hydraulic conductivity.

4.3 Aquifer Transmissivity and Hydraulic Conductivity

In this study, the Cooper-Jacob straight-line time-drawdown method was used to analyse the

Table 1: Resistivity values of common rocks and soil materials (Keller & Frischknecht, 1996).

Material	Resistivity (Ωm)
Alluvium	10 – 800
Sand	60 – 1000
Clay	1 – 100
Groundwater (fresh)	10 – 100
Sandstone	8 – 4,000
Shale	20 – 2,000
Limestone	5,000 – 1,000,000

Table 2: Resistivity values of different water types (Keller & Frischknecht, 1996).

Type of water	Resistivity (Ωm)
Precipitation	30 – 1000
Surface water in areas of igneous rock	30 – 500
Surface water in areas of sedimentary rock	10 – 100
Groundwater in areas of igneous rock	30 – 150
Groundwater in areas of sedimentary rock	> 1
Seawater	0.2
Freshwater	10 – 100
Drinking water (max. salt content 0.25%)	> 1.8
Water for irrigation and stock watering (max. salt content 0.25%)	> 0.65

pumping test data. Several assumptions were considered. The Cooper-Jacob solution assumes that the aquifer is confined, homogenous, isotropic and of uniform thickness over the area of pumping. In addition, we assumed that thegeneral assumption for determining aquifer parameters from time-drawdown data assumes that the pumping well is screened throughout the entire thickness of the aquifer being tested (Fetter, 2001).

Transmissivity is defined as the rate at which water passes through a unit width of the aquifer under a hydraulic gradient unit. From the pumping rate (Q) and changes in drawdown ($h_0 - h$) of the water level, the transmissivity (T) is calculated from Eq.2 (Cooper & Jacob, 1946):

$$T = \frac{2.3Q}{4\pi(h_0 - h)} \qquad (2)$$

High aquifer transmissivity values are desirable for groundwater irrigation. Standard numerical values for transmissivity and classification of the aquifer are given in Table 3 (Sen, 2015).

From the calculated transmissivity (T) and the aquifer thickness (b), the hydraulic conductivity (K) was calculated using Eq. 3:

$$K = \frac{T}{b} \qquad (3)$$

5. Results and Discussion

5.1 2D Resistivity Model and Groundwater Zone

An electrical resistivity study was carried out at the Labi agricultural site to delineate subsurface geological formations, structures and groundwater potential. The study area's 2D resistivity inversion model revealed the resistivity variations to 100 m depth below the ground surface (Fig. 4). Resistivity values in the model ranges from 5 to 700 ohm-m. Two zones were interpreted; the topsoil and the groundwater zone. The topsoil is distinctive of resistivity values from 100 to 700 ohm-m, with a depth of 10 m to 40 m from the ground surface. In the study area, the topsoil overlies the potential groundwater zone. The groundwater zone is distinctive of resistivities ranging from 5 to 100 ohm-m. Resistivity values of less than 100 ohm-m are typical of soils below the water

Table 3: Aquifer classification based on Transmissivity values.

Transmissivity (m^2/day)	Aquifer Classification
<5	Negligible
5 – 50	Weak
50 – 500	Moderate
>500	High

table due to groundwater effects (Keller & Frischknecht, 1996). In contrast, resistivity values of soils above the water table are typically higher as they tend to be much drier (Riwayat et al., 2018). A Borehole drilling target was identified at the horizontal distance of 100 mof the survey line, considering the favourable and well-defined resistivity contrast to the surrounding geological formations at a depth of about 20 m to 80 m.

5.2 Borehole Lithology and Resistivity Correlation

A new borehole was drilled to 80 m below the ground surface to investigate the geological formation in the study area. Borehole drilling encountered multiple saturated layers of sands and sandstones between the depth of 4 and 78 m. Interbedded layers of clay and mudstone were also recorded throughout the borehole log. Lithological description of the borehole and resistivity correlations are shown in Fig. 5. With careful correlation with lithology differences, resistivity surveys can be helpful to detect anomalous bodies or potential groundwater zones (Saad et al., 2012; Annuar & Nordiana, 2018; Ashraf et al., 2018; Aziman et al., 2018; Kumar et al., 2020). The saturated sandy layers found from the borehole drilling was characterised as the groundwater zone, inferred from the resistivity model. Our findings indicate that due to the inhomogeneous properties of the soil materials comprising mainly alternating sand and clay, the resistivity values often overlap, resulting in an ambiguous interpretation. Therefore, future studies should include drilling groundwater test wells to further determine the soil properties.

5.3 Borehole Pumping Tests and Aquifer Characterisation

Borehole pumping tests are vital for understanding the aquifer performance in various hydrogeological settings. The pumping test was conducted to investigate water table responses and groundwater availability in the study area. The time-drawdown and recovery curves from the newly drilled borehole are shown in Fig. 6. The water level measurements from the open borehole showed that the static water level is approximately 4.5 m below the ground surface, suggesting a shallow water table in the area. The results of the pumping test with a constant rate showed that the maximum drawdown was 1.52 m after 24 hours of the test. During the recovery test, the water table was recovered to the final drawdown of 0.02 m at 4 hours after the stop of the pumping up. Based on the pumping test results, the groundwater was produced at a steady rate of 288 m^3/day (12 m^3/hr), suggesting the well has sufficient groundwater for withdrawal and distribution for irrigation purposes.

The pumping test provided an estimate of aquifer transmissivity and hydraulic conductivity. The sandy aquifer is assumed to be confined for estimating aquifer characteristics. The thickness of the aquifer is 40 m. Based on the unsteady Cooper-Jacob time-drawdown method, the estimated transmissivity value is 109 m^2/day, showing moderate potentiality for groundwater usage in the study area for irrigation purposes (Table 3). Aquifer parameters in this study suggest that the hydraulic conductivity is 2.75 m/day, typically associated with unconsolidated deposits of alluvial and fine sand (Spitz & Moreno, 1996).

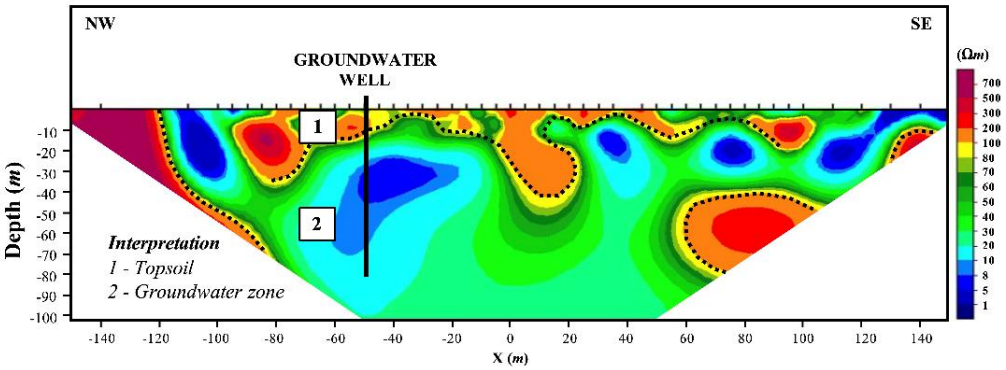

Fig. 4: The 2D resistivity model of the survey line.

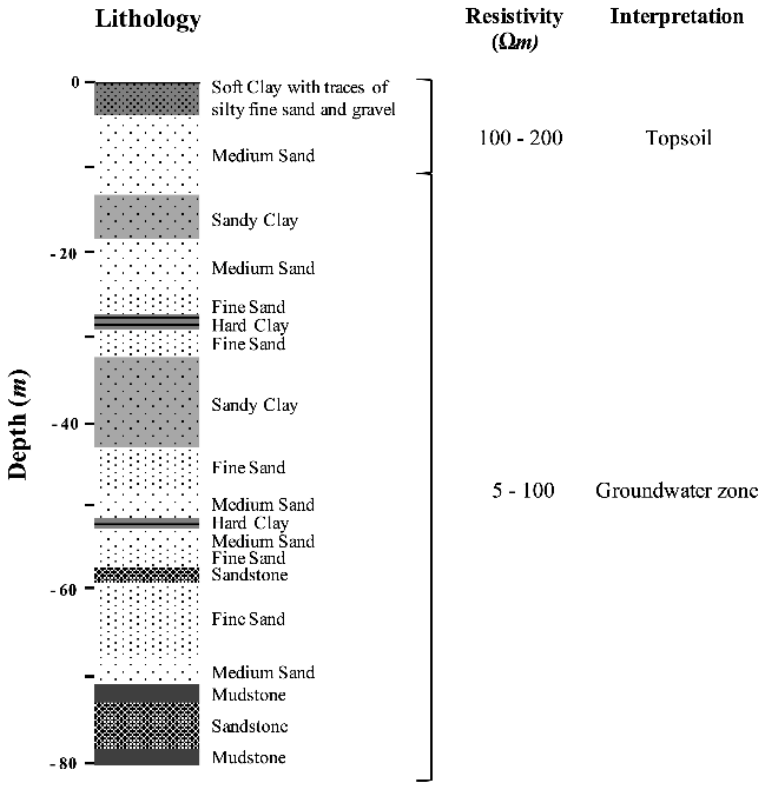

Fig. 5: Correlation of 2D resistivity model with the borehole lithology at a distance of 100 m of the survey line.

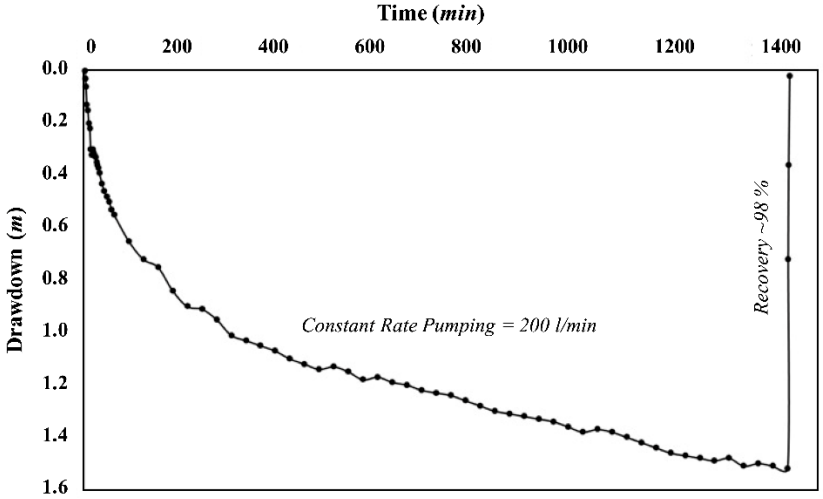

Fig. 6: Time-drawdown and recovery curves of the newly drilled borehole in the study area.

6. Conclusions

Electrical resistivity tomography conducted at the Labi agricultural site provided an understanding of the subsurface geological formations and structures through variation in resistivity. Resistivity values ranged from 5 to. 700 ohm-m in the obtained resistivity inversion model. The 2D resistivity model showed two distinctive subsurface layers: the topsoil and the groundwater zone. The identified groundwater zone was characterised by distinctive resistivities ranging from 5 to 100 ohm-m. Based on resistivity datasets, a suitable drilling target was identified.

The 2D resistivity model was correlated with borehole lithology from the executed target well to 80 m depth. Borehole drilling encountered multiple saturated layers of sand and sandstone at depths of 4 to 78 m from the ground surface. The groundwater was produced at a steady rate of 288 m^3/day. The pumping test indicated that the well could be used for irrigation purposes. The aquifer characterisation based on the pumping test analysis revealed an estimated transmissivity of 109 m^2/day and a hydraulic conductivity of 2.75 m/day.

The resistivity datasets and borehole lithology have immensely helped in a realistic conceptualisation and understanding of the study area's aquifer system. The present study helped decision-makers take suitable measures to place future irrigation wells and to achieve significant groundwater exploration results in the study area and other regions of similar geological settings.

References

Annuar, U. M., & Nordiana, M. M. (2018). Aquifer detection using 2D resistivity method and porosity calculation. *Jurnal Teknologi (Sciences & Engineering) 80 (6)*, 149-158.

Ashraf, M. A., Yusoh, R. S., & Abidin, M. H. (2018). Aquifer characterisation and groundwater potential evaluation in sedimentary rock formation. *Journal of Physics: Conference Series Volume 995*.

Azhar, A. S., Abdul Latiff, A. H., Lim, L. H., & Gödeke, S. H. (2019). Groundwater investigation of a coastal aquifer in Brunei Darussalam using seismic refraction. *Environmental Earth Sciences, 78:220*.

Aziman, M., Hazreek, Z. A., Azhar, A. T., Fahmy, K. A., Faizal, T. B., Sabariah, M., . . . Ismail, M. A. (2018). Electrical resistivity technique for groundwater exploration in Quaternary deposit. *Journal of Physics: Conference Series Volume 995*.

Bailie, P., Darman, H., & Fraser, T. H. (2004). Deformation of Cenozoic basins of Borneo and West Sulawesi. *Proceedings of Deepwater and Frontier Exploration In Asia & Australasia Symposium.* Jakarta: Indonesian Petroleum Associations.

BDMD (2021). *Climate*. Retrieved from Brunei Darussalam Meteorological Department: www.bruneiweather.com.bn

Cooper, H. H., & Jacob, C. E. (1946). A generalised graphical method for evaluating formation constants and summarising well-field history. *Transactions, American Geophysical Union ,27;526-34*.

DAA (2018). *Full Report of Electrical Imaging (Resistivity) and Soil Sampling in Brunei Darussalam.* Bandar Seri Begawan: Department of Agriculture and Agrifood.

DEPS (2019). *Population*. Retrieved from Department of Economic Planning and Statistics, Ministry of Finance and Economy: www.deps.gov.bn

FAO (2011). *AQUASTAT Country Profile - Brunei Darussalam.* Rome, Italy: Food and Agriculture Organisation of the United Nations (FAO).

Fetter, C. W. (2001). *Applied Hydrogeology Fourth Edition.* New Jersey: Pearson Education International.

Galazoulas, E. C., Mertzanides, Y. C., Petalas, C. P., & Kargiotis, E. K. (2015). Large scale electrical resistivity tomography survey correlated to hydrological data for mapping groundwater salinisation: A case study from multilayered coastal aquifer in Rhodope, Northeastern Greece. *Environmental Process 2*, 19-25.

Hall, R., & Nichols, G. (2002). Cenozoic sedimentation and tectonics in Borneo: climatic influences on orogenesis. In S. J. Jones, & L. Frostick, *Sediment flux to basins: causes, controls and consequences* (pp. 5-22). Geological Society London, Special Publications.

Keller, G. V., & Frischknect, F. C. (1996). *Electrical methods in geophysical prospecting.* Oxford: Pergamon Press Inc.

Kumar, D., Rajesh, K., Mondal, S., Warsi, T., & Rangarajan, R. (2020). Groundwater exploration in limestone-shale-quartzite terrain through 2D electrical resistivity tomography in Tadipatri, Anantapur district, Andhra Pradesh. *Journal of Earth System Sciences, 129(1)*.

Lambiase, J. J., & Cullen, A. B. (2013). Sediment supply systems of the Champion "Delta" of NW Borneo: Implications for deepwater reservoir sandstones. *Journal of Asian Earth Sciences 76*, 356-371.

Lech, M., Skutnik, Z., Bajda, M., & Markowska-Lech, K. (2020). Applications of electrical resistivity surveys in

solving selected geotechnical and environmental problems. *Applied Sciences 10:2263*.

Loke, M. H. (2012). Tutorial: 2D and 3D electrical imaging surveys. 172.

Riwayat, A. I., Ahmad Nazri, M. A., & Zainul, M. H. (2018). Application of Electrical Resistivity Method (ERM) in Groundwater Exploration. *Journal of Physics: Conference Series, Volume 995*.

Saad, R., Nawawi, M. N., & Mohamad, E. T. (2012). Groundwater detection in alluvium using 2-D Electrical Resistivity Tomography (ERT). *Electronic Journal of Geotechnical Engineering*, 369-376.

Samouëlian, A., Cousin, I., Tabbagh, A., Bruand, A., & Richard, G. (2005). Electrical resistivity survey in soil science: a review. *Soil & Tillage Research 83*, 173-193.

Sandal, S. T. (1996). *The geology and hydrocarbon resources of Negara Brunei Darussalam.* Bandar Seri Begawan: Brunei Shell Petroleum.

Sen, Z. (2015). Basic porous medium. In Z. Sen, *Practical and applied hydrogeology 1st Edition* (pp. 43-97). Elsevier.

Spitz, K., & Moreno, J. (1996). *A practical guide to groundwater and solute transport modelling.* New York: Wiley.

Sudha, K., Israil, M., Mittal, S., & Rai, J. (2009). Soil characterisation using electrical resistivity tomography and geotechnical investigation. *Journal of Applied Geophysics 67*, 74-79.

Torres, J., Gartrell, A., & Hoggmascal, N. (2011). Redefining a sequence stratigraphic framework for the Miocene to present in Brunei Darussalam: roles of local tectonics, eustacy and sediment supply. *International Petroleum Technology Conference.* Bangkok.

Zawawi, M. H., Syafalni, & Abustan, I. (2011). Detection of groundwater aquifer using resistivity imaging profiling at Beriah landfill site, Perak, Malaysia. *Advanced Materials Research Volume 250-253*, 1852-1855.

Thai Geoscience Journal 3(3), 2022, p. 10-19

ISSN-2730-2695; DOI-10.14456/tgj.2022.2

BOOSTING THE PROMOTION OF MALAYSIAN GEOSITES THROUGH DIGITAL PLATFORM IN THE NEW NORMAL TIMES

Muhammad Mustadza Mazni[1*], Norbert Simon[2], Anuar Ishak[1], Abd Rahim Harun[1], Zamri Ramli[1], Dana Badang[3], Che Aziz Ali[2]

[1] *Department of Mineral and Geoscience Malaysia, Headquarters*
[2] *Geology Program, Department of Earth Science and Environment, Universiti Kebangsaan Malaysia*
[3] *Department of Mineral and Geoscience Malaysia, Sarawak*
**Corresponding author: mustadza@jmg.gov.my*
Received 17 March 2021; Accepted 22 July 2021.

Abstract

Undeterred by the interrupted local and global activities due to the current health crisis, the Department of Mineral and Geoscience Malaysia (JMG) has boosted its promotion of geological sites and related information to the public. The JMG has initiated the creation of a smartphone application called '**MYGeotapak**', which directly translates to 'Malaysian Geosites' in English. Initially, the application was solely for within-department and expert use. Given the significance of sharing such a platform to the public, its second version will be soon available for public use. Both versions include information on Malaysian geosites. The first version was successfully launched in early March 2020 in collaboration with the Malaysian Geoheritage Group and local university representatives. Surprisingly, it garnered 205 views on YouTube, 241 application downloads and 240 user manual downloads in eight months. The sites containing this material were also visited by more than 1,047 viewers. However, the first version is not available in the Apple Store and Google Play Store. The continuous effort by the JMG to promote Malaysian geosites resulted in the second version of the application, which contains hundreds of potential geosites around the country. The current version also boasts innovative and interactive tools, which are an improvement from its predecessor. This latest application, which is currently in its prototype phase, follows the ISO MS1759 (geology) standard. This user-friendly application suits the requirements of the general public. This application is part of JMG's effort to promote awareness amongst the public on the significance and wonders of geological heritage in the country. It also serves as an alternative for the roadshows often carried out around the country before the pandemic. Other efforts for conservation and promotion of geosites in Malaysia are currently being planned and will be utilising the digital platform.

Keywords: Digital Platform, Geoheritage, Malaysian Geosites, MYGeotapak

1. Introduction

Geotourism is a national effort under the sustainable tourism programmes, which has gain momentum in recent years. However, this initiative would be for nothing if not shared with the public (Filocamo, 2020). Aside from its economic benefits, people learn the history of the earth through its concepts. Hence, the promoted sites can become the natural capital of the people (Gray, 2019). The term 'natural capital' refers to the world's stock of natural assets, which also includes geology (https://naturalcapitalforum.com/about/).

Digital devices and platforms have altered science and are driving new ways to deal with geoheritage and geotourism education, communication and interaction amongst the public (Tormey, 2019). Few applications or digital platforms for geotourism contain geosite descriptions, glossary, geological itineraries, sketch maps and other non-geological sites, such as cultural and natural sites (Filocamo et al., 2020).

Researchers (e.g. Norbert et al., 2018) from the Malaysian Geoheritage Group and the Department of Minerals and Geoscience (JMG) utilised web applications to promote geosites around the country. They employed the Story

Map tool, which is an opensource web application made by ESRI. The proposed web applications present geothermal sites with basic scientific information for the Gombak-Hulu Langat National Geopark and different rock types and their petrographic minerals around the famous Dayang Bunting Geoforest Park in the Langkawi UNESCO Global Geopark.

Digital platforms have greatly contributed to many aspects during the current pandemic. Nowadays, government agencies, education institutions and businesses are rapidly changing their ways to adapt to this new norm without comprising the quality of service as provided before. The current pandemic situation has highlighted the significance of advance technologies for governments and businesses to continue their activities. The education sector also has the same needs (Tejedor et al., 2020).

On the basis of the above discussion, introducing geology to the public is relevant, especially during the current health crisis where social gatherings are prohibited, and travel is minimal and supervised. Thus, the JMG, together with the Malaysian Geoheritage Group and pool of educators, has initiated the creation of a smartphone application called 'MYGeotapak' (Malaysian Geosites). This application provides graphic information on some of the geosites around Malaysia. This project aims to create awareness and promote these sites continuously even during these trying times. This study presents the proposed design, achievements and future improvements of the MYGeotapak application.

2. Methodology

Ease of use and satisfactory user experience are the primary focus in designing applications for public use. In general, geology is not a common subject to lay people, and apprehending specific fields in geology, such as geoconservation, geotourism and 'geosites', would be more difficult to the public. The schematic in Fig. 1 presents the application design. The design flow is as follows: Users are first presented with a walkthrough page, which contains a tutorial on how to use the application, followed by a 'discover' page that displays the application's main themes (geosite, geopark and geodiversity). Users can navigate these themes through their menu, which contains the definition and list of locations. The menu also provides other information, such as glossary, disclaimer and tutorial pages apart from simple explanations on each site.

The first version of MYGeotapak mainly includes 348 geosites in 11 states and the Federal Territory (Table 1). However, the application does not yet include all the geosites in Malaysia. This inventory thus requires further studies and continuous updates. To date, the sites provided in the application have almost complete information.

a) Geodiversity Option

The application categorises the sites for each state into different geodiversity groups. Some sites naturally have multiple geodiversity categories. This option helps users discover the uniqueness of each state on the basis of the given categories. These categories involve nine geodiversity groups as follows: rock types, minerals, fossils, geological structures, stratigraphy, geological process, landforms/landscapes, geohazards and geological sites (e.g. mining area). These sites showcase the geodiversity of each state. Table 2 presents the site distribution.

b) Site Information

The site description includes no geological jargons or complex terms to facilitate understanding amongst the public. Each site has six information headings. Table 3 shows the information and rationale of each heading for end users.

c) Geological Map

The geological map provided in the application is for geologists and non-experts who wish to know about the distribution of rock types and their ages in Malaysia. The location of the geosites is overlaid on top of the map provided for users. In this way, users can easily identify them with geological information provided with the geological map. Users can simply click on the map to view or read the geological attribute of their choice.

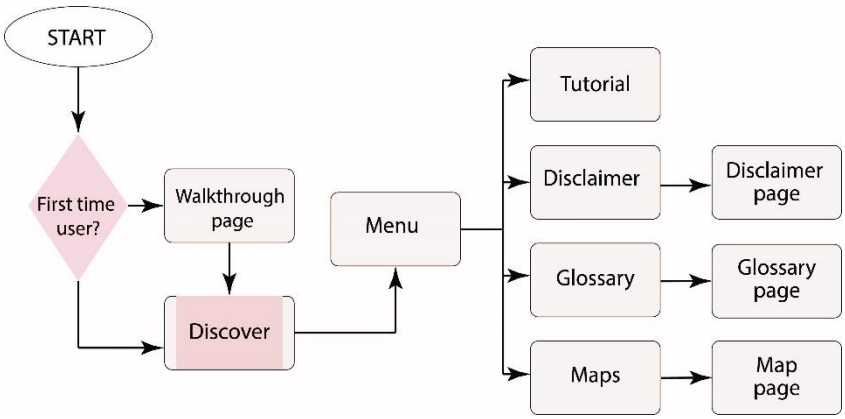

Fig. 1: Workflow schematic diagram for the MYGeotapak App.

Table 1: Number of geological sites and geosites in Malaysia.

State	Number of Geological site/geosite
Negeri Sembilan	53
Sarawak	52
Johor	43
Kelantan	36
Pahang	33
Terengganu	30
Sabah	27
Kedah	24
Perak	18
Perlis	12
Labuan	11
Selangor	9
Total	**348**

Table 2: The distribution in percentage of sites that have various geodiversity in each state.

State	Sites	Rock	Min	Fos	Struc	Strat	Proc	Land	GeoH	GeoS
Negeri Sembilan	53	15%	-	-	24%	-	-	46%	-	3%
Sarawak	52	23%	9%	7%	15%	-	9%	35%	-	3%
Johor	43	39%	3%	3%	16%	4%	-	36%	-	-
Kelantan	36	22%	5%	6%	30%	-	2%	3%	-	4%
Pahang	33	42%	-	10%	-	-	-	48%	-	-
Terengganu	30	42%	6%	7%	24%	-	-	18%	-	4%
Sabah	27	36%	5%	-	18%	-	-	38%	3%	-
Kedah	24	39%	12%	6%	-	6%	-	24%	6%	6%
Perak	18	34%	7%	7%	17%	-	-	34%	-	-
Perlis	12	5%	14%	29%	-	14%	-	24%	-	14%
Labuan	11	-	33%	8%	21%	8%	-	8%	-	21%
Selangor	9	-	-	-	56%	-	-	33%	-	11%

Note: Rock = rock type; Min = Mineral; Fos = Fossil; Struc = Geological structure; Strat = Stratigraphy; Proc = Geological process; Land = Landform/landscape; GeoH = Geohazard; GeoS = Geological site (e.g. mining area).

Table 3: Description of each information group provided for end user in the application.

Information	Description
Name of geological site/ geosite	Conventional geological site/geosite's name that is commonly practiced in geoheritage.
Location	Based on known location that is familiar to the local such as district, place of attraction
GPS Coordinate	For better accuracy, user can use the coordinates to find ways to get to the site's location
Age	Given in 'numbers' (e.g 15 million years instead of geological age (e.g. Miocene)
Geoheritage value	The values which are often described as scientific, recreational, aesthetic
Short description	Some explanation on the site and what can be expected when the user reaches the location

They can also acquire site information by tapping the location icon on the geological map.

d) User Manual

The application includes a user manual as one of the promotional efforts by the JMG. This feature allows users to be familiarised with the application and its system requirements. The manual also explains the contents and the distribution of geosites for each state. The manual design is similar to a catalogue. In this way, users can obtain relevant information before installing the application without taking the fun out of the process.

3. Result and Discussion

The first version was successfully launched in early March 2020 in collaboration with the Malaysian Geoheritage Group and a pool of scholars (Fig. 2). However, this version is not available in the Apple Store and Google Play Store. Initially, the application was created specifically for internal use only. Later on, the JMG perceived the significance of the application on the promotion of the valuable sites in Malaysia amongst the public.

Hence, the application's user manual and montage video was made available in the JMG official websites for the public to download. From mid-March to 28 November 2020, the application garnered 205 views on YouTube, 241 application downloads, 240 user manual downloads and 1,047 viewers (Fig. 3). These numbers are encouraging as this application has been only made available on the web for around eight months, and this subject is somewhat new to the public. The JMG believes that the above statistics will reach new records if the application becomes available in the Google Play Store.

The second version of MYGeotapak application is a complete revamp of the previous version. It contains better interactive features and additional information, which are valuable for geologists and non-expert users. The second version introduces the following innovative features:

a) Step-by-step tutorial on how to use the application
b) Splash screen
c) Definition of terms, such as 'what is geodiversity', for each page
d) Three selections to view sites in Malaysia (geosite, geopark and geodiversity)
e) Glossary
f) Search and filter capability
g) Number of sites displayed for each state
h) Point location on a map for each site
i) Biosites

The second version of the application comprises a step-by-step tutorial displayed at the launch screen. This feature is a great improvement from the previous version and a good starting point for users to learn about geological heritage (Fig. 4). The application also defines special geological terms, especially on the main categories (geosite, geopark and geodiversity; Fig. 5). Each category design follows the significance of geological heritage and geoconservation fields.

Fig. 2: The framework for the first version of MYGeotapak app (a) Geological map of the area (b) Google map (c) Menu bar (d) Developer contact (e) Manual on using the app (f) The main interface (g) Distribution of geosites (h) Information for each geosite.

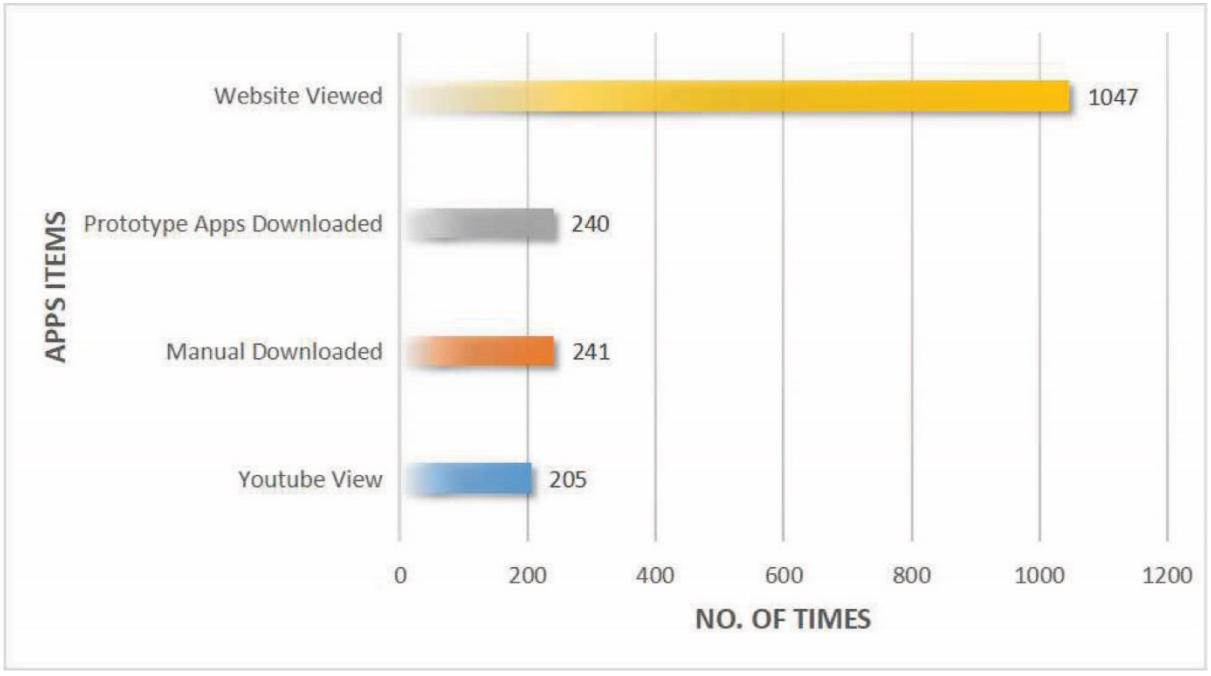

Fig. 3: Statistics of visitors viewing and downloading the 1st verstion MYGeotapak Apps and manual.

The geosite category comprises geological sites in each state (Figs. 6 and 7), and the geopark category includes UNESCO Geopark and National Geopark in Malaysia (Fig. 8). The division of the featured geosites follows their geodiversity category. Users can obtain information about each site by pinpointing their location on the map (Fig. 9). A glossary of scientific terms is also available for those terms that geologists commonly use, facilitating understanding amongst non-experts (Fig. 10; Filocamo et al., 2020).

The current version and innovations of the application are all products of detailed consultation with experts and fruitful investigations on users' requirements. The application follows the recommended standard practice for geology in Malaysia (i.e. ISO MS1759) and the technology of geographic information systems (GIS). The updates of the GIS-based application can be done through its GIS platform. To date, the application is at the last phases of its testing stage and will be soon be available for public use. Similar to its previous version, the JMG believes that this innovation will promote further information dissemination to the public. Li et al. (2015) indicated that smartphone applications would accelerate information sharing on geopark and geoeducation amongst the public. Connecting the importance of geoheritage values to the people at large will foster the appreciation of geoconservation and geoheritage (Tormey, 2019).

4. Conclusion

Although the current health crisis has disrupted many governmental projects and scholarly activities, the JMG has taken proactive steps to maximise the efforts to promote geology to the public through technological and digital approaches. The JMG hopes that the launching of the MYGeotapak application and other upcoming digital innovations will help instil geoconservation awareness to each user.

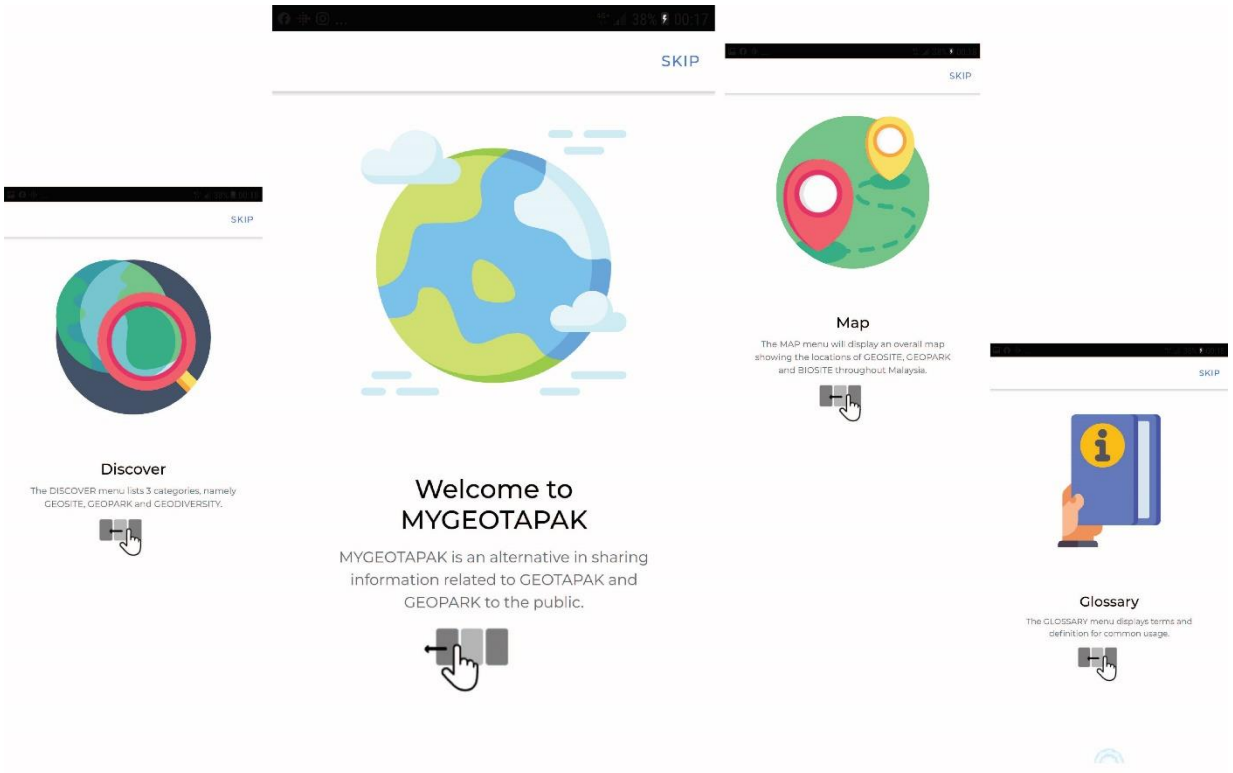

Fig. 4: The welcoming screen displays basic information and short tutorial for user to get familiar with the apps.

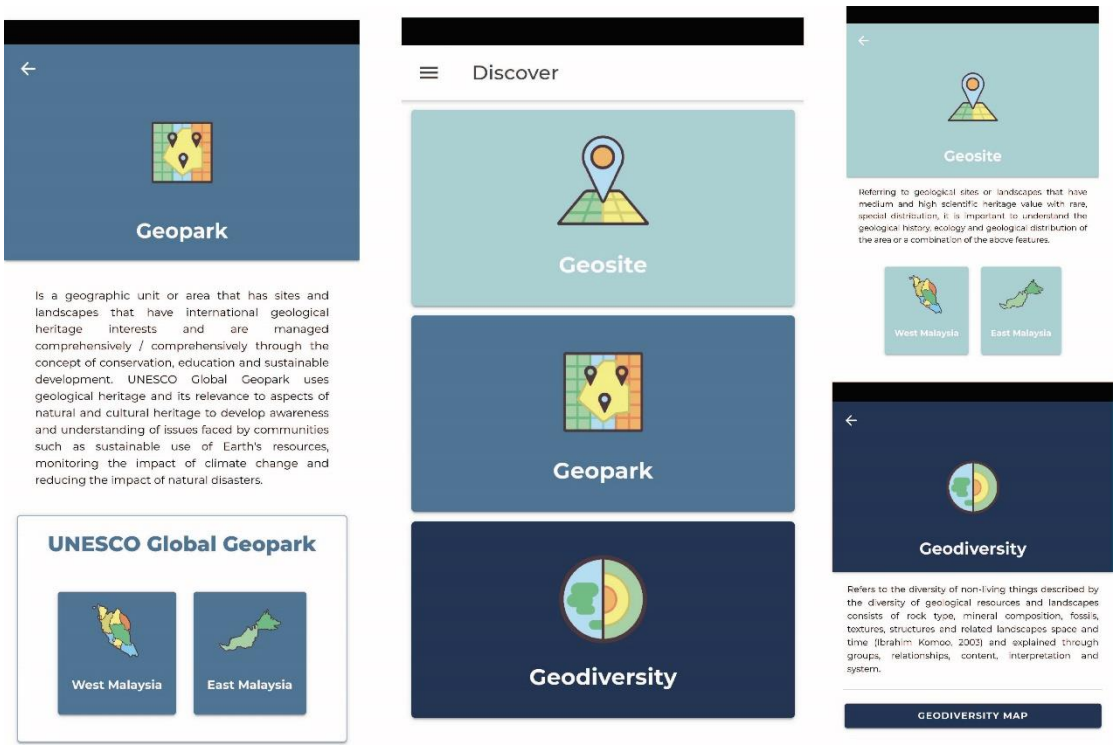

Fig. 5: Three categories for site selections. The Geosite category shows the distribution and information of each geosites in Malaysia; the Geopark tab showcases the UNESCO Global Geopark and National Geoparks; and the Geodiversity tab displays different groups of geodiversity in each geosite.

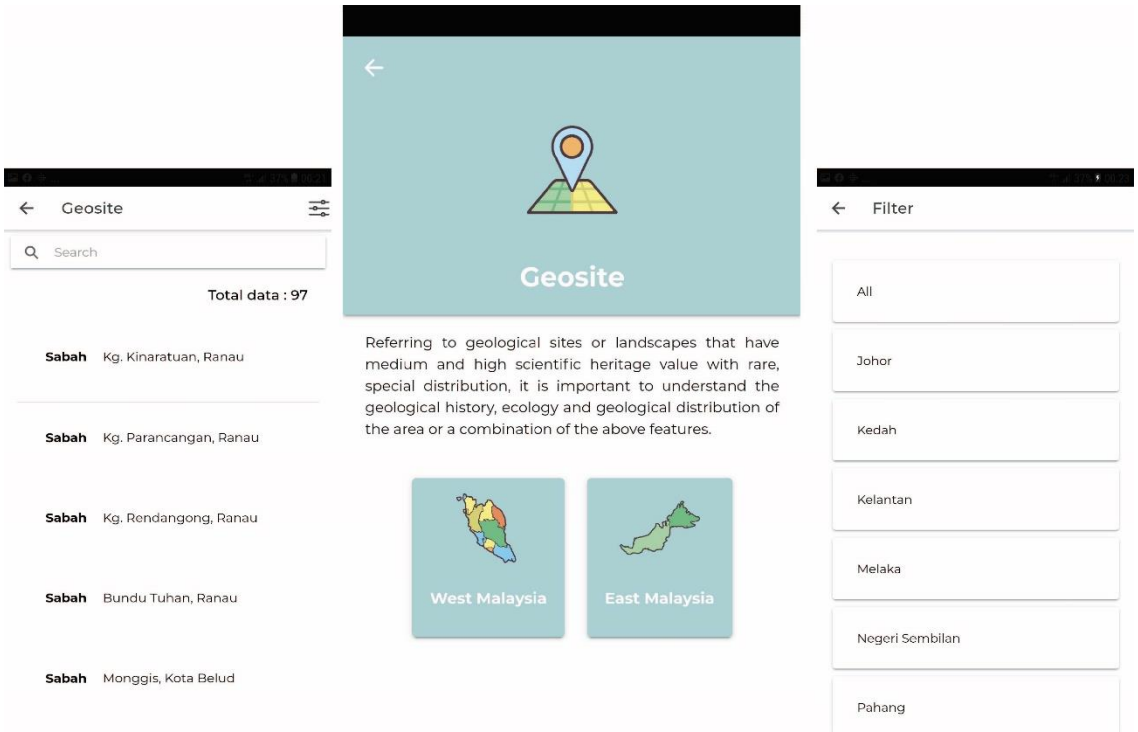

(b) (a) (c)

Fig. 6: Information on each geosite can be viewed through different filters (a) West and East Malaysia (b) Through different states (c) Example of geosites in the state of Sabah.

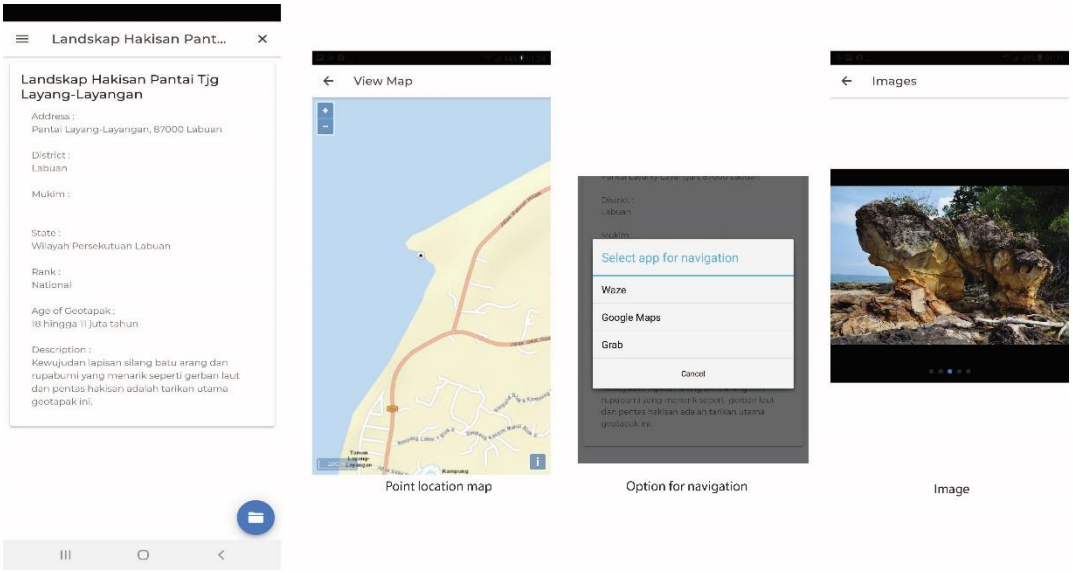

(a) (b) (c) (d)

Fig. 7: Comprehensive information on a geosite and location (a) Information on a geosite (b) Its location on a map (c) Geosite picture and (d) Ways to get there.

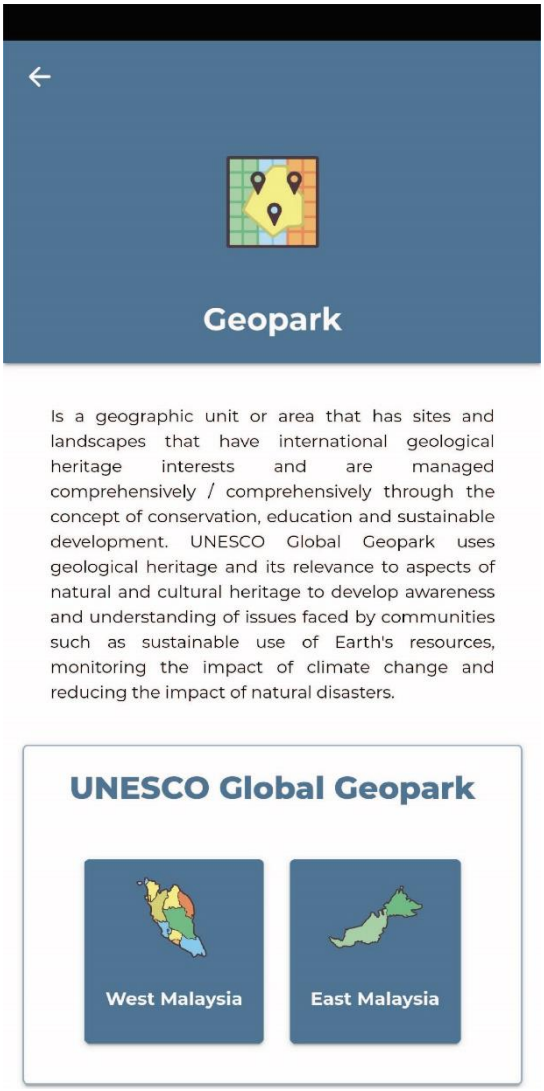

Fig. 8: This page displays the geopark tab in the West and East Malaysia.

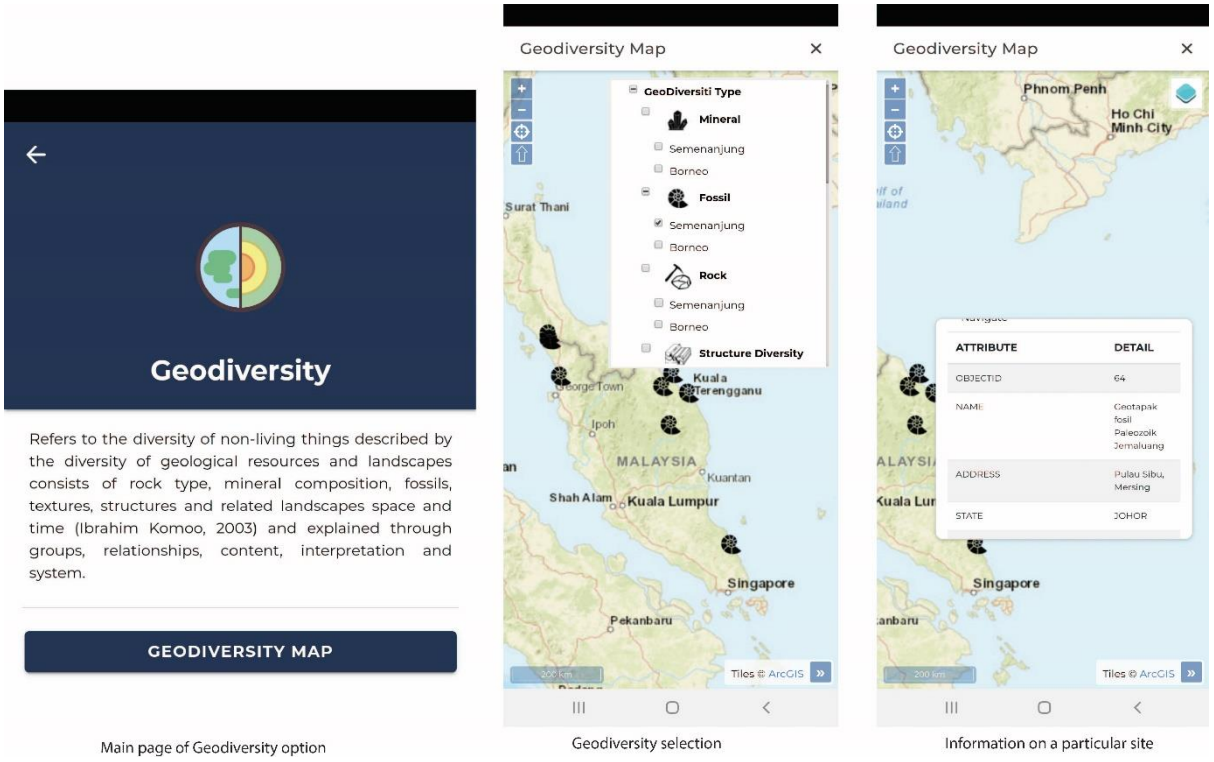

Fig. 9: Web pages showing various information on geodiversity in the application.

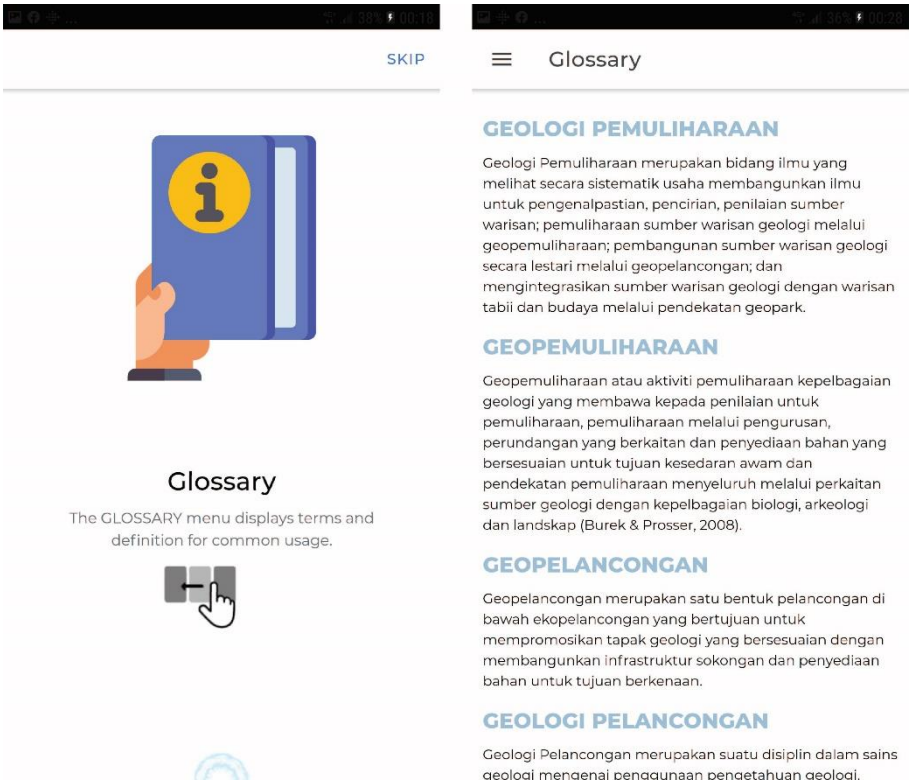

Fig. 10: Web page showing the glossary for speciic terms in the application. At the moment, only terms in Malay are provided in the app.

Acknowledgments

The authors would like to thank the Director General of Department of Mineral and Geoscience Malaysia (JMG), Geoscience Planning Unit, JMG Headquarters, all JMG Geoscience Officers in every state for their advice and contributions. Also a special thanks to researchers from the Malaysian Geoheritage Group (KWGM) and the Geology Department of the Universiti Kebangsaan Malaysia for their expertise and contributions.

References

Filocamo F., Di Paola, G., Mastrobuono L., & Rosskopf, C.M. (2020). MoGeo, a mobile application to promote geotourism in Molise Region (Southern Italy). *Resources*, 9(31), doi:10.3390/resources9030031.

Gray, M. (2019). Geodiversity, geoheritage and geoconservation for society. *International Journal of Geoheritage and Parks*, 7, 226-236.

Li, Q., Tian, M., Li, M., Shi, Y., and Zhou, X. (2015). Toward smartphone applications for geoparks information and interpretation systems in China. *Open Geoscience*, 1, 663-677.

Saliola, F. & Islam, A.M. (2020, September 24) How to harness the digital transformation of the Covid Era. *Harvard Business Review*, https://hbr.org/2020/09/how-to-harness-the-digital-transformation-of-the-covid-era

Simon, N., Ali, C. A., Sarman, M., Badang, D., Unjah, T., & Rahman M. N. (2018). AN Inventory Database For Geoeducational Outreach Based On Volunteered Geographic Information (VGI) Approach In Malaysia. *GeoJournal of Tourism and Geosites*, 23(3), 684–-701. https://doi.org/10.30892/gtg.23306-320

Tejedor, S., Cervi, L., Perez-Escoda, A., & Jumbo, F.T. (2020). Digital Literacy and Higher Education during COVID-19 Lockdown: Spain, Italy, and Ecuador. Publications, 8(48). doi:10.3390/publications8040048

Tormey, D. (2019). New approaches to communication and education through geoheritage. *International Journal of Geoheritage and Parks*, 7, 192-198.

Thai Geoscience Journal 3(3), 2022, p. 20-31

ISSN-2730-2695; DOI-10.14456/tgj.2022.3

Tectonic setting of late Cambrian to early Ordovician meta-tuffs in Kanchanaburi Province, Western Thailand

Suwijai Jatupohnkhongchai[1*], Burapha Phajuy[1], Sirot Salyapongse[2]

[1]Department of Geological Sciences, Faculty of Science, Chiang Mai University, Chiang Mai, Thailand
[2]Geoscience Program, Mahidol University Kanchanaburi Campus, Kanchanaburi, Thailand
** Corresponding author: suwiijai@gmail.com*
Received 17 March 2021; Accepted 6 July 2021.

Abstract

Meta-tuffs are mapped as a Silurian-Devonian unit in Kanchanaburi Province, Western Thailand. These rocks were discovered and described for the first time in 1976 and mentioned in the 1:250,000 Suphanburi geologic map sheet (ND47-7). The detailed petrography and geochemistry of these rocks are still unclear and insufficient. Petrographically, the meta-tuffs can be named as a meta-quartz-K-feldspar crystal tuff and meta-lithic tuff. They are made up of pyroclasts (volcanic rock, quartz, K-feldspar, devitrified glass) and epiclasts (granitic and meta-sedimentary rocks) embedded in a very fine-grained matrix. The whole-rock composition shows enrichment in SiO_2 and K_2O and a strong depletion in CaO and Na_2O which is related to alteration and low-grade metamorphism. The meta-tuffs are divided into two groups based on immobile element classification. Group 1 rocks can be classified as dacitic-rhyolitic rocks which belong to the calc-alkaline series. Group 2 rocks are considered to be transitional rocks. Their chondrite-normalized patterns of both groups display light REE enrichment with nearly flat heavy REE and a negative Eu anomaly, typical for calc-alkaline volcanic rocks. Moreover, these meta-tuffs obviously show a negative Nb-Ta anomaly in the primitive mantle immobile-normalized spider diagram suggested volcanic arc environment. Both REE patterns and spider diagrams are coincident with the tectonic discrimination diagrams, which confirm that these meta-tuffs were formed in a volcanic arc environment. The zircon U-Pb dating of the meta-tuffs yield ages of 498.4+2.40/-3.0 Ma and 482.7+3.6/-1.0 Ma. These meta-tuffs are basement of Sibumasu Terrane. They were formed during the late Cambrian-early Ordovician possibly related to the closure of a proposed Proto-Tethys ocean along the margin of Gondwana.

Keywords: Late Cambrian-early Ordovician tuff, Proto-Tethys ocean, Sibumasu Terrane, Silurian--Devonian unit, Volcanic arc

1. Introduction

The pre-Cenozoic extrusive rocks of Thailand have been divided into four volcanic belts (Barr and Macdonald, 1991; Barr and Charusiri, 2011). However, there are occurrences of poorly investigated meta-tuffs in western Thailand. In particular, the Kanchanaburi study area, the mapped Silurian--Devonian meta-tuffs first time appeared in the 1:250,000 Suphan Buri geologic map sheet and the report (in Thai) in 1976 and 1980 respectively (Bunopas, 1976, 1980). No detailed petrography and geochemistry have been previously published. The 'Silurian-Devonian unit' in Kanchanaburi, is the Bo Phloi Formation which has a type section at Khao Yai-Ka, and consists of quartzite, shale, chert, tuff, tuffaceous sandstone, tuffaceous shale, phyllite, and thin crystalline limestone (Bunopas, 1981). "*Tentaculites* cf. *elegans"* has been reported from Khao Ka in the upper part of the Bo Phloi Formation which is probably Lower Devonian, while the unfossiliferous lower part is probably Silurian (Bunopas and Bunjitradulya, 1975). Although the formation is considered to be a result of an active margin from westward dipping subduction beneath the Shan-Thai related to a possible back-arc environment based primarily on regional stratigraphy and relative age (Bunopas, 1981; Bunopas and Vella, 1978), reliable data insufficient. The purposes of this

study are to analyze the geochemical composition and classify the tephra as well as to evaluate the tectonic setting of these pyroclastic rocks in Kanchanaburi Province, Thailand.

2. Geological background

Thailand is subdivided into four major tectonic zones, from west to east: Sibumasu Terrane, Inthanon Suture Zone, Sukhothai Terrane, and Indochina Terrane (Sone and Metcalfe, 2008). The Sibumasu Terrane and Inthanon Suture Zone dominate Western Thailand. The Inthanon Suture Zone is a large accretionary complex that formed with the closure of the Palaeo-Tethys Ocean in the Triassic (Barr and Macdonald, 1991; Ueno, 1999; Sone and Metcalfe, 2008). Suture zone rocks include Permian basaltic volcanics, Carboniferous-Permian limestones, Devonian--Triassic radiolarian cherts, Triassic S-type granitoids, and mylonitic/migmatitic gneisses (Sone and Metcalfe, 2008), with Sibumasu basement thrust slices in the western part of suture zone (Metcalfe, 2013). Sibumasu Terrane (or Shan Thai) composed of Precambrian metamorphic rocks (Tabsila Gneiss) with Paleozoic sedimentary rocks (Bunopas, 1981). The Silurian-Devonian Unit in Kanchanaburi area is situated at the boundary between the Sibumasu Terrane and Inthanon Suture Zone. By using U-Pb zircon dating, Jatupohnkhongchai et al. (2020) revealed that the mapped Silurian--Devonian meta-tuffs were emplaced in the late Cambrian-early Ordovician (ca. 498-482 Ma). As a result of their age and the lack of reported Cambro-Ordovician rocks in the Inthanon Suture Zone, these meta-tuffs belong in the Sibumasu basement.

The study area (Fig. 1) is located in Muang District, Kanchanaburi Province, and was mapped between 1968 to 1971 by the German Geological Mission in cooperation with the Department of Mineral Resources of Thailand. The following are the five periods that the study area can be divided according to its age into: 1) Cambrian Chao Nen Formation which consist of biotite-muscovite-quartz schistose hornfels, quartzo-biotite schistose hornfels, quartzo-feldsparthic-biotite -muscovite schistose hornfels, calc-silicate hornfels, quartz schist, quartzite (Nanorn, 2016); 2) Ordovician Tha Manao Limestone Formation which consists of metalimestone, slate, marble, feldspathic quartzite, calc-silicate, hornfel, tremolite marble hornfels (Nanorn, 2016; Panjamart, 2016); 3) Silurian-Devonian Bo Phloi formation which consists of feldspathic quartzite, meta argillaceous sandstone, and shale (Jatupohnkhongchai, 2018); 4) Triassic S-type granite (Nanorn, 2016); and 5) Quaternary old alluvial fan, colluvial, old and recent flood plain.

3. Methodology

Representative rock samples were collected during field observation for petrographic and geochemical analyses. The petrographic studies have been carried out at the Geoscience Program Mahidol University, Kanchanaburi Campus and Department of Geological Sciences, Faculty of Science, Chiang Mai University. The bulk geochemical analysis was determined using Bruker Pioneer S4 X-ray fluorescence (XRF) spectrometer for major elements at the NAWI Graz Geocenter--Institute of Earth Sciences (Petrology and Geochemistry), University of Graz, Austria. Samples were prepared to a glass bead using one gram of sample powder and seven grams of $Li_2B_4O_7$ flux. Loss on ignition (LOI) was determined by heating the powdered rock material to 1030 °C for one hour. A selected subset of five samples were analyzed for trace and rare earth elements by an Agilent 7700 quadrupole inductively mass spectrometer (ICP-MS) at the Institute of Chemistry--Analytical Chemistry, University of Graz, Austria. Sample powders (40-50 mg) were dissolved at the cleanroom facility of the NAWI Graz Geocenter.

For U-Pb zircon age dating, sample CHK11A and sample CHK27 were selected. A plastic gold pan was used to separate the heavy minerals from the light minerals after crushing and sieving about 1-2 kg of each sample. In the divided heavy minerals, zircons are maintained. The zircon grains were then hand-picked under a binocular microscope and mounted in epoxy resin. The zircon mount was polished until the

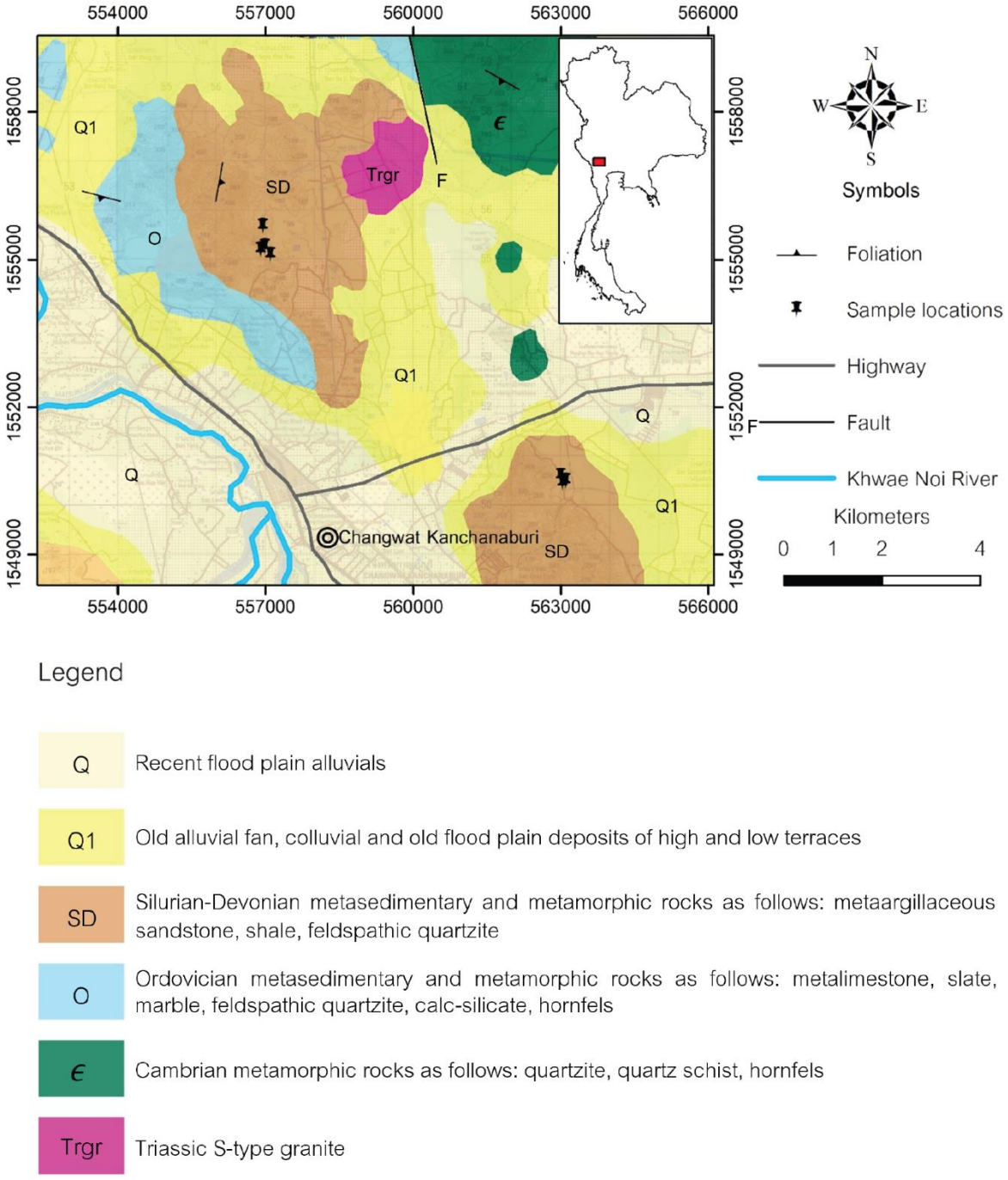

Fig. 1: Geological map of the study area and sample locations. (modified after Bunopas, 1976).

core of most of the grains was exposed. Zircon U-Pb isotopic analyses were measured using laser ablation-multi collector-inductively coupled plasma-mass spectrometryt (LA-MC--ICP-MS) at the Graz University of Technology cooperation within NAWI Graz Geocenter. The TuffZirc algorithm in the Isoplot program (Ludwig, 2008) was devised to reduce the possible effect of xenocrysts and Pb-loss in tuff zircon, and the results are displayed in Fig. 4.

4. Results

4.1 Field observation and petrography

The meta-tuffs were carefully collected from outcrops and float rocks along slope toe at Mueang District, Kanchanaburi Province. Field observation shows their outcrops are trending NW-SE direction. The elongated outcrop is around 15-20 meters high and extend more than 10 kilometers (Fig. 2a-c).

The meta-tuffs consist of various fragments which display lineation parallel to foliation (Fig. 2d). Some exposures of the meta-tuffs are weathered and altered to clay minerals and fine-grained white mica, showing a silky sheen to the foliation surface.

Fisher and Schmincke (1984) terminology for volcaniclastic particles is adapted here. Terms of volcaniclastic particles refer to the processes by which the fragments originate. The term pyroclast is commonly used to refer only to volcanic materials ejected from a volcanic vent. Epiclasts are lithic clasts and minerals released by ordinary weathering processes from pre-existing consolidated rocks, and volcanic epiclasts are clasts of older volcanic rocks derived from weathering and erosion. We use term pyroclast for all volcaniclastic particles, including volcanic epiclast, and use term epiclast for nonvolcanic particles. It is difficult to distinguish each type of clasts of the Cambrian-Ordovician tuff that have already metamorphosed and deformed.

The hand specimens are commonly greyish-white and consist of crystals and lithic fragments. They can be named as a meta-quartz-K-feldspar crystal tuff and meta-lithic tuff, showing pyroclastic texture (Fig. 3). They are made up mainly of pyroclasts and mixed with epiclasts embedded in a very fine--grained matrix. The meta-quartz-K-feldspar crystal tuff consists of pyroclasts (quartz with small amount K-feldspars) (Fig. 3e, f), while the meta-lithic tuff comprises both pyroclasts (volcanic rock, quartz, K-feldspar, devitrified glass) (Fig. 3a, d) and epiclasts (granitic and meta-sedimentary rocks) (Fig. 3b, c). The quartz crystals reacted with the melt and show rounded edges or embayed outlines due to resorption. The matrix shows foliated texture, comprising quartz, feldspar, micas, clay minerals, and sericite.

4.2 U-Pb age results

Zircon grains are primarily colorless, with a few yellow grains, and have well-developed oscillatory zoning. They're prismatic, euhedral

Fig. 2: Outcrop photographs of meta-tuff (a) at Khao Yai (The woman is 155 cm height), (b) close up view of outcrop (a) (Hammer is 35 cm long), (c) at Khao Tong (The woman is 158 cm height). (d) Meta-tuff float rock sample at Khao Yai (Hammer head is 15 cm long).

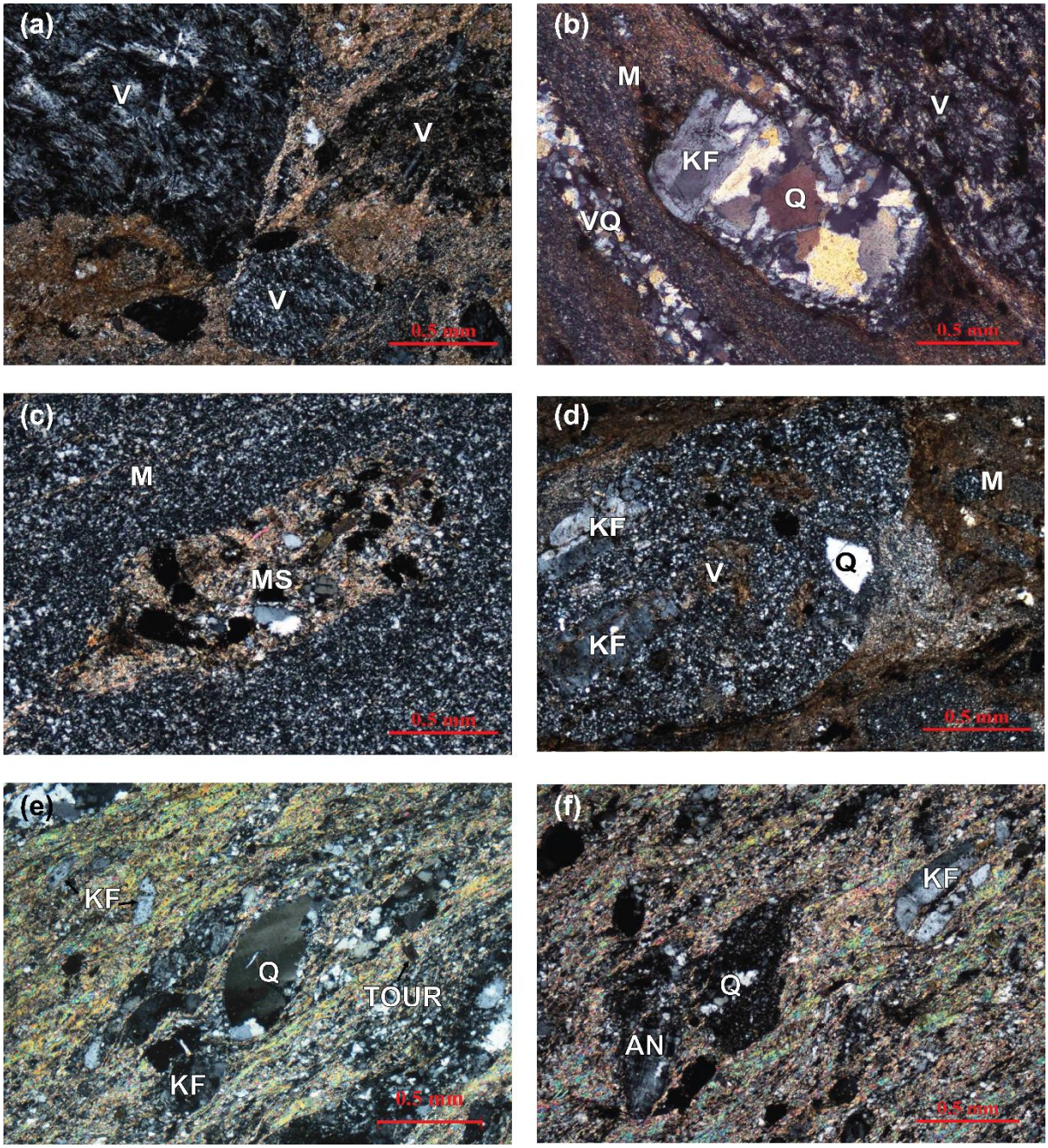

Fig. 3: Photomicrograph of meta-tuffs showing (a) pyroclast of volcanic rock containing plagioclase laths, (b) epiclast of granitic rock comprising K-feldspar and quartz, (c) epiclast of meta-sedimentary rock, (d) pyroclast of volcanic rock comprising K-feldspar and quartz, (e) pyroclasts of quartz and K-feldspar, (f) pyroclasts of quartz, K-feldspar, and anorthoclase. V=volcanic rock, M=matrix, KF=K-feldspar, Q=quartz, MS= meta-sedimentary rocks, AN=anorthoclase, Q= quartz, VQ=vein quartz, TOUR=tourmaline.

to subhedral, and come in the form of elongated grains. Based on 17 and 21 zircon grains, the Tuffzirc ages for the meta-lithic tuffs in the mapped Silurian--Devonian unit, Bo Phloi Formation are 498.4+2.40/-3.0 Ma and 482.7+3.6/-1.0 Ma, respectively (Fig. 4 and Table 1).

4.3 Major and trace elements

The geochemical data of the meta-tuffs are presented in Table 2. The whole-rock composition shows enrichments in SiO_2 and K_2O and a strong depletion in CaO and Na_2O which is related to alteration and low-grade metamorphism. They can be classified as trachyandesite,

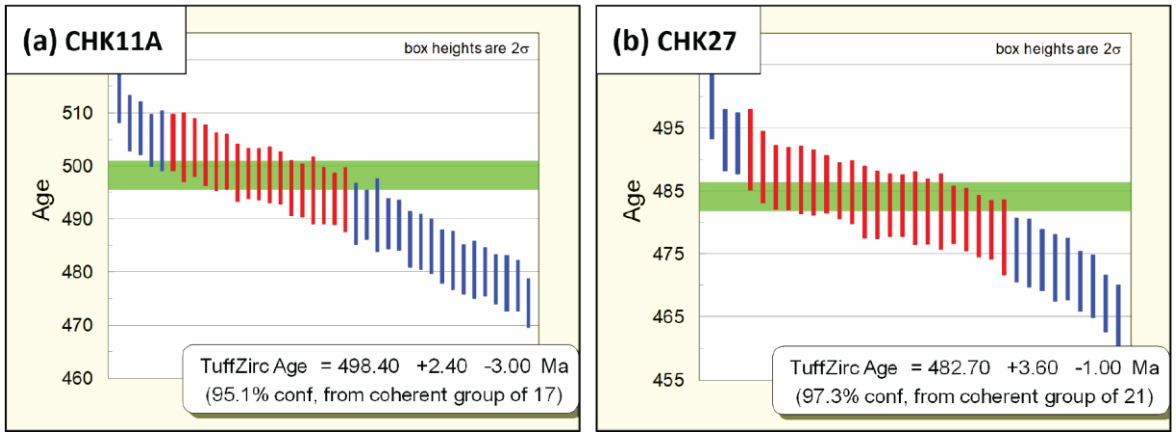

Fig. 4: TuffZirc Age calculation for meta-lithic tuffs a) CHK11A and b) CHK27. (After Jatupohnkhongchai et al., 2020).

Table 1: Summary of zircon U-Pb ages for meta-tuffs formerly assigned as Silurian-Devonian.

Formation: Bo Phloi Formation Formerly inferred age: Silurian-Devonian Sample	CHK11A (Group 2)	CHK27 (Group 1)
Zircon U-Pb data		
Number of all data (n)	39	33
Number of coherent data (n)	17	21
TuffZirc Age (Ma)	498.4+2.40/-3.0	482.7+3.6/-1.0

dacite and rhyolite in Zr/Ti-Nb/Y diagram (Fig. 5) (Pearce, 1996) which belong to the alkaline and calc-alkaline series. Chondrite--normalized REE patterns of these rocks display light REE enrichment with nearly flat heavy REE with the negative Eu anomalies, typical for calc--alkaline volcanic rocks (Fig. 6). Moreover, the REE patterns also show slightly to strongly negative Ce anomalies. The meta-tuffs obviously show negative Nb-Ta anomalies in their primitive mantle-normalized spider diagrams, which indicate magmatic arc signature (Fig. 7). Most samples fall in the volcanic arc granites field in the granite discrimination diagrams (Fig. 8) (Pearce, 1984). The Th-Hf-Ta, Th-Zr-Nb, and Th-Hf-Zr discrimination diagrams likewise show that all of the meta-tuffs fall in the calc-alkaline basalt field (Fig. 9) (Wood, 1980).

5. Discussion and Conclusion

Petrographically, the meta-tuffs from Kanchanaburi can be named as a meta-quartz--K-feldspar crystal tuff and meta- lithic tuff. They are made up of pyroclasts (volcanic rock, quartz, K-feldspar, devitrified glass) and epiclasts (granitic and meta-sedimentary rocks) embedded in a very fine-grained matrix. The matrix shows foliated texture and comprises quartz, feldspar, clay minerals, micas, and sericite, that is probably reflecting the influence of low-grade metamorphism. Geochemically**,** the meta-tuffs can divide into two groups. Group 1 rocks can be classified as dacite-rhyolite which belong to calc-alkaline series. Group 2 rocks are considered to be transitional rocks because there is a contrast between the classification diagram and REE pattern indicating alkaline rocks and calc--alkaline rocks, respectively. The discri-mination diagram for basalts and silicic lavas also indicates that both groups are calc-alkaline affinity. The REE patterns of group 1 and 2 rocks display negative Eu anomalies that may denote the removal of plagioclase from a felsic melt by crystal fractionation or the partial melting of rock in which plagioclase is retained

Table 2. Major oxide and trace element compositions of the meta-tuffs.

Sample Number	CHK07	CHK07I2	CHK09A	CHK11A	CHK27	CHK28	CHK30
Group	1	1	1	2	1	2	1
Lithology	mQKT	mLT	mLT	mLT	mLT	mLT	mLT
Major oxide (wt%)							
SiO_2	70.51	81.76	82.24	64.00	61.54	79.84	84.19
TiO_2	0.22	0.06	0.08	0.56	0.54	0.28	0.10
Al_2O_3	15.40	9.14	7.24	17.67	18.10	9.88	7.68
FeOt	3.37	1.11	0.77	4.93	6.71	1.94	1.92
MnO	0.00	0.00	0.00	0.01	0.00	0.00	0.00
MgO	0.92	0.13	0.10	0.66	0.91	0.34	0.07
CaO	b.d.l.	b.d.l.	b.d.l.	b.d.l.	0.06	b.d.l.	b.d.l.
K_2O	6.85	6.51	5.63	9.59	8.83	6.12	5.90
Na_2O	b.d.l.	b.d.l.	b.d.l.	b.d.l.	b.d.l.	b.d.l.	b.d.l.
P_2O_5	0.03	0.02	0.01	0.05	0.08	0.03	0.01
LOI	2.14	0.52	0.45	1.72	2.18	0.99	0.34
Total	99.46	99.25	96.53	99.20	98.96	99.42	100.22
Trace (ppm)							
Ni	15.40	2.58	1.50	11.20	12.60	5.48	2.94
Rb	225	115	98	309	272	145	104
Sr	43	140	71	44	55	54	27
Y	32.20	35.80	14.20	19.90	34.30	11.10	22.60
Zr	207	60	52	273	286	150	67
Nb	14.40	11.60	7.28	19.80	20.70	11	10.10
Sn	4.36	4.17	2.17	3.53	3.98	2.35	3.32
Ba	379	2253	852	486	546	356	122
La	33.90	28.40	13.70	27.40	47.70	12.20	11.40
Ce	53.50	53.20	17.90	27.90	88.10	24.50	19.80
Nd	22.60	27.80	9.02	17.80	41.20	7.07	10.40
Sm	3.95	5.81	2.11	3.63	7.41	1.53	2.61
Eu	0.76	1.51	0.47	0.81	1.71	0.31	0.47
Gd	4.25	5.48	2.06	3.50	6.94	1.56	2.77
Tb	0.66	0.86	0.33	0.54	1.01	0.25	0.50
Dy	3.68	4.57	1.87	2.83	5.10	1.44	2.95
Ho	0.76	0.88	0.35	0.55	0.97	0.28	0.59
Er	2.32	2.59	1.13	1.80	2.95	0.97	1.85
Tm	0.33	0.38	0.19	0.29	0.45	0.18	0.29
Yb	1.93	2.37	1.20	1.95	3.08	1.24	1.88
Lu	0.26	0.34	0.16	0.28	0.51	0.18	0.26
Hf	5.84	2.13	1.70	6.12	6.27	3.29	2.21
Ta	1.40	1.21	0.82	1.52	1.59	0.84	1.07
Pb	6.30	4.98	6.07	6.95	5.73	6.21	7.71
Th	8.91	22.20	14.50	12.40	16.70	6.43	9.63
U	1.15	0.70	1.30	2.70	3.08	1.35	0.62
La_N/Sm_N	0.99	1.71	1.34	1.47	1.76	1.12	0.80
Sm_N/Yb_N	0.12	0.18	0.06	0.08	0.17	0.04	0.08
Eu/Eu*	0.26	0.26	0.24	0.24	0.25	0.23	0.25
Nb/Y	0.45	0.32	0.51	1.00	0.60	0.99	0.45
Zr/Ti	0.09	0.10	0.07	0.05	0.05	0.05	0.07

Explanation of abbreviations: mQKT=meta-quartz-K-feldspar crystal tuff; mLT=meta-lithic tuff; FeOt=FeO+Fe_2O_3; b.d.l.=below detection limit.

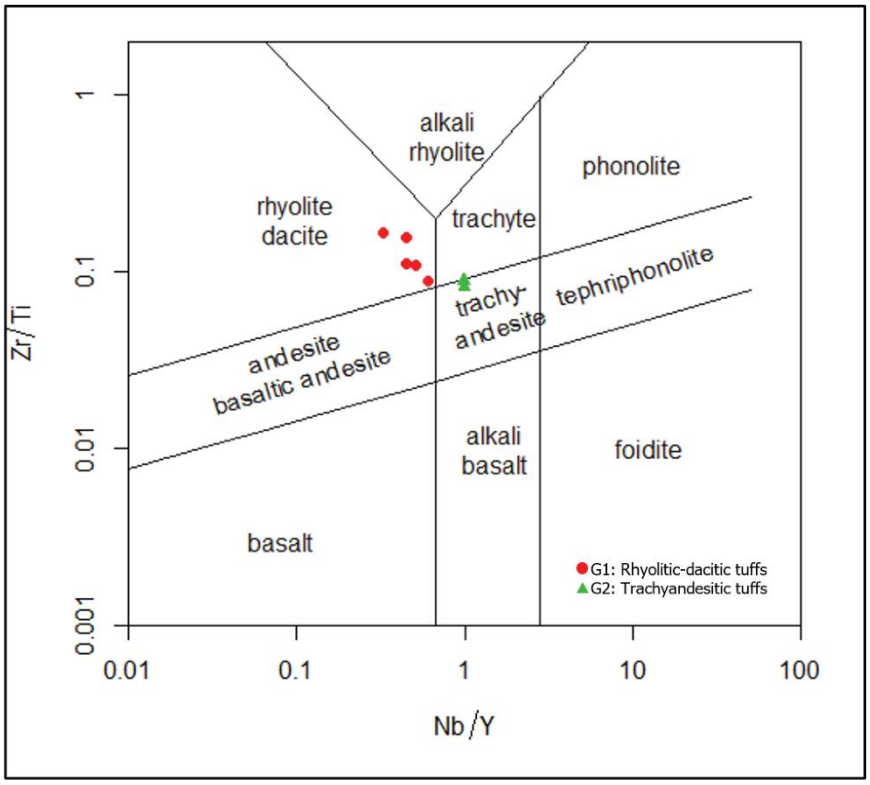

Fig. 5: The Nb/Y vs. Zr/Ti diagram for meta-tuffs (Pearce, 1996; Janoušek, 2006).

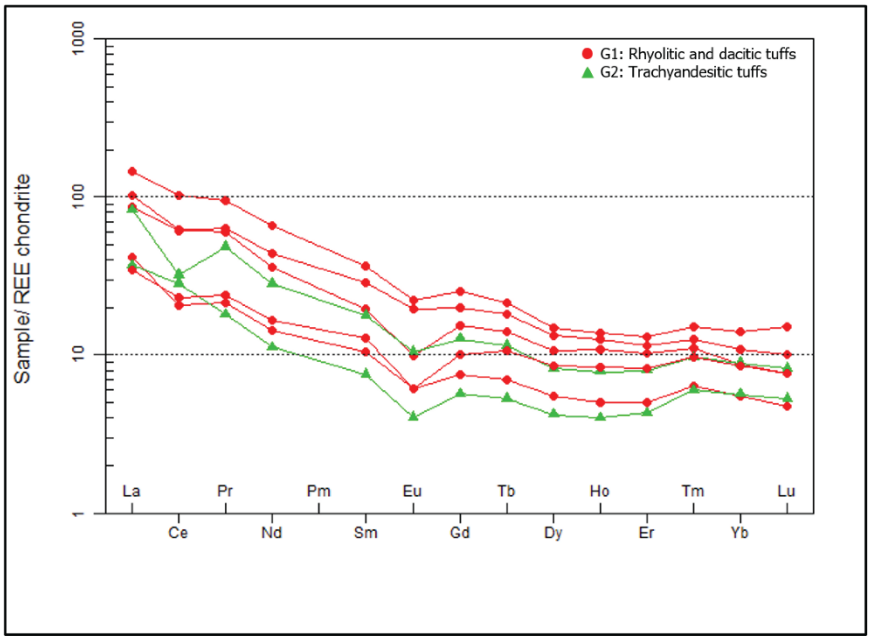

Fig. 6: Chondrite-normalized REE diagram for meta-tuffs (Nakamura, 1974; Janoušek, 2006).

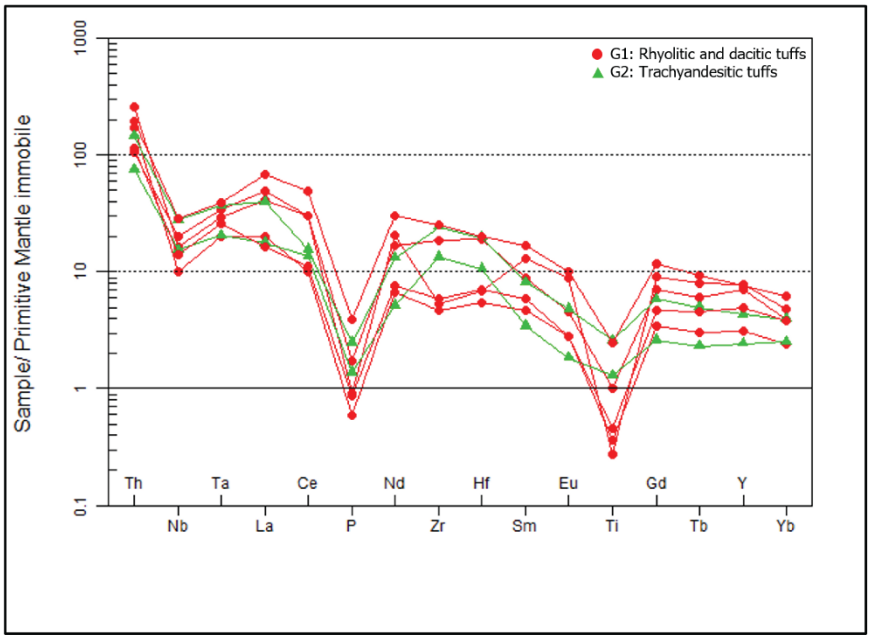

Fig. 7: Primitive mantle-normalized spider diagrams for meta-tuffs (Sun and McDonough, 1989; Janoušek, 2006).

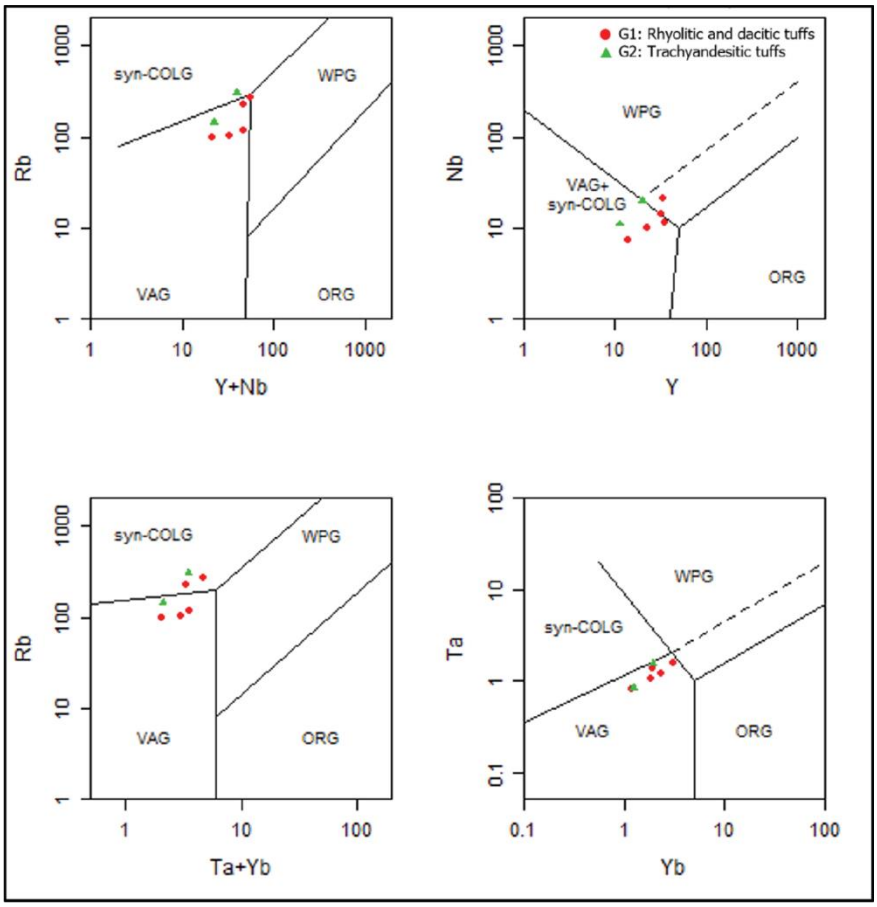

Fig. 8: The Rb-Y-Nb and Rb-Yb-Ta tectonic discrimination diagrams for granites (Pearce et al., 1984; Janoušek, 2006). VAG=volcanic arc granites, WPG=within-plate granites, syn-COLG=syn-collisional granites, ORG=oceanic-ridge granites.

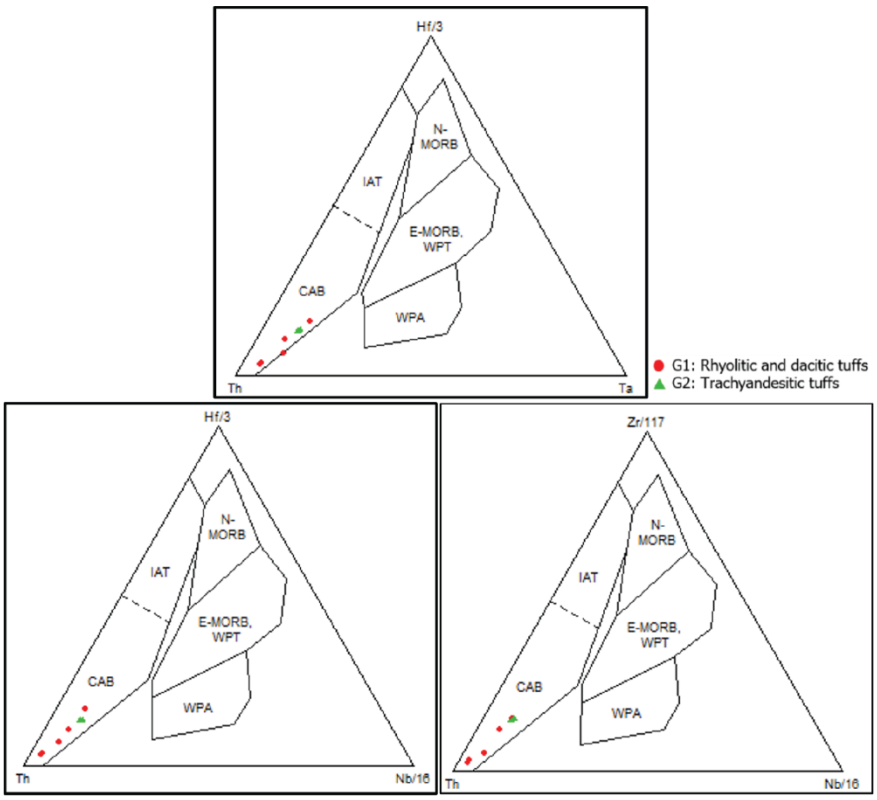

Fig. 9: The Th-Hf-Ta, Th-Zr-Nb, Th-Hf-Nb discrimination diagram for basalts and silicic lavas (Wood, 1980; Janoušek, 2006). WPT=within-plate tholeiites, WPA=within-plate alkaline basalts, CAB=calc-alkaline basalts (Hf/Th < 3), IAT=island-arc tholeiites or primitive arc tholeiites (Hf/Th > 3).

in the source (Weill and Drake, 1973; Drake and Weill, 1975). The negative Ce anomalies possibly indicate a subducted slab of sediment migrated into the mantle wedge source region of the arc because Ce^{3+} is generally fractionated from other REEs to Ce^{4+} under oxidizing conditions in near-surface environments (Class and Roex, 2008).

In the Sibumasu Terrane, Thailand, Cambrian-Ordovician magmatism is rarely found. The zircon U-Pb dating of Kao Tao gneiss in Hua Hin area (Lin *et al*., 2013) and Khao Dat Fa granite in Khanom area (Kawakami *et al*., 2014) yields ages of 501± 7 Ma and 477±7 Ma, respectively. According to our U-Pb zircon dating, the meta-tuffs are 498.4+2.40/-3.0 Ma and 482.7+3.6/-1.0 Ma. These meta-tuffs (ca. 498-482 Ma) support the Cambrian Kao Tao gneiss and Ordovician Khao Dat Fa granite, which related to the closure of a Proto-Tethys (Lin *et al*., 2013). These meta-tuffs mark the most significant magmatic event in that period and represented the Sibumasu basement.

Therefore, the synthesis of all data suggests that group 1 and 2 rocks were emplaced in a volcanic arc environment possibly related to the closure of a Proto-Tethys ocean along the margin of Gondwana in the late Cambrian to early Ordovician (Fig. 10), extending from Turkey, Iran, Tibetan Plateau, Tengchong, Baoshan, Western Thailand (Ustaomer et al., 2009; Ramezani & Tucker, 2003; Cawood et al., 2007; Zhao et al., 2017; Zhang *et al*., 2019; Wang et al., 2012; Wang *et al*., 2013; Lin et al., 2013; Kawakami et al., 2014; Zhu et al., 2012; Hu et al., 2013; Ding et al., 2015).

Acknowledgements

The first authors thank Geoscience Program Mahidol University, Kanchanaburi Campus and Department of Geological Sciences, Faculty of Science, Chiang Mai University for supporting the petrographic study. Professor Dr. Christoph Hauzenberger, Heads of the NAWI Graz Geocenter, University of Graz, has kindly given valuable advice about geochemical analysis throughout the work.

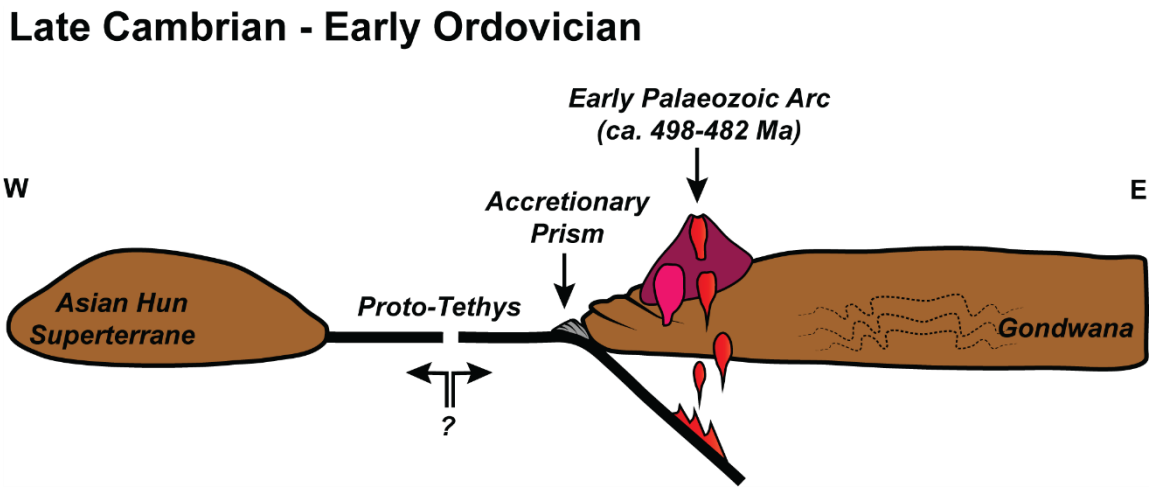

Fig. 10: Cartoon showing the tectonic evolution of western margin of Gondwana from the late Cambrian-early Ordovician.

Moreover, thanks to the Development and Promotion of Science and Technology Talents Scholarship (DPST) for funding this project.

References

Barr, S. M., & Macdonald, A. S. (1991). Toward a late Palaeozoic-early Mesozoic tectonic model for Thailand. *Journal Thai Geoscience*, 1, 11 – 22.

Barr, S. M., & Charusiri, P., (2011). Volcanic rocks. In: Ridd, M. F., Barber, A. J., & Crow, M. J. (Eds.), *The Geology of Thailand* (pp. 415-439). Geological Society of London.

Bunopas, S., (1976). Geologic map of Changwat Suphanburi, Sheet ND 47-7. Geologic map of Thailand, Series 1:250,000. Department of Mineral Resources, Bangkok.

Bunopas, S., (1980). *Geological Survey Report No 2, Sheet Suphan Buri (ND 47-7), Scale 1:250,000.* Department of Mineral Resources, Thailand.

Bunopas, S. (1981). *Paleographic history of western Thailand and adjacent parts of Southeast Asia: A plate tectonics interpretation* (Doctoral dissertation). Victoria University of Wellington, New Zealand.

Bunopas, S., & Bunjitradulya, S. (1975). Geology of Amphoe Bo Phloi north Kanchanaburi with special notes on the Kanchanaburi Series. *Journal of Geological Society of Thailand*, 1, 51-67.

Bunopas, S., & Vella, P. (1978). Late Palaeozoic and Mesozoic structural evolution of northern Thailand, a plate tectonic model. In *Regional conference on geology and mineral resources of Southeast Asia 3*(pp. 133-140).

Cawood, P. A., Johnson, M. R., & Nemchin, A. A. (2007). Early Palaeozoic orogenesis along the Indian margin of Gondwana: Tectonic response to Gondwana assembly. *Earth and Planetary Science Letters*, *255*(1-2), 70-84.

Class, C., & le Roex, A. P. (2008). Ce anomalies in Gough Island lavas—trace element characteristics of a recycled sediment component. *Earth and Planetary Science Letters*, *265*(3-4), 475-486.

Ding, H., Zhang, Z., Dong, X., Yan, R., Lin, Y., & Jiang, H. (2015). Cambrian ultrapotassic rhyolites from the Lhasa terrane, south Tibet: evidence for Andean-type magmatism along the northern active margin of Gondwana. *Gondwana Research*, *27(4)*, 1616-1629.

Drake, M. J., & Weill, D. F. (1975). Partition of Sr, Ba, Ca, Y, Eu^{2+}, Eu^{3+}, and other REE between plagioclase feldspar and magmatic liquid: an experimental study. *Geochimica et Cosmochimica Acta*, *39*(5), 689-712.

Fisher, R.V., & Schmincke, H.U. (1984) *Pyroclastic Rocks.* Springer Berlin Heidelberg, New York.

Hu, P., Li, C., Wang, M., Xie, C., & Wu, Y. (2013). Cambrian volcanism in the Lhasa terrane, southern Tibet: record of an early Paleozoic Andean-type magmatic arc along the Gondwana proto-Tethyan margin. *Journal of Asian Earth Sciences*, *77*, 91-107.

Janoušek, V., Farrow, C. M., & Erban, V. (2006). Interpretation of whole-rock geochemical data in igneous geochemistry: introducing Geochemical Data Toolkit (GCDkit). *Journal of Petrology*, *47*(6), 1255-1259.

Jatupohnkhongchai, S. (2018). *The discovery of ignimbrite and associates in Western Shan-Thai, Kanchanaburi* (Unpublished undergraduate thesis). Mahidol University, Kanchanaburi campus, Thailand [In Thai].

Jatupohnkhongchai, S., Salyapongse, S., Phajuy, B., Gallhofer, D., & Hauzenberger, C. (2020). Pyroclastic rocks from Kanchanaburi and Uthai Thani

Province, Inthanon Zone, Western Thailand. In *EGU General Assembly Conference Abstracts* (p. 19604).

Kawakami, T., Nakano, N., Higashino, F., Hokada, T., Osanai, Y., Yuhara, M., Charusiri, P., Kamikubo, H., Yonemura, K., & Hirata, T. (2014). U-Pb zircon and CHIME monazite dating of granitoids and high-grade metamorphic rocks from the Eastern and Peninsular Thailand—A new report of Early Paleozoic granite. *Lithos*, *200*, 64-79.

Lin, Y. L., Yeh, M. W., Lee, T. Y., Chung, S. L., Iizuka, Y., & Charusiri, P. (2013). First evidence of the Cambrian basement in Upper Peninsula of Thailand and its implication for crustal and tectonic evolution of the Sibumasu terrane. *Gondwana Research*, *24*(3-4), 1031-1037.

Ludwig, K. R. (2008). *Manual for isoplot 3.7*. Berkeley Geochronology Center Special Publication.

Metcalfe, I. (1984). Stratigraphy, paleontology and paleogeography of the Carboniferous of Southeast Asia. *Mémoires de la Société géologique de France (1924)*, (147), 107-118.

Metcalfe, I. (2013). Gondwana dispersion and Asian accretion: Tectonic and palaeogeographic evolution of eastern Tethys. *Journal of Asian Earth Sciences*, *66*, 1-33.

Nanorn, S. (2016). *Increasing grades of metamorphism due to the intrusion of S-type granite pluton in Khao Tham (Khun Krai) and adjacent areas, Maung district, Kanchanaburi province* (Unpublished undergraduate thesis). Mahidol University, Kanchanaburi campus, Thailand.

Panjamart, H. (2016). *A Study on Structural Geology in Khao Noen Prang, Khao Hua Lan, KhaoPhu Rang and Khao Phra Tumbon Kaeng Sian, Amphoe Muang, Changwat Kanchanburi* (Unpublished undergraduate thesis). Mahidol University, Kanchanaburi campus, Thailand.

Pearce, J. A. (1996). A user's guide to basalt discrimination diagrams. *Trace element geochemistry of volcanic rocks: applications for massive sulphide exploration. Geological Association of Canada, Short Course Notes*, *12*(79), 113.

Pearce, J. A., Harris, N. B., & Tindle, A. G. (1984). Trace element discrimination diagrams for the tectonic interpretation of granitic rocks. *Journal of petrology*, *25*(4), 956-983.

Ramezani, J., & Tucker, R. D. (2003). The Saghand region, central Iran: U-Pb geochronology, petrogenesis and implications for Gondwana tectonics. *American journal of science*, *303(7)*, 622-665.

Sone, M., & Metcalfe, I. (2008). Parallel Tethyan sutures in mainland Southeast Asia: new insights for Palaeo-Tethys closure and implications for the Indosinian orogeny. *Comptes Rendus Geoscience*, *340*(2-3), 166-179.

Ueno, K. (1999). Closure of the Paleo-Tethys caused by the collision of Indochina and Sibumasu. *Chikyu Monthly*, *21*, 832-839 [in Japanese].

Ustaömer, P. A., Ustaömer, T., Collins, A. S., & Robertson, A. H. (2009). Cadomian (Ediacaran–Cambrian) arc magmatism in the Bitlis Massif, SE Turkey: magmatism along the developing northern margin of Gondwana. *Tectonophysics*, *473*(1-2), 99-112.

Wang, X., Zhang, J., Santosh, M., Liu, J., Yan, S., & Guo, L. (2012). Andean-type orogeny in the Himalayas of south Tibet: Implications for early Paleozoic tectonics along the Indian margin of Gondwana. *Lithos*, *154*, 248-262.

Wang, Y., Xing, X., Cawood, P. A., Lai, S., Xia, X., Fan, W., Liu, H., & Zhang, F. (2013). Petrogenesis of early Paleozoic peraluminous granite in the Sibumasu Block of SW Yunnan and diachronous accretionary orogenesis along the northern margin of Gondwana. *Lithos*, *182*, 67-85.

Weill, D. F., & Drake, M. J. (1973). Europium anomaly in plagioclase feldspar: experimental results and semiquantitative model. *Science*, *180*(4090), 1059-1060.

Wood, D. A. (1980). The application of a ThHfTa diagram to problems of tectonomagmatic classification and to establishing the nature of crustal contamination of basaltic lavas of the British Tertiary Volcanic Province. *Earth and planetary science letters*, *50*(1), 11-30.

Zhang, L. K., Li, G. M., Santosh, M., Cao, H. W., Dong, S. L., Zhang, Z., Fu, J. G., Xia, X. B., Huang, Y., Liang, W., & Zhang, S. T. (2019). Cambrian magmatism in the Tethys Himalaya and implications for the evolution of the Proto-Tethys along the northern Gondwana margin: A case study and overview. *Geological Journal*, *54*(4), 2545-2565.

Zhao, T., Feng, Q., Metcalfe, I., Milan, L. A., Liu, G., & Zhang, Z. (2017). Detrital zircon U-Pb-Hf isotopes and provenance of Late Neoproterozoic and Early Paleozoic sediments of the Simao and Baoshan blocks, SW China: Implications for Proto-Tethys and Paleo-Tethys evolution and Gondwana reconstruction. *Gondwana Research*, *51*, 193-208.

Zhu, D. C., Zhao, Z. D., Niu, Y., Dilek, Y., Wang, Q., Ji, W. H., Dong, G. C., Sui, Q. L., Liu, Y. S., Yuan, H. L., & Mo, X. X. (2012). Cambrian bimodal volcanism in the Lhasa Terrane, southern Tibet: record of an early Paleozoic Andean-type magmatic arc in the Australian proto-Tethyan margin. *Chemical Geology*, *328*, 290-30.

Thai Geoscience Journal 3(3), 2022, p. 32-50

ISSN-2730-2695; DOI-10.14456/tgj.2022.4

Late Triassic freshwater conchostracan, ostracods, and stromatolites from Huai Hin Lat Formation, northeastern Thailand.

Anisong Chitnarin[a*], Stephen Kershaw[b], Anucha Promduang[a], Prachya Tepnarong[a]

[a] *Geological Engineering Program, School of Geotechnology, Institute of Engineering, Suranaree University of Technology, 111 University Avenue, Suranaree subdistrict, Mueang, Nakhon Ratchasima 30000, Thailand*
[b] *Department of Life Sciences, Brunel University London, UB8 3PH, UK; and Earth Sciences Department, The Natural History Museum, Cromwell Road, London, SW7 5BD, UK*
**Corresponding author, email: anisong@sut.ac.th*
Received 15 August 2021; Accepted 2 December 2021.

Abstract

Although ostracods are well-known in marine environments, their study in non-marine facies is less understood. In the Khorat Plateau region of northeast Thailand, a well-exposed example of fluvial-lacustrine facies in the Dat Fa Member of the Huai Hin Lat Formation (Norian, Late Triassic), contains abundant ostracods that in the oldest known non-marine sedimentary sequence in Thailand. *Euestheria buravasi*, the Late Triassic index fossil is recovered for the first time at the studied section. Associated with the ostracods is a restricted non-marine stromatolite, together with non-marine clastic sediments. A combined study of ostracod faunas and sedimentary characters herein provides more detail of the nature of the environments of the Huai Hin Lat Formation. The ostracods are from the superfamily Darwinulidae, thus are a low diversity assemblage of exclusively non-marine forms that confirms the freshwater nature of the beds. The stromatolite layer consists of some stromatolite domes of hybrid construction combining laminae with filamentous structure (suspected to be cyanobacteria) together with probable inorganic layers of fine-grained carbonate. The stromatolite represents an episode of carbonate-rich waters available in these freshwater facies to create a hybrid stromatolite deposit in this non-marine setting. The sum of facies study in this investigation makes an interpretation of the setting as being very shallow water, in contrast to other studies that proposed the lacustrine setting was deeper.

Keywords: Huai Hin Lat Formation, Khorat Plateau, Late Triassic, Ostracods, stromatolite

1. Introduction

Ostracods are crustaceans with small size (average 1 mm in length) living in (semi) aquatic environments, from lakes, springs, lagoons, shallow shelves to deep oceans. They were entirely marine during the Early Paleozoic (e.g., Salas et al. 2007; Ghobadi Pour et al. 2011), then invaded non-marine environments during the Carboniferous (e.g., Bennett, 2008; Iglikowska, 2014; Williams et al. 2006; Bennett et al. 2012). Marine ostracods were inten-sively affected by the end-Permian mass extinction (i.e., Crasquin & Forel, 2015), yet opportunely, some ostracods survived in a specific condition related to microbialites (i.e., Kershaw et al. 2007; 2012; Forel, 2012; 2015; 2018). In contrast, non-marine ostracods survived and radiated during the Mesozoic and through the Cenozoic (Horne & Marten, 1998; Horne, 2003). In Thailand, marine Permian and Triassic ostracods have been reported from northern, central and northeastern regions (Chitnarin et al. 2008; 2012; 2017; Burrett et al. 2014; Ketmuang-moon et al. 2018). However, the study of fossil non-marine ostracods is uncommon. This study focuses on the occurrence of the oldest known non-marine ostracods in Thailand, as well as a conchostracan found in the same level as the ostracods, and associated sedimentary facies that include a stromatolite deposit (also the oldest non-marine stromatolite in Thailand) found in the Dat Fa Member of the Huai Hin Lat Formation. The aim is to record the occurrence of these fossil arthropods, enhance understanding of their associated facies, and their applications in analysis of the depositional environment of the Huai Hin Lat Formation using a key study section.

2. Geological setting and locality

The Huai Hin Lat Formation is part of the oldest non-marine Mesozoic Erathem on the Khorat Plateau in northeastern Thailand (Fig. 1) which accumulated in half-graben basins as a result of the Indosinian I Orogeny (Bunopas & Kositanon, 2008; Booth & Sattayarak, 2011). Although there is evidence that natural gas in northeastern Thailand reservoirs has a lacustrine source signature (Chinoroje & Cole, 1995; Sattayarak et al. 1989), knowledge of the depositional setting of the Huai Hin Lat Formation is not completely developed (Asairai et al. 2014; 2016; Phujaranchaiwon et al. 2021). Facies of the Huai Hin Lat Formation consist of mainly clastic sedimentary rocks deposited in fluvial-lacustrine environments during the Late Triassic (Chonglakmani & Sattayarak, 1978; Chonglakmani, 2011) and is exposed extensively at the western and rim of the Khorat Plateau (Wongprayoon & Saengsrichan, 2004.; Treerotchananon, 2012; Phujaranchaiwon et al. 2021). Various fossils including vertebrates (Ingavat & Janvier 1981; Buffetaut et al. 1993, Laojumpon et al. 2012; 2013), invertebrates (Hayami, 1968; Kobayashi, 1973; 1975), and floral groups (Endo & Fujiyama, 1966; Kon'no & Asama 1973; Haile, 1973) have been reported. A Late Triassic age is assigned due to presence of Norian plants and palynomorphs (Kon'no & Asama 1973; Haile, 1973) and conchostracans (Kobayashi, 1973; 1975). The equivalent rock formation of the Huai Hin Lat Formation is in the subsurface under the Khorat Plateau, and is recognized as one of petroleum source rocks in northeastern Thailand (Booth, 1998; Racey, 2011). The formation is overlain unconformably by a thick succession of the younger Upper Triassic to Jurassic Nam Phong Formation and the Jurassic-Cretaceous 'Red Beds' of the Khorat Group (Ward & Bunnag, 1964; Sattayarak, 1983; Meesook, 2001; Racey, 2011) (Fig. 2A). The maximum thickness of the Khorat Group as recognized from seismic profiles is approximately 6,000 meters in the center of the Khorat Plateau. Hydrocarbon production is achieved from reservoirs below these rocks (Booth & Sattayarak, 2011; Racey, 2011).

Terrestrial Triassic sedimentary rocks named as Huai Hin Lat formation were primarily recognized by Iwai and Asama (1964) for the lowest succession of the Khorat Group which lies unconformably on the Permian limestone and is overlain by sandstones of the Nam Phong Formation in Loei and the Khon Kaen areas. Later on, Bunopas (1971) erected the Nam Pha Formation for sequences of conglomerate, sandstone and shale in Chiyaphum area further to the south. Lithology and relative age of both formations are similar, thus Chonglakmani & Sattayarak (1978) correlated and compiled these two formations and formally proposed the Huai Hin Lat Formation with details of five members, from bottom to top (Fig. 2).

- The Pho Hai Member: consisting mainly of volcanic rocks including tuff, agglomerate, rhyolite and andesite with intercalations of sandstone and conglomerate (210 meters thick).

- The Sam Khaen Member: consisting mainly of basal conglomerates intercalated with red siltstone, shale, and local limestone beds (100 meters thick).

- The Dat Fa Member: comprised of a thick sequence of gray to black, carbon-rich, calcareous, well bedded shale and numerous argillaceous limestone beds (390 meters thick).

- The Phu Hi Member: consisting of gray sandstone, shale and argillaceous limestone with some conglomerate beds (650-850 meters thick).

- The I Mo Member: consisting of diorite and volcanic clastic rocks intercalated with well-bedded gray shale, sandstone and limestone (300 meters thick), locally exposed.

Among these units, the Dat Fa Member, the lacustrine facies, is emphasized in this study. The Dat Fa Member is characterized by a thick sequence of shale with intercalations of fine-grained sandstone in the lower part and with argillaceous limestone in the upper part (Chonglakmani & Sattayarak, 1978; Wongproyoon & Saengsrichan, 2004.; Treerotchana-non, 2012). The outcrops vary from place to place: the thick sequence of carbonaceous shale is interpreted as

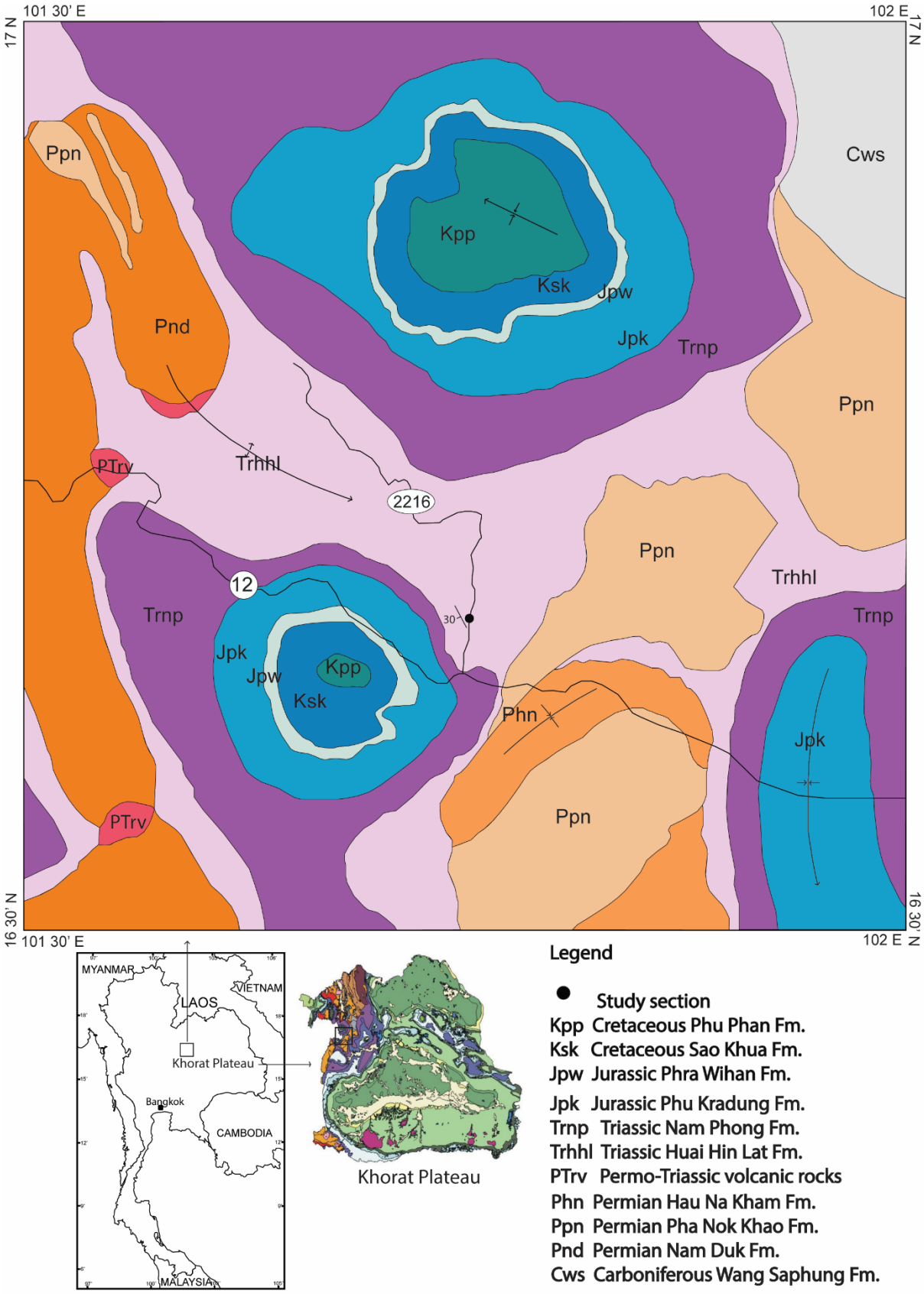

Fig. 1: Geologic map and location of the study section (modified after Chonglakmani & Sattayarak, 1979)

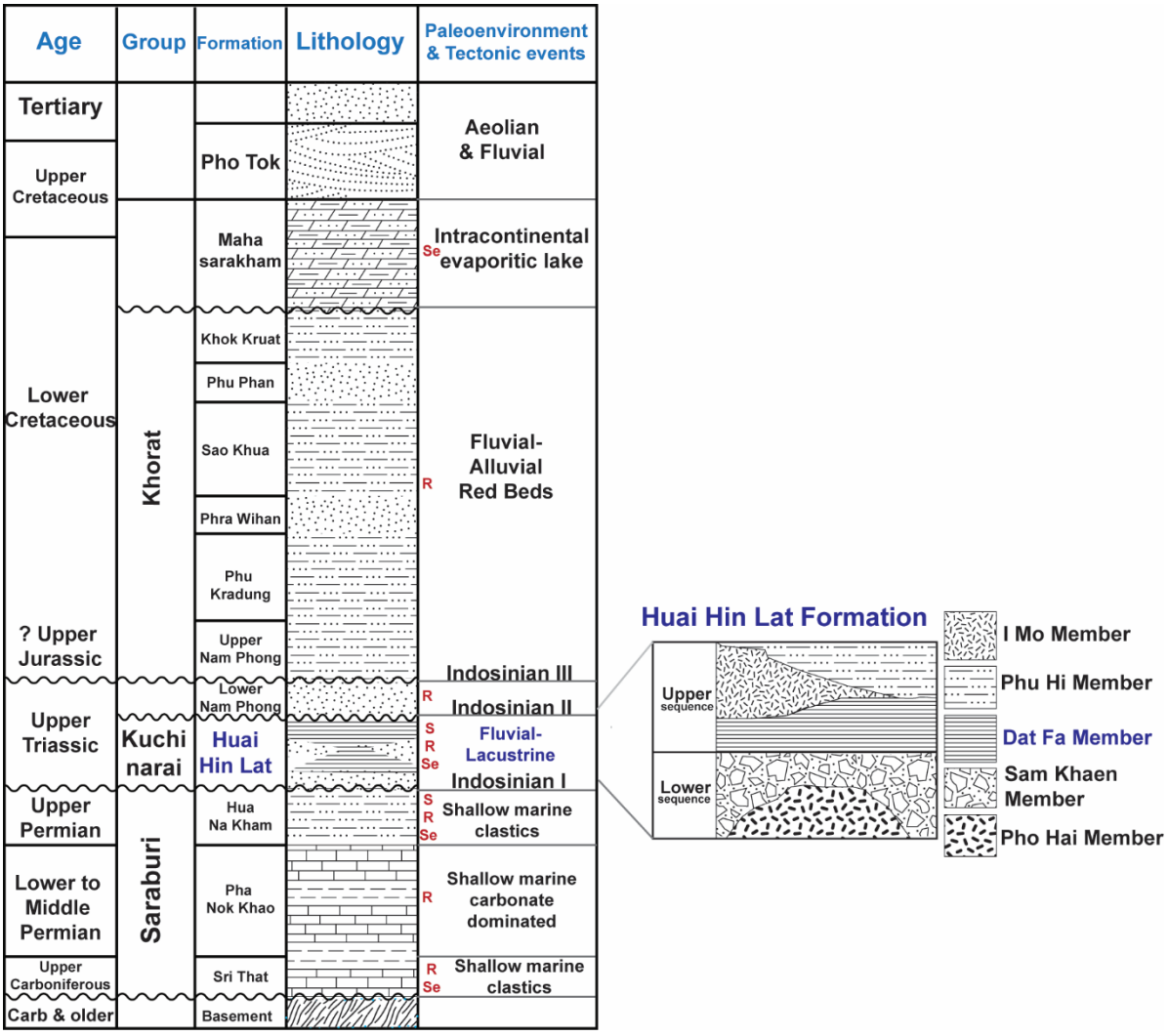

Fig. 2: General lithostratigraphy of northeastern Thailand, modified after Chonglakmani and Sattayarak (1978) and Racey (2011). Letters in red represent the petroleum play: S-source rock; R-reservoir; Se-seal. See text for description.

the middle part of the lake (Phujaranchaiwon et al. 2021), the calcareous siltstone and limestone beds are in the shallower zone; sandstones, siltstones and coals are uncommonly exposed (Asairai et al. 2012; 2016).

The study section is located at 101˚44’30.4”E, 16˚40’59.3”N, at km 2 on highway No.2216, in Nam Noa Subdistrict, Phetchabun Province and belongs to the Dat Fa Member (Figs. 1, 2). The section is approximately 40 meters thick, exposed on both sides of the road, but partly covered by asphaltic pavement. It is composed of well bedded calcareous mudstone in the lower part, intercalations of calcareous mudstone and shale in the middle part, and silty sandstone with coal-bearing strata in the upper part (Fig. 3). The bedding attitude is 30^{o}/240 (dip/dip direction). Fig. 4A shows outcrops of the upper part of the section, Fig. 4B shows the middle part. The lower part of the section exposed on the east side of the road consists of medium-, to thick-bedded, dark grey to black, calcareous mudstone containing abundant ostracods which can be seen on rock surfaces (Fig. 5), and rare stromatolites. During field mapping in 1976-1977, approximately ten stromatolite mounds were found in an argillaceous limestone bed (exposed length of the bed was 2 meters) at this location (Nares Sattayarak, 2020, PTTEP, pers com). They are possibly the oldest freshwater stromatolites known in Thailand, and of the observed stromatolite mounds, samples from two are available. One mound is exhibited at Sirindhorn Museum in

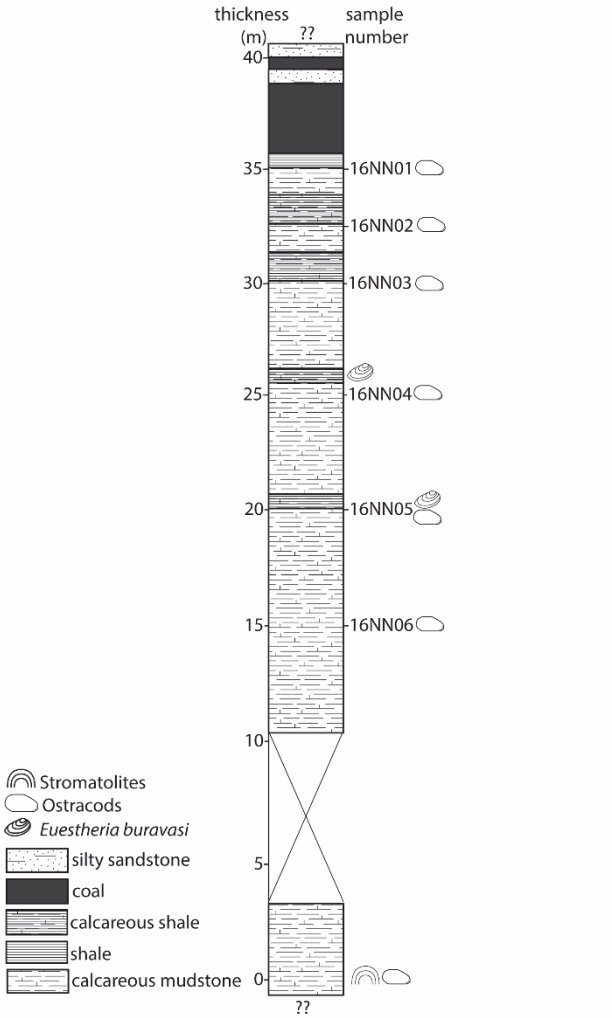

Fig. 3: Lithologic log of the study section, Dat Fa Member, Huai Hin Lat Formation.

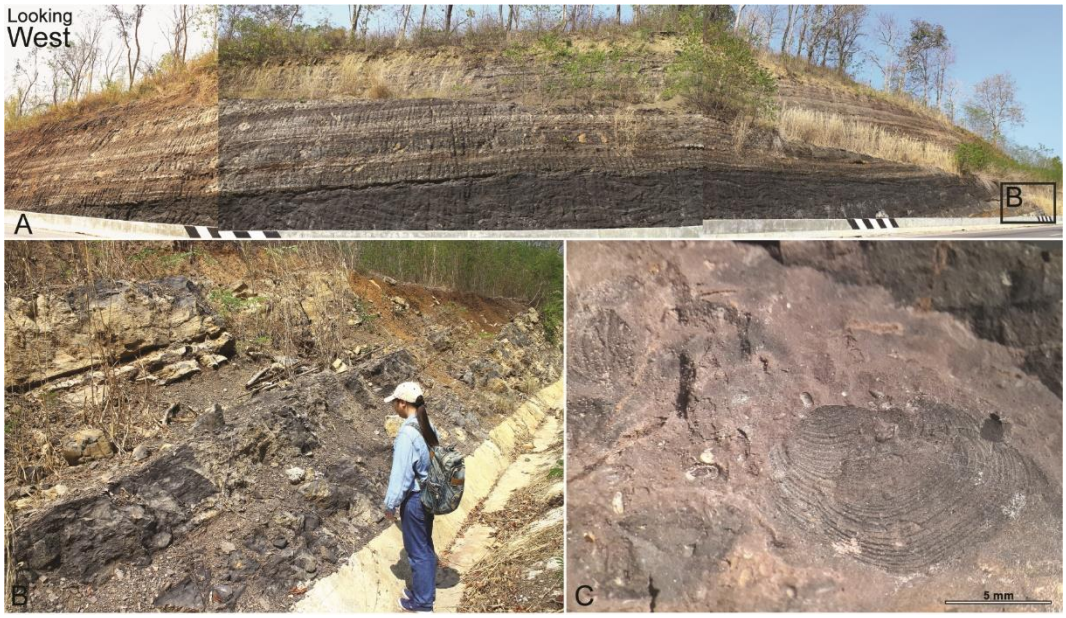

Fig. 4: Field photographs of the study section: A, sandstone and coal beds in the upper part; B, calcareous mudstone and shale in the middle part; C, *Euestheria buravasi* found on calcareous mudstone surface in the middle part (sample No. 16NN04).

Kalasin Province (Fig. 6A), and another is in the collection of Suranaree University of Technology in Nakhon Ratchasima Province (Figs. 6B - C).

3. Methods

Field logging was used to collect samples for sedimentological study, including the microbialite, and palaeontological assessment of the ostracods and the conchostracan. Six calcareous mudstone samples were collected and labelled as NN01-NN06 (Fig. 3); thin sections of sediment and microbial structures are used for analysis. For ostracods, the calcareous mudstone samples were processed by hot acetolysis (Lethiers & Crasquin-Soleau, 1988; Crasquin-Soleau et al. 2005). Few specimens could be freed from the rock matrix due to their low calcareous content. The preservation and density of the ostracods can be seen on these mudstone surfaces as shown in Fig. 5. In general, the ostracod carapaces are well preserved and embedded tightly within the matrix. They are more obvious on the naturally broken or weathered surfaces than on the parting surfaces broken by hammer. There are many ostracods but it is not possible to estimate their abundance. The carapaces are thin,

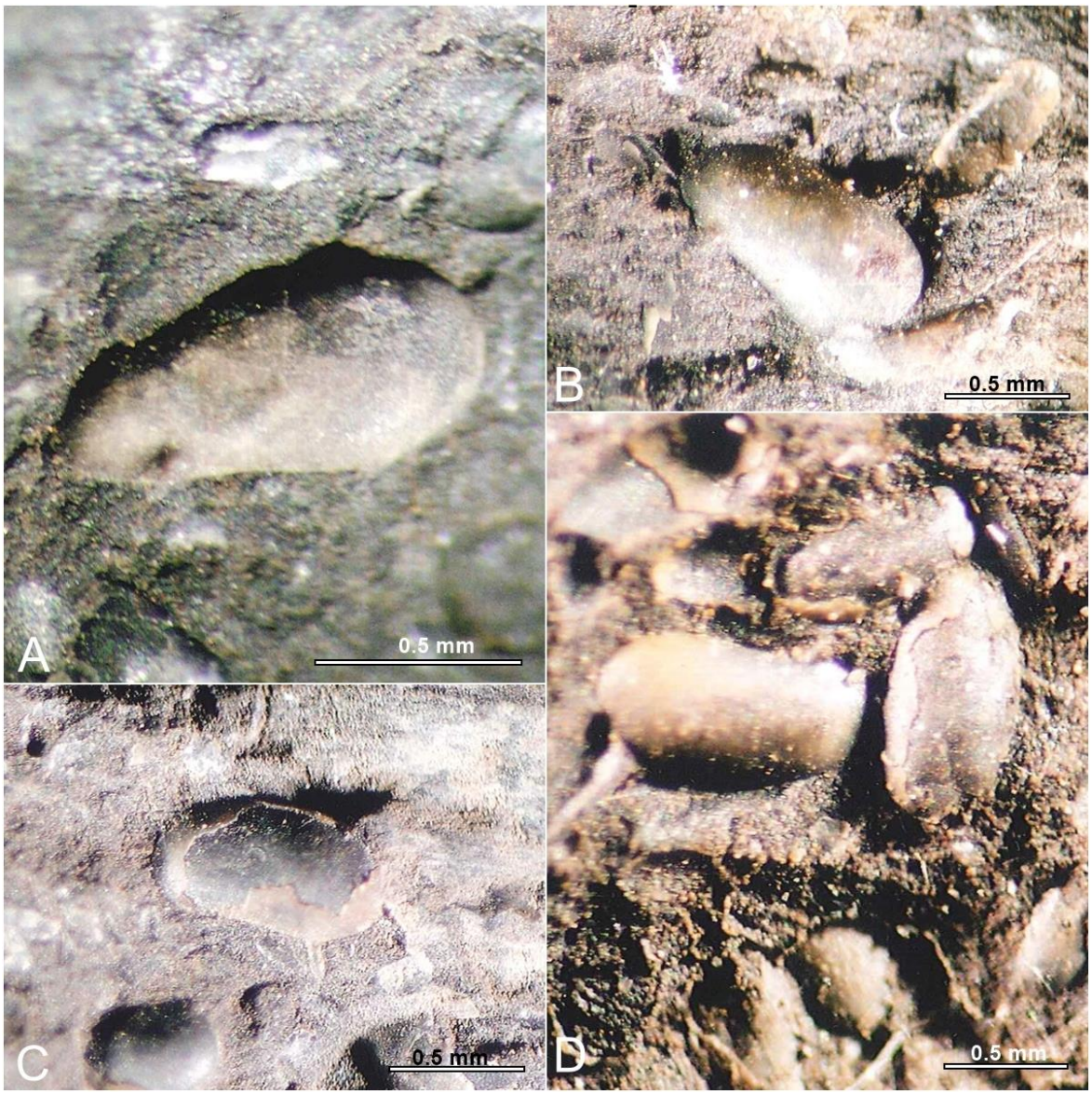

Fig. 5: Steromicrographs of ostracods found in calcareous mudstone in the lower part of the section with associated to stromatolite deposit: A, *Suchonellina* sp.4; B, *Suchonellina* sp.1; C, *Suchonellina* sp.5; C, D, showing rosette pattern of central muscle scars.

delicate and closed, muscle scars are preserved on internal casts (Fig 5 C, D). Ostracod identification is in section 4.3. On the other hand, the conchostracan is rare, occurs as incomplete cast and mold (Fig 4C). Characteristics of the valves are used for identification (section 4.2.1).

4. Methods

4.1 Age of strata

Few specimens of the conchostracan are found in samples NN04 and NN05 (Fig. 3). The fossils are embedded in the calcareous mudstones, they can be observed on naturally weathered surfaces or surfaces parallel to bedding planes (and 4C). The specimens are cast and mold, only the species *Euestheria buravasi* Kobayashi, 1975 can be identified and confirmed (Fig. 4C). *Euestheria buravasi* is important because it demonstrates the freshwater nature of the facies.

In 1973 Kobayashi identified *Euestheria mansuyi* from the basal part of Nam Pha formation at Nam Prom Dam (renamed as Chulabhorn Dam), located about 12 km to the Southwest of the studied section. The *E. mansuyi*-bearing strata were assigned to the Upper Triassic because they are correlated to the

Fig. 6: A stromatolites form the study section: A, stromatolite mound exhibited at Sirindhorn Museum in Kalasin Province; B, unpolished section of the stromatolite mound scrutinized in this study; C, polished section of the studied mound.

lower part of the contemporaneous Huai Hin Lat formation (exposed to the north), and plants collected from the middle part of the Huai Hin Lat formation were dated to Norian age (Kon'no & Asama, 1973). Later in 1975, Kobayashi identified six more species and one new genus (also called the mansuyi faunule by Kobayashi) from the rocks collected at the same locality including *Euestheria thailandica* Kobayashi, 1975; *E. buravasi*, Kobayashi, 1975; *Khoratestheria macroumbo* Kobayashi, 1975; *Cyclestherioides bunopasi* Kobayashi, 1975; *Metahabdosticha*? sp. and *Asmussia symmetrica* Kobayashi, 1975. He also classified these materials as belonging to the Dido Conchostracan Group whose members were dispersed in Japan, Vietnam and Yunnan and confined to the Norian. In 1978, Chonglakmani & Sattayarak compiled the geological map in this area and merged the Nam Pha and the Huai Hin Lat formations to the newly established Huai Hin Lat Formation, thus, the mansuyi faunule can be used as index fossils for the Huai Hin Lat Formation. Since then, fossil conchostracans have been mentioned in reports of geological investigations especially for the Huai Hin Lat Formation, but without taxonomic details.

Kozur & Weems (2010) reviewed the occurrences of the conchostracans in the northern hemisphere including Europe, Asia and America, and established a conchostracan zonation for Late Permian to Early Jurassic time (including 34 biozones in the Triassic). They recorded that *E. buravasi* was found in the United States of America (North Carolina), Germany (Thuringia) and Thailand (Chaiyaphum Province). Kozur & Weems (2010) placed *Euestheria buravasi – Euestheria* n. sp. zone at Middle Lacian Substage (Lower Norian). Weems & Lucas (2015) investigated new localities of the Upper Triassic Systems in North America, then revised and simplified the Upper Triassic conchostracan zonation. The *Shipingia weemsi – Euestheria buravasi* zone was place at the base of the Norian to indicate the whole Lacian Substage in North America. According to the biostratigraphic zonation of conchostracans as mentioned above, the *E. buravasi* and the mansuyi faunule is confined in the Lower Norian (Lacian Substage). The presence of *E. buravasi* in the studied section suggests the Early Norian age and indicates that the section is the base of the Huai Hin Lat Formation (correlated with the formal Nam Pha formation at the Chulabhorn Dam - Kobayashi, 1973).

4.2 Systematic Paleontology

4.2.1 Conchostracan

We follow the systematic classification of Astrop & Hegna (2015) for the higher levels. Method of conchostracan classification of Scholze and Schneider (2015) is followed as much as possible. The description of *Euestheria buravasi* by Kobayashi (1975) is adopted.

Class Branchiopoda Latreille, 1817

Order Spinicaudata Linder, 1945

Superfamily Eosestherioidea Zhang and Chen in Zhang et al., 1976 *sensu* Chen and Shen, 1985

Family Euestheriidae Defretin-Lefranc, 1965

Genus *Euestheria* Depéret & Mazeran, 1912

Type species. *Posidonia minuta* von Zieten, 1833

Euestheria buravasi Kobayashi, 1975
Fig. 4 C

Materials: one incomplete carapace and one incomplete cast.

Remarks: The specimens are incomplete; the carapace is partly embedded in rock matrix and is overlain by another cast. However, carapace shape and concentric ribs are observed. They are identified to *Euestheria buravasi* due to diagonally elongated carapace with submedial umbo. The growth lines and concentric ribs are coarse in the medial region and narrower on the umbonal side. Sizes of both specimens are very large; length of the carapace is approximately 12.5 mm.; length of the cast is approximately 13.3 mm. *E. buravasi* can be differentiated from *E. mansuyi* by having coarser growth lines and concentric ribs, and from *E. thailandica* by more diagonal carapace which causes the diagonal curvature of the growth line and ribs at medial region. Weems

& Lucus (2015) constructed a sketch of complete *E. buravasi* (fig. 3, p. 305) showing the finer growth lines bounded along the carapace rim, though; this feature cannot be observed in our specimens.

4.2.2 Ostracods

The circular outline and pattern of the muscle scars imprinted on internal molds of the ostracods recovered indicate that they belong to Superfamily Darwinulidae (Figs. 5 and 7). The characters observable here are external features of the carapace (shape, size). The shell characters such as marginal inner teeth and keels which are normally used to identify extant materials (Rossetti and Martens, 1998) are not observed. In this study, we classify fossil darwinulocopines following Antonietto et al. (2017; 2018), Liebau (2005) for above family level and Molostovskaya (2000) for lower ranks. The distinct characters of most studied specimens are ovate to sub-rectangular shape with rounded posterior margin which led us to the attribution of the materials to genus *Suchonellina* Spizharsky, 1937 (Antonietto et al. 2017). Thus, five species are recognized: *Suchonellina* sp.1, *Suchonellina* sp.2, *Suchonellina* sp.3, *Suchonellina* sp.4, and *Suchonellina* sp.5 (Fig. 8, A-L). The systematic attributions are discussed as follows.

Abbreviations used in this study: LV, left valve; RV, right valve; DB, dorsal border; ADB, antero-dorsal border; AB, anterior border; AVB, anteroventral border; VB, ventral border; PVB, postero-ventral border; PB, posterior border; PDB, postero-dorsal border; H, height; L, length. The length of specimen is indicated as very small (0.40-0.50 mm), medium (0.51-0.70 mm), large (0.71-0.90 mm) and very large (> 0.90 mm).

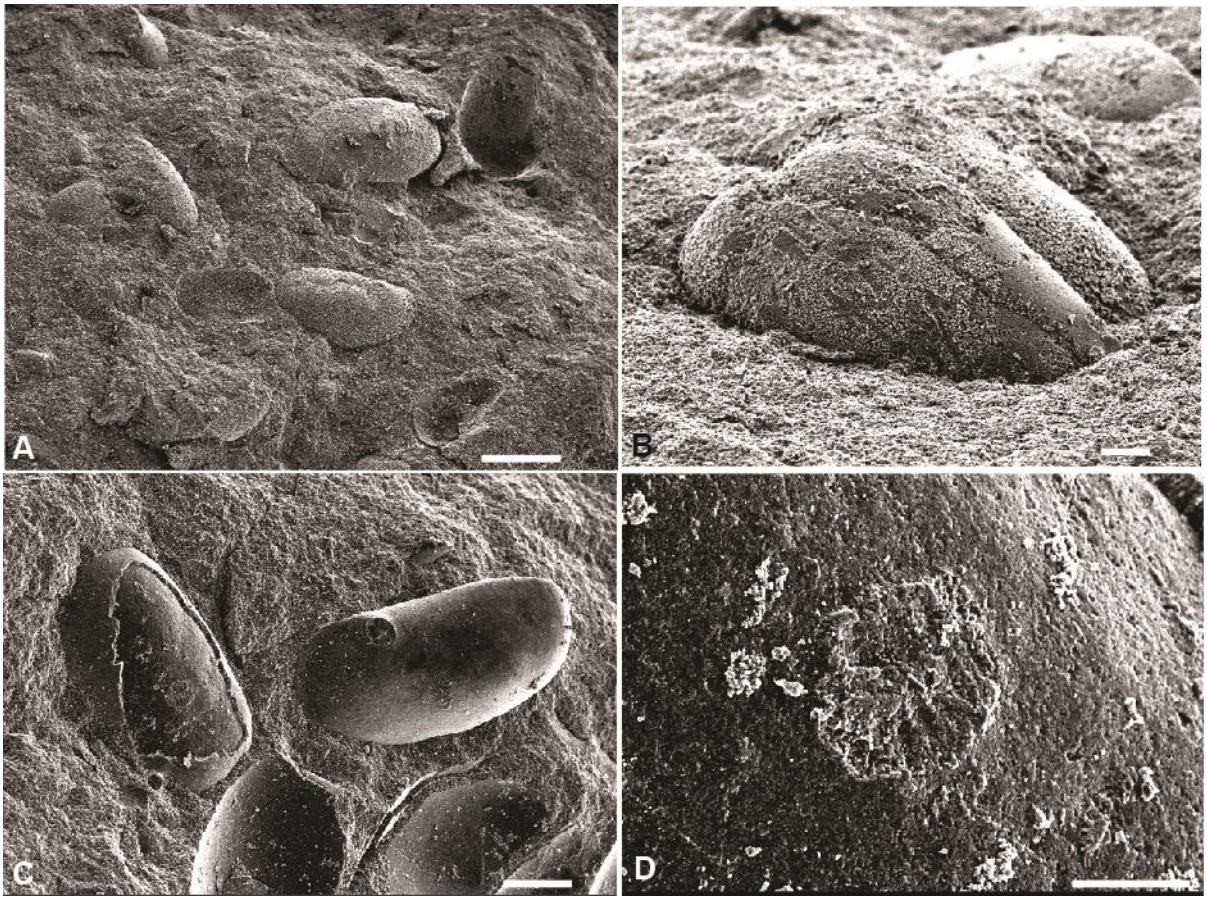

Fig. 7: Pictures from scanning electron microscope showing ostracods embedded in calcareous mudstone in the lower part of the section with associated to stromatolite deposit: A, carapaces and valves partly exposed from the matrix, scale bar = 0.5 mm.; B, carapace partly exposed from the matrix, scale bar = 0.1 mm.; C, carapaces, casts and mold with imprinted central muscle scar, scale bar = 0.2 mm.; D, central muscle scar, scale bar = 0.1 mm.

Class Ostracoda Latreille, 1802

Superorder Podocopomorpha Kozur, 1972

Order Podocopida Sars, 1866

Suborder Darwinulocopina Sohn, 1988

Superfamily Darwinuloidea Brady and Norman, 1889

Family Suchonellinidae Kukhtinov, 1985

Genus *Suchonellina* Spizharsky, 1937

Type species. *Suchonellina inornata* Molostovskaya, 1980

***Suchonellina* sp.1**

Fig. 8, A-D

Materials: more than 12 incomplete carapaces.

Measurement: (figured specimens) H = 0.433-0.727 mm; L = 0.811-1.309 mm; H/L = 0.52-0.57.

Remarks: This species is characterized by its long and sub-rectangular carapace in lateral view. DB is short (25% of L) and straight to slightly convex, ADB is straight and incline at 30°. AB of both valves is rounded with small radius of curvature and maximum convexity is located at 30% of H. VB is long (70% of L) and straight. PVB and PDB are rounded. PB is rounded with large radius of curvature and maximum convexity is located at 50% of H.

Maximum H is located at 50% of L, maximum L is located at 30% of H. Carapace is flattened laterally. The carapace size ranges from large to very large. Surface is smooth. The lateral outline of the carapace looks similar to *Darwinula accuminata* Belousova, 1961 which was described from Wayaobu Formation (Upper Triassic) of Tongchun, Shaanxi (Plate 2, fig. 12 in Xu, 1988).

***Suchonellina* sp.2**

Fig. 8, E-F

Materials: more than 5 incomplete carapaces.

Measurement: (figured specimens) H = 0.400-0.600 mm; L = 0.833-1.183 mm; H/L = 0.48-0.50.

Remarks: This species is characterized by elongated carapace and a rounded PB which maximum of convexity is located above mid of H. DB is longer than 50% of L and straight. ADB is straight and slightly inclined at 30°. AB of both valves is rounded with medium radius of curvature; maximum convexity is located just below 50% of H. VB is long (80% of L) and straight. PVB is slightly convex. PB is rounded with medium size of curvature and maximum convexity is located above 50% of H. PDB is very short. Carapace is flattened laterally. The carapace size ranges from medium to very large. Surface is smooth. *Suchonellina* sp. 2 can be differentiated from *S.* sp. 1 by the longer carapace, position of maximum convexity of PB, and the less H/L ratio.

***Suchonellina* sp.3**

Fig. 8, G-I

Materials: more than 5 incomplete carapaces.

Measurement: (figured specimens) H = 0.228-0.550 mm; L = 0.521-1.183 mm; H/L = 0.43-0.46.

Remarks: *Suchonellina* sp. 3 can be differentiated from *S.* sp. 2 by the longer carapace, position of maximum convexity of PB which located below 50% of H, and the less H/L ratio. Shape of the carapace resemble genus *Praesuchonellina* which has been found from Upper Paleozoic rocks of Russia (Molostovskaya et al. 2000).

***Suchonellina* sp.4**

Figs. 5, A; 8, J

Materials: more than 6 incomplete carapaces.

Measurement: (figured specimen) H = 0.600 mm; L = 1.183 mm; H/L = 0.52.

Remarks: This species is characterized by having a distinct antero-ventral knob on LV as shown in Figs. 5A and 8J. DB is long and straight, and sloped at 20° to anterior. ADB is short, AB is rounded with small radius of curvature, maximum convexity is located at 25% of H. AVB is short, VB is long and straight,

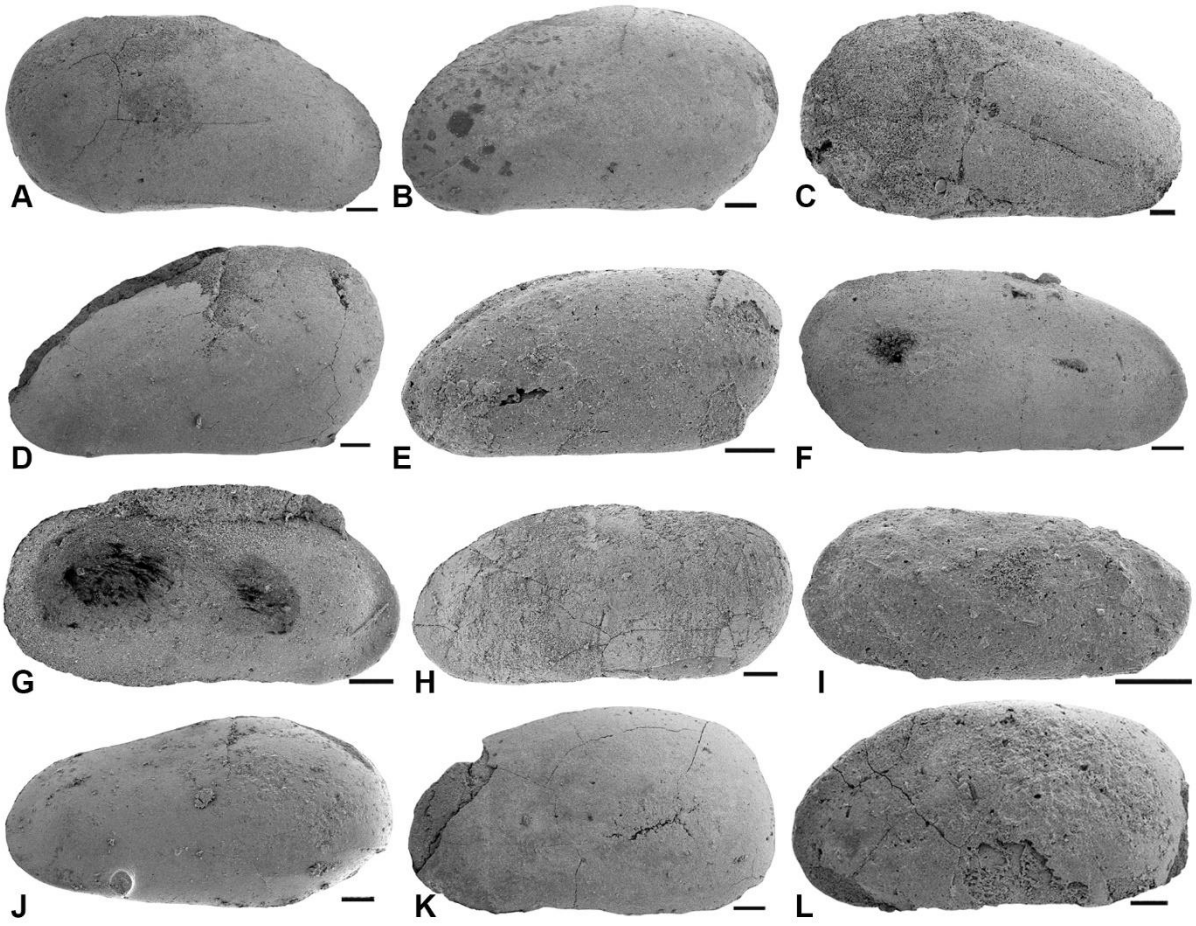

Fig. 8: Late Triassic ostracods from Dat Fa Member, Huai Hin Lat Formation, Phetchabun Province, northeastern Thailand: A-D, *Suchonellina* sp.1, A, right lateral view of complete carapace, sample No. 16NN02, SUT-16-001; B, left lateral view of complete carapace, sample No. 16NN03, SUT-16-002; C, right lateral view of complete carapace, sample No. 16NN03, SUT-16-003; D, left lateral view of complete carapace (partly embedded), sample No. 16NN05, SUT-16-004; E-F, *Suchonellina* sp.2, E, left lateral view of complete carapace, sample No. 16NN03, SUT-16-019; F, right lateral view of complete carapace, sample No. 16NN04, SUT-16-017;G-I, *Suchonellina* sp.3, G, left lateral view of complete carapace, sample No16NN04, SUT-16-023; H, left lateral view of complete carapace, sample No. 16NN04, SUT-16-021; I, right lateral view of complete carapace, sample No. 16NN05, SUT-16-020; J *Suchonellina* sp.4, left lateral view of complete carapace, sample No. 16NN06, SUT-16-016; K-L, *Suchonellina* sp.5, K, left lateral view of complete carapace, sample No. 16NN06, SUT-16-005; L, left lateral view of complete carapace, sample No. 16NN05, SUT-16-006. Scale bars = 0.1 mm.

PVB is long. PB is rounded with medium radius of curvature, maximum convexity is located above 50% of H. Carapace is flattened laterally. The size is very large. Surface is smooth. This species cannot be compared to any known species.

Suchonellina sp. 5

Fig. 8, K-L

Materials: more than 4 incomplete carapaces.

Measurement: (figured specimens) H = 0.58-0.66 mm; L = 1.166-1.183 mm; H/L = 0.50-0.55.

Remarks: This species is characterized by its short and sub-rounded carapace. DB is slightly convex, ADB is sloped at 25°. AB is rounded with medium radius of curvature and located at 30% of H. AVB is short and slightly convex. VB is slightly concave in middle part, PVB is short and convex. PB is rounded with large

radius of curvature, maximum convexity is located at 30% of H. PDB is convex. Carapace is flattened laterally. The size is very large. Surface is smooth. Shape of the carapace resemble genus *Wjatkellina* which has been found from Upper Paleozoic rocks of Russia (Molostovskaya et al. 2018). Unfortunately, more precise identification cannot be made because the ostracods were tightly embedded in rock matrix.

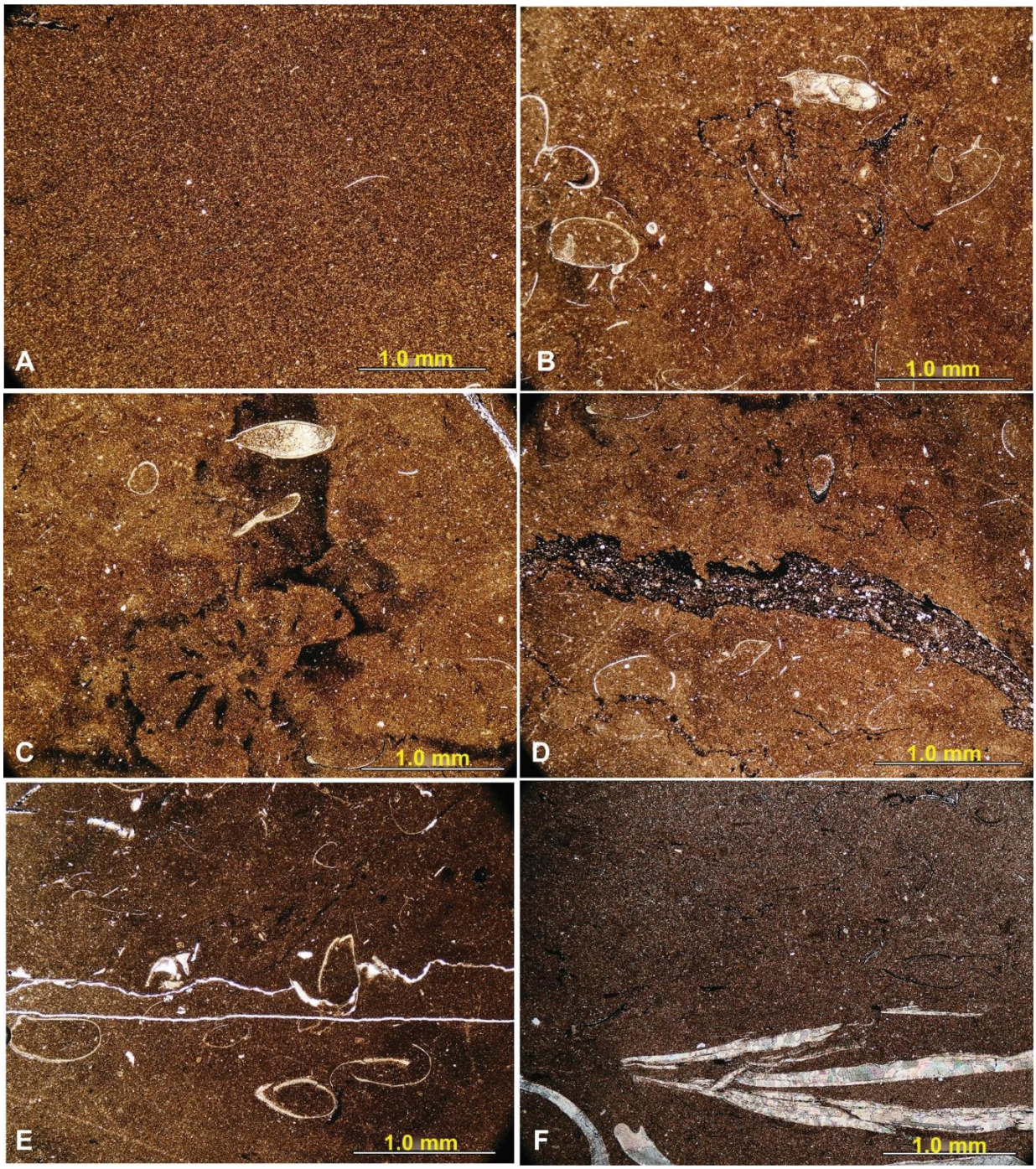

Fig. 9: Photomicrographs of massive carbonates facies from the Dat Fa Member, Huai Hin Lat Formation: A, sample No. 16NN01, massive carbonate mudstone (regular light); B-D, sample No.16NN02, massive carbonate wackestone with bioclasts (regular light); E, sample No.16NN03, massive carbonate wackestone with bioclasts and stylolite (regular light); F, sample No. 16NN04, massive carbonate wackestone with bivalve shell fragments (polarized light).

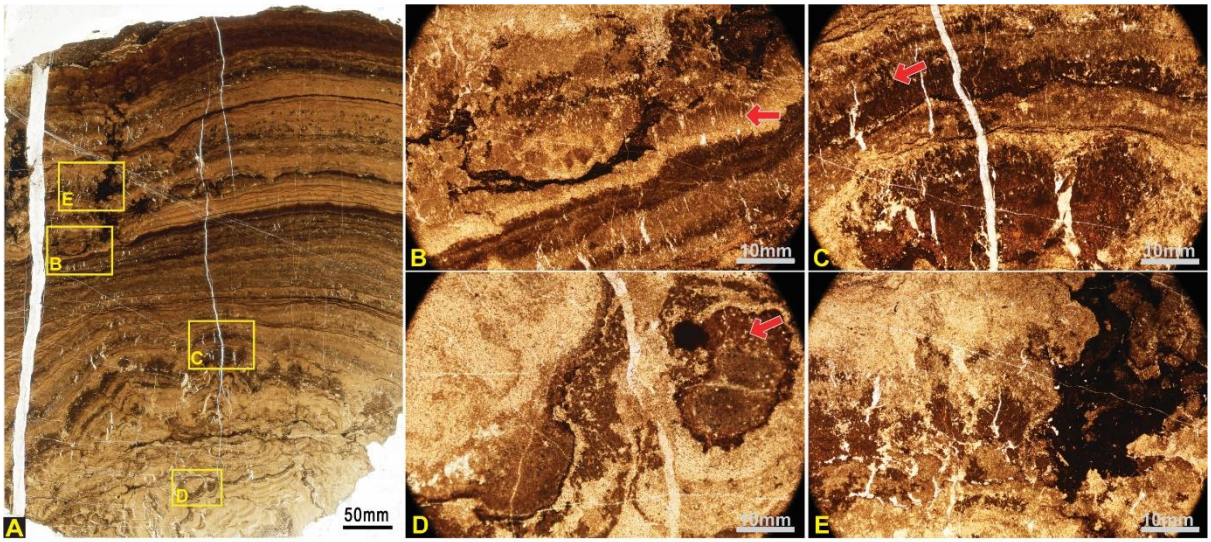

Fig. 10: Photomicrographs of vertical sections of stromatolite from microbial carbonates facies from the Dat Fa Member, Huai Hin Lat Formation: A, laminated structure of stromatolite clearly demonstrated; B-E, enlargements of the yellow boxes in A. In B and C, the filamentous structure is shown (arrows). In D, part of the stromatolite is shown in transverse section due to curvature of the laminations; the filamentous structure is arrowed. E, the stromatolite is broken and partially infilled with carbonate matrix.

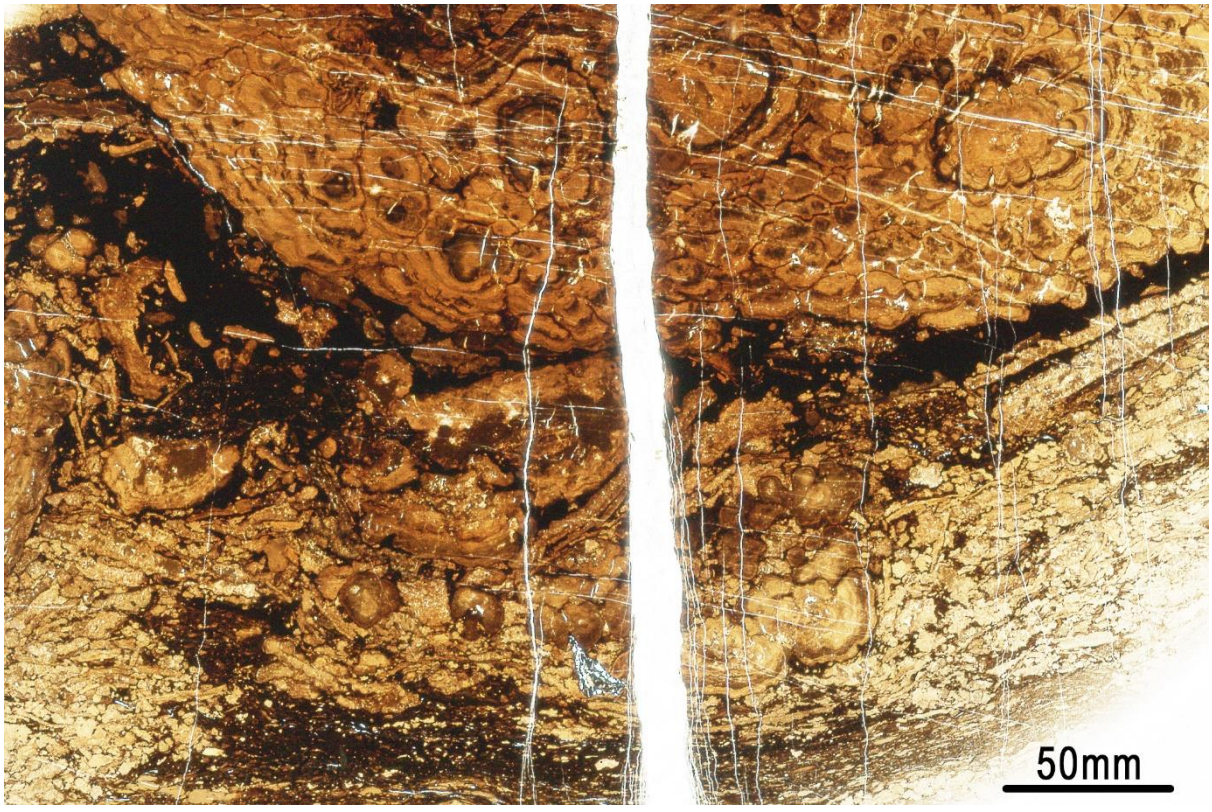

Fig. 11: Photomicrograph of stromatolite from microbial carbonates facies from the Dat Fa Member, Huai Hin Lat Formation. This photograph shows the complex laminated structure in transverse section in the upper two thirds of the picture; in the lower part are abundant fragments, probably formed due to high energy events affecting the surface environments.

4.3 Sedimentary facies from log and thin sections

The studied section is composed of well bedded calcareous mudstone (with stromatolite mounds) in the lower part, intercalations of calcareous mudstone and shale in the middle part, and coal-bearing strata in the upper part (Fig.3). The succession is dominated by fine--grained, grading to coarser grained, clastic rocks and terminated by the coal seams and silty sandstone; altogether this assemblage indicates a fluvial-lacustrine facies association (Renaut & Gierlowski-Kordesch, 2010). The stromatolite can be classified to microbial carbonates facies and described in section 4.4. All thin sections of the calcareous mudstone from the middle part (16NN01-16NN06) are identical and can be classified as massive carbonates facies by lacking sedimentary structure except some bioturbation (Fig. 9). Fossils such as ostracods and bivalve fragments are found.

4.4 Stromatolite and associated sediments

Rock slabs and thin sections were prepared from the stromatolite mound (Figs.10-11). The stromatolite (Figs. 6, 10, 11) at the base of the section indicates higher levels of carbonate input than other parts of the study site. Fig. 6 shows vertical sections of the two stromatolite samples available, and Figs. 10 and 11 show representative thin section views of the stromatolite fabric. Fig. 10 demonstrates the stromatolite has variable structure but a key component is layers containing a vertical fabric of filaments likely to be of cyanobacterial composition. Between filament layers are fine-grained calcium carbonate layers of possible bacterially-mediated, or perhaps inorganic, origin. Some of the stromatolite was fragmented (Fig. 11) indicating episodic events of higher energy, possibly storms, that affected the region and damaged the stromatolite.

5. Discussion

5.1 Taxonomy of conchostracan and ostracod from the Dat Fa Member, Huai Hin Lat Formation

Conchostracans and ostracods are groups of arthropods which belonged to Subphylum Crustacea, and Class Branchiopoda and Class Ostracoda, respectively (Ahyong et al. 2011). They are different from each other by biology and evolution (Negera et al. 1999; Yamaguchi & Endo, 2003; Newman, 2005). Both are known as fossils and living animals, but detailed studies are rare in Thailand.

Conchostracan is a common name of animals in Superorder Conchostraca Sars, 1867, they are also called spinicaudatan which means the animals in Order Spinicaudata Linder, 1945 (Negrea et al. 1999). The name conchostracan however is more familiar to paleontologists (Scholze & Schneider, 2015). A phylogenetic study between living and fossil spinicaudatan was carried out by Astrop & Hegna (2015) and their classification is adopted in this study. The Late Triassic conchostracan genus *Euestheria* identified by Kobayashi (1973 and 1975) is therefore moved from Family Lioestheriidae Kobayashi, 1954 to Family Euestheriidae under Superfamily Eosestherioidea. It should be noted that a common name estheriid which is assigned for animals in Family Estheriellidae (Superfamily Estherielloidea), is not the same as the taxa identified by Kobayashi (1973, 1975). According to him, genus *Estheria* was not described from the Huai Hin Lat Formation. The Rhaetian *Estheria* sp. found in the Nam Pha Formation by Bunopas 1971 (cited in Sattayarak, 1983, p. 132) should thus be reviewed. So far, Thai conchostracans have been recorded from the Upper Triassic, Huai Hin Lat Formation in Chaiyaphum Province (Kobayashi, 1973; 1975), Phetchabun Province (this study) and the ?Middle Jurassic, ? Phra Wihan Formation in the Nan-Phrae area (Heggeman et al. 1990).

The ostracods recovered from the Huai Hin Lat Formation belong to the Superfamily Darwinulidae, which can be recognized by their smooth carapaces and rosette-pattern muscle scar with circular outline. Though the Darwinulid ancestors were marine in origin since the Paleozoic, the extant animals are entirely non-marine, benthic organisms (Horne and Martens, 1998; Martens and Horne, 2009; Karanovic, 2012). During the Mesozoic, members of the Superfamily Darwinulidae

were known to be wholly non-marine inhabitants and the maximum number of species was recorded in Late Triassic rocks (Horne and Marten, 1998). Their abundance declined in the Jurassic due to evolution of other freshwater ostracod groups (Cypridoidea and Cythe-roidea), so that less than ten species have been recorded from the Middle Jurassic to the Cretaceous (Horne and Martens, 1998).

Late Paleozoic Darwinulid ostracods were recorded and well studied from the Russian Plate, three Superfamilies including Darwinuloidea, Suchonelloidea, Darwinuloidoidea and nine genera were classified (Molostovskaya, 2000). The Darwinulid ostracods were also recovered from the Permian-Triassic boundary beds of several sections of the East European platform (Kukhitnov et al. 2008). According to them, the Triassic sediments at the studied sections were marked by species of the Early Triassic *Gerdalia* (Gerdaliidae) and the Late Permian and Early Triassic assemblages might share some taxa in common. On the contrary, the complete stratigraphic record during Late Permian to Middle Triassic is unknown in Northeastern Thailand. The ostracods scrutinized in this study are from the Huai Hin Lat Formation which was deposited after the Indosinian I Orogeny. There is a big gap between the upper Middle Permian marine sediments and the Upper Triassic terrestrial sediments that conceals the evolution of the ostracods from marine to freshwater realms. Most of the studied materials are embedded in the rock matrix, identification to the genus *Suchonellina* is based on the observable features of the carapaces. More research is needed especially if there were suitable sedimentary facies or well-preserved materials.

5.2. Paleoenvironmental reconstruction

Chonglakmani et al. (2006) preliminarily reported occurrence of freshwater stromatolites associated with the ostracods from the same locality of this study and concluded that the microbial and micro-invertebrate communities thrived in a shallow lake during the time of deposition. Co-occurrence of the Darwinulids and conchostracan supports the interpretation of a freshwater lake or pond environment. For example, an assemblage described from lacustrine Late Carnian claystone at Krasiejów in southwestern Poland (Olemska, 2004) was interpreted to be deposited in shallow, still water pools. The conchostracans are non-marine, aquatic biotopes, but occasionally they occur in more saline environments (i.e., large playa lakes, coastal salt flats) where they usually die when water salinity reaches about 5‰ (Olemska, 2004). A well-known Darwinulid ostracod genus *Darwinula* is known as a non-swimming, infaunal ostracod which inhabits muddy substrates in fresh to slightly brackish water (Carbonel et al. 1988; Van Doninck et al., 2003). Members of the Darwinuloidea preferred lakes with terrigenous sediments with minor bicarbonate (Molostovskaya, 2000) . Freshwater stromatolites can be found in fluvial-lacustrine deposits, and indicate water chemistry, generally carbonate and salinity, of the environments (Renaut and Gierlowski-Kordesch, 2010). The stromatolites are found in lacustrine environments (Gierlowski-Kordesch, 2010) and can be formed in fluvial deposits (Arenas-Abad et al. 2010). Our study reveals that sedimentary facies of the middle part of the study section contains massive carbonate facies (structureless with bioturbation) that corresponds with the lacustrine carbonates (Gierlowski-Kordesch, 2010), but lack oncoidal facies or alignment of bioclastic materials representing directional current, thus do not resemble fluvial carbonates (Arenas-Abad et al. 2010). The lake was shallowing upward as shown by presence of the coarser-grained clastic rocks and coal seams in the upper part. This facies corresponds with shoreline deposits including the proximal deltaic sediments and coals of the overfilled lake type (Renaut and Gierlowski-Kordesch, 2010). The sedimentary facies in the study section is different from the deeper facies of the Dat Fa Member previously studied (Asairai et al. 2016; Phujaranchaiwon et al. 2021).

6. Conclusions

We present an analysis of sedimentary facies of the study section, a part of the Dat Fa Member (Huai Hin Lat Formation) in Nam Nao area, Phetchabun Province, including dark grey to black calcareous mudstone (in the

lower part), calcareous mudstone interbedded with calcareous shale in the middle part, and silty sandstone with coal seams in the upper part. The calcareous mudstone in the lower part contains stromatolite mounds with ostracods. We report the occurrence of *Euestheria buravasi* (conchostracan) which indicates the Late Triassic (Early Norian age) in the middle part of the section. The stromatolite is constructed of layers of carbonate containing filamentous structure, and shows contemporaneous fragmentation, probably caused by episodes of higher energy affecting the surface environments. Abundant ostracods are found in the lower to middle parts, five ostracod species are identified, all belong to the family Suchonellinidae. The microbial carbonate facies and massive carbonate facies are determined for the lower and middle parts of the section, respectively. The facies and associated microfossils suggest a shallow lacustrine environment. The silty sandstone and coal seams in upper part of the section correspond to proximal deltaic sediments in the shoreline area of an overfilled lake.

Acknowledgements

This project was funded by Suranaree University of Technology. We are grateful to Dr. Clive Burrett (Mahasarakham University, Thailand) and Prof. Dr. Che Aziz Ali (Universiti Kebangsaan Malaysia) for their constructive advices that improved an earlier version of this manuscript The first author would like to express her deepest gratitude to Dr.Chongpan Chonglakmani and Mr.Nares Sattayarak who made intensive investigations on the Huai Hin Lat Formation, and provided an opportunity to study the stromatolite mound. She is also extremely grateful to Dr.Assanee Meesook and Mr. Wirote Saengsrichan (former DMR geologists) for their encouragement and support during her Ph.D. fieldwork in Phetchabun area. The authors would like to thank Dr.Marie-Béatrice Forel (Muséum National d'Histoire Naturelle, Paris) and Associate Professor Dr.Sukonthip Savatenalinton (Mahasarakham University) for discussions about the ostracods, to Miss Wansiri Boonla (geologist at Sirindhorn Museum, Kalasin Province) for providing pictures of the museum's stromatolite.

References

Ahyong, S.T., Lowry, J.K., Alonso, M., Bamber, R.N., Boxshall, G.A., Castro, P., Gerken, S., … & Svavarsson, J. (2011). Subphylum Crustacea Brünnich, 1772. In: Zhang, Z.-Q. (Ed.) Animal biodiversity: An outline of higher-level classification and survey of taxonomic richness. *Zootaxa*, 3148, 165–191.

Antonietto, L. & Boush, L.P. (2017). Some comments on the systematics of Paleozoic-Early Mesozoic Darwinulocopina Sohn, 1988. Proceedings of 18th International Symposium on Ostracoda. Abstract. p.73.

Antonietto, L.S., Boush, L.P., Suarez, C.A., Milner, A.R.C. & Kirkland, J.I. (2018). The 'Last Hurrah of the Reigning Darwinulocopines'? Ostracoda (Arthropoda, Crustacea) from the Lower Jurassic Moenave Formation, Arizona and Utah, USA. *Journal of Paleontology*, 92, 648–660.

Arenas-Abad, C., Vázquez-Urbez, M., Pardo-Tirapu, G., Sancho-Marcén, C., 2010. Fluvial and Associated Carbonate Deposits. In, Alonso-Zarza, A.M., Tanner, L.H. (Eds.), Carbonates in continental settings–Facies, environments and processes. *Developments in Sedimentology*, 61, 33-175.

Arsairai, B. (2014). Depositional environment and petroleum source rock potential of the Late Triassic Huai Hin Lat Formation, northeastern Thailand. Ph.D. Thesis. Suranaree University of Technology. 311 p.

Arsairai, B., Wannakomol, A., Feng, Q. & Chonglakmani, C. (2016). Paleoproductivity and Paleoredox Condition of the Huai Hin Lat Formation in Northeastern Thailand. *Journal of Earth Science*, 27(3), 350–364.

Astrop, T. I. & Hegna, T. A. (2015). Phylogenetic relationships between living and fossil spinicaudant taxa (Branchiopoda Spinicaudata): reconsidering the evidence. *Journal of Crustacean Biology*, 35(3), 339-354.

Bennett, C. E. (2008). A review of the Carboniferous colonisation of non-marine environments by ostracods. *Senckenbergiana Lethaea*, 88, 37–46.

Bennett, C. E., Siveter, D. J., Davies, S. J., Williams, M., Wilkinson, I. P., Browne, M. & Miller, C. G. (2012). Ostracods from freshwater and brackish environments of the Carboniferous of the Midland Valley of Scotland: the early colonization of terrestrial water bodies. *Geological Magazine*, 149(3), 366–396.

Booth, J. & Sattayarak, N. (2011). Subsurface Carboniferous-Cretaceous geology of NE Thailand. In: Ridd, M. F., Barber, A. J., and Crow, M. J. (eds.) The

Geology of Thailand. *Geological Society*, London, 185-222.

Brady, G.S. & Norman, A.M. (1889). A monograph of the marine and freshwater Ostracoda of the North Atlantic and of northwestern Europe, Section 1, *Podocopa: Scientific Transactions of the Royal Dublin Society*, 4, 63–270.

Bunopas, S. and Kositanon, S. (2008). Did Shan-Thai twice marry Indochina and then India?: A Review. *Bulletin of Earth Sciences of Thailand*, 1 (1-2), 1-27.

Buffetaut, E., Suteethorn, V., Martin, V., Chaimanee, Y. & Tong, H. (1993). Biostratigraphy of the Mesozoic Khorat Group of Northeastern Thailand: the contribution of vertebrate palaeontology. In: Thanasuthipitak, T. ed., Proceedings of the International Symposium on Biostratigraphy of Mainland Southeast Asia (BIOSEA), 51-62. Department of Geological Sciences, Chiangmai University, Chiangmai.

Carbonel, P., Colin, J.−P., Danielopol, Dan L., Löffler, H., & Neustrueva, I. (1988). Paleoecology of limnic ostracodes: a review of some major topics. *Palaeogeography, Palaeoclimatology, Palaeoecology*, 62, 413–461.

Chinoroje, O. & Cole, M. R. (1995). Permian Carbonates in the Dao Ruang#1 exploration well-implications for petroleum potential, Northeast Thailand, In: Wannakao, L., Youngeme, M., Srisuk, K. and Lertsirivorakul, R (eds.) International Conference on Geology, Geotechnology and Mineral Resources of Indochina (Geo-Indo 95), 563-576. Khon Kaen University, Khon Kaen.

Chitnarin, A., Crasquin, S., Chonglakmani, C., Broutin, J., Grote., J. & Thanee, N. (2008). Middle Permian ostracods from Tak Fa Limestone, Phetchabun Province, Central Thailand. Geobios, 41(3), 341-353.

Chitnarin, A. Crasquin, S., Charoentitirat, T., Tepnarong, C. & Thanee, N. (2012). Ostracods (Crustacea) of the Early - Middle Permian from Central Thailand (Indochina Block). *Part 1: Order Palaeocopida. Geodiversitas*, 34(4). 801–835.

Chitnarin, A., Crasquin, S., Forel, M.-B., Tepnarong, P. (2017). Ostracods (Crustacea) of the Early-Middle Permian (Cisarulian-Guadalupian) from Central Thailand (Indochina Block): part II, Orders Podocopida, Platycopida and Myodocopida. *Geodivesitas*, 39(4): 651-690.

Chonglakmani, C. (2011). Triassic system. In: Ridd, M. F., Barber, A. J., and Crow, M. J. (eds.) The Geology of Thailand. *Geological Society, London*, 137-150.

Chonglakmani, C. & Sattayalak, N. (1978). Stratigraphy of the Huai Hin Lat Formation (Upper Triassic) in Northeastern Thailand. In: Nutalaya, P. (ed.) Proceedings of the 3rd Regional Conference on the Geology and Mineral Resources of SE Asia, 739--762. Department of Mineral Resources. Bangkok.

Chonglakmani, C. & Sattayalak, N. (1979). Geological map of Thailand on 1: 250,000 scale: sheet Changwat Phetchabun (NE47-16). Bangkok: Department of Mineral Resources.

Crasquin, S., & Forel, M.-B. (2015). Ostracods (Crustacea) through Permian-Triassic events. *Earth--Science Reviews*, 137, 52–64.

Endo, S. and Fujiyama, I. (1966). Some late Mesozoic and late Tertiary plants and fossil insects from Thailand. *Geology and Paleontology of Southeast Asia*, 2.

Forel, M.-B. (2012). Ostracods (Crustacea) associated with microbialites across the Permian- Triassic boundary in Dajiang (Guizhou Province, South China). *European Journal of Taxonomy*, 19, 1–34.

Forel, M.-B. (2015). Heterochronic growth of ostracods (Crustacea) from microbial deposits in the aftermath of the end-Permian extinction. *Journal of Systematic Palaeontology*, 13 (4), 315–349.

Forel, M.-B. (2018). Ostracods (Crustacea), microbialites and their long shared history. Symposium of Amazing Geological Research for Sustainable Development: Case Study of Global Geopark Satun, Mineral Resources Research and Development Center, Department of Mineral Resources, Bangkok, Thailand, 33.

Ghobadi Pour, M., Mohibullah, M., Williams, M., Popov, L. E. & Tolmacheva, T. (2011). New, early ostracods from the Ordovician (Tremadocian) of Iran: systematic, biogeographical 414 and palaeoecological significance. Alcheringa 35(4), 517–529.

Haile, N.S. (1973). Note on Triassic fossil pollen from the Nam Pha Formation, Chulabhorn (Nam Phrom) Dam, Thailand, Geological Society of Thailand, *Newsletter*, 6 (1), 15–16.

Hayami, I. (1968). Some non-marine bivalves from the Mesozoic Khorat Group of Thailand. Geol.Pal.SE.Asia. vol.4.311-

Heggemann, H., Kohring, R. & Schlüter, T. (1990). Fossil plants and arthropods from the Phra Wihan Formation, presumably Middle Jurassic of northern Thailand. *Alcheringa*, 311–316.

Horne, D. (2003). Key events in the ecological radiation of the Ostracoda. *Paleontological Society Papers*, 9, 181-201.

Horne, D. & Martens, K. (1998.) An assessment of the important of the resting eggs for the evolutionary success of Mesozoic non-marine cypridoidean Ostracoda (Crustacea). Arch. Hydrobiol. Spec. Issues Advanc. Limnol: *Evolutionary and ecological aspects of crustacean diapause*, 52, 549–561.

Iglikowska, A. (2014). Stranded: The Conquest of Fresh Water by Marine Ostracods. *Paleontological Research* 18(3), 125–133.

Ingavat, R. & Janvier, P. (1981). Cyclotosaurus cf. posthumus Fraas (Capitosauridae, Stereospondyli) from the Huai Hin Lat Formation (Upper Triassic), Northeastern Thailand, with a note on capitosaurid biogeography. *Geobios*, 14, 711–725.

Iwai, J. & Asama, K. (1964). Geology and palaeontology of the Khorat Plateau and the plant–bearing Permian Formations, Report on the Stratigraphical and Palaeontological Reconnaissanic in Thailand and Malaysia, 1963–64, Overseas technical Cooperation Aqency, Tokyo.

Iwai, J., Asama, K., Veeraburus, M. & Hongnusonthi, A. (1966). Stratigraphy of the so–called Khorat Series and a note on the fossil plant–bearing Paleozoic strata in Thailand, Geology and Paleontology of the SE Asia. *Tokyo University Press*, v.2, 179–196.

Kershaw, S., Li, Y., Crasquin-Soleau, S., Feng, Q.L., & Mu, X. (2007). Earliest Triassic microbialites in the South China block and other areas: control on their growth and distribution. *Facies*, 53, 409–425.

Kershaw, S., Crasquin, S., Li, Y., Collin, P.-Y., & Forel, M.-B. (2012). Microbialites and global environmental change across the Permian–Triassic boundary: a synthesis. *Geobiology*, 10, 25–47.

Ketmuangmoon, P., Chitnarin, A., Forel, M.-B. & Tepnarong, P. (2018). Diversity and paleoenvironmental significance of Middle Triassic ostracods (Crustacea) from northern Thailand: Pha Kan Formation (Anisian, Lampang Group). *Revue de micropaléontologie*, 61(1), 3–22.

Kozur, H. Z. & Weems, R. E. 2010. The biostratigraphic importance of conchostracans in the continental Triassic of the northern hemisphere. In: Lucus, S. G. (ed.) The Triassic Timescale. *Society London*, 334, 334–410.

Kukhtinov, D.A. (1985). Sistema ostrakod nadsemeystva Darwinulaceae: *Paleontological Journal*, v1985, 64–69.

Laojumpon, C., Deesri, U., Khamha, S., Wattanapituksakul, A., Lauprasert, K., Suteethorn, S. & Suteethon, V. (2013). New vertebrate-bearing localities in the Triassic of Thailand. *Journal of Science and Technology Mahasarakham University*. 335–343.

Laojumpon, C., Matkhammee, T., Wathanapitaksakul, A., Suteethorn, V., Suteethorn, S., Lauprasert, K., Srisuk, P., & Loeuff, J. (2012). Preliminary report on coprolites from the late Triassic of Thailand, Vertebrate Coprolites, *New Mexico Museum of Natural History and Science, Bulletin*, 57, 207–213.

Latreille, P.A. (1802). Histoire Naturelle, Generale et Particulière, des Crustacés et des Insectes, Principes Élémentaires, Volume 1: Paris, F. Dufart, 382 p.

Liebau, A. (2005). A revised classification of the higher taxa of the Ostracoda (Crustacea). *Hydrobiologia*, 538, 115–137. doi: 10.1007/s10750-004-4943-7.

Meesook, A. (2001). Jurassic-Cretaceous Environments of Northeastern Thailand. Technical Report. Geological survey Division. Department of Mineral Resources. 43 p.

Meesook, A. (2011). Cretaceous. In: M.F., Ridd, A.J., Barber, & M.J., Crow. (eds.), *The geology of Thailand. Geological Society of London*. London. 169–184.

Meesook, A. and Saengsirchan, W. (2011). Jurassic. In: M.F., Ridd, A.J., Barber, M.J., Crow. (eds.), *The geology of Thailand*. Geological Society of London. London. 151–167.

Meisch, C., Smith, & R.B., Martens, H. 2019. A subjective global checklist of the extant non-marine Ostracoda (Crustacea). *European Journal of Taxonomy* 492, 1-135. https://doi.org/10.5852/ejt.-2019.492.

Molostovskaya, I.I. (2000). The evolutionary history of Late Permian Darwinulocopina Sohn, 1988 (Ostracoda) from the Russian Plate*: Hydrobiologia*, 419, 125–130.

Molostovskaya, I.I., Naumcheva, M.A., & Golubev, V.K. (2018). *Severodvinian and Vyatkian ostracodes from the Suchona River Basin, Vologda region, Russia*, In: Nurgaliev, D.K. (ed.) Advances in Devonian, Carboniferous and Permian Research: Stratigraphy, Environments, Climate and Resources: Bologna, Italy, Filodiritto Editore, 179–187.

Newman, W.A. (2005). Origin of the Ostracods and their maxillopodan and hexapodan affinities. *Hydrobiologia* 538, 1-21.

Negrea, S., Botnariuc, N. & Dumont, H. J. (1999). Phylogeny, evolution and classification of the Branchiopoda (Crustacea). *Hydrobiologia*, 412, 191--212.

Olempska, E. (2004). Late Triassic spinicaudatan crustaceans from southwestern Poland. *Acta Palaeontologica Polonica*, 49 (3), 429–442.

Phucareanchaiwon, C., Chenrai, P. & Laitrakull, K. (2021). Depositional environment and petroleum source rock using outcrop gamma-ray log spectrometry from the Huai Hin Lat Formation, Thailand. *Frontiers in Earth Science*, 9: 1-18. Doi: 10.3389/feart.2021.638862.

Racey, A. (2011). Petroleum geology. In: Ridd, M. F., Barber, A. J., and Crow, M. J. (eds.) The Geology of Thailand. *Geological Society, London*, 351–392.

Renaut, R. W. and Gierlowski-Kordesch, E. H. (2010). Lakes. In: Noel, P. J. & Robert, W. D. Facies Models 4, Geotext 6, 541–757. Geological Association of Canada.

Rossetti, G., Pinto, R.L. & Martens, K. (2011) Description of a new genus and two new species of Darwinulidae (Crustacea, Ostracoda), from Christmas Island (Indian Ocean) with some considerations on the morphological evolution of ancient asexuals. *Belgian Journal of Zoology*,141, 55–74

Kon'no, E. & Asama, K. (1973). *Mesozoic plants from Khorat Thailand. Geology and Palaeontology of Southeast Asia*, 12, 149-172. Tokyo University Press, Tokyo.

Kobayashi, T. (1973). The Norian Conchostracan from the Basal Part of the Khorat Group in Central Thailand. Proceedings of the Japan Academy, 49, 825–828.

Kobayashi, T. (1975). Upper Triassic estheriids in Thailand and the conchostracan development in Asia in Mesozoic Era. Geology and Palaeontology of Southeast Asia, 16, 57–90. Tokyo University Press, Tokyo.

Kozur, H. (1972). Einige Bemerkungen zur Systematik der Ostracoden und Beschreibung neuer Platycopida aus der Trias Ungarns und der Slowakei: Geologisch-Paläontologische Mitteilungen Innsbruck, 2(10), 1–27.

Sakagami, S. and Iwai, J. (1974). Permian Fusulinacean from the Pha Duk Chik Limestone and in the Limestone Conglomerate in its environ, north Thailand. *Geology and Palaeontology of Southeast Asia*, Vol 14.

Salas, M. J., Vannier, J., & Williams, M. (2007). Early Ordovician Ostracods from Argentina: 460 their bearing on the origin of Binodicope and Palaeocope clades. *Journal of Paleontology*, 81(6), 1384–1395.

Sars, G.O. (1866). Oversigt af Norges marine ostracoder: Forhandlinger I Videnskabsselskabet, v. 7, 130 p.

Sattayarak, N. (1983). Review of the continental Mesozoic stratigraphy of Thailand. In: Nutalaya, P. (ed.) Proceedings of a workshop on stratigraphic correlation of Thailand and Malaysia, 1, 127-140.

Sattayarak, N., Srisulawong, S. and Pum-im, S. (1989). Petroleum potential of the pre-Khorat intermontane basins of northeastern Thailand. In: Thanasuthipitak, T. and Ounchanum, P. (eds.) Proceedings of Symposium oh Intermontane basins: Geology and Resources, 45-48. Chiang Mai University, Chiang Mai, Thailand.

Scholze, F. and Schneider, J.W. (2015). Improved methodology of conchostracan (Crustacea: Branchiopoda) classification for biostratigraphy. Newsletters on Stratigraphy, 48/3, 287-298.

Sohn, I.G. (1988). Darwinulocopina (Crustacea: Podocopa), a new suborder proposed for nonmarine Paleozoic to Holocene Ostracoda: Proceedings of the Biological Society of Washington, v. 101, p. 817--824.

Spizharsky, T.N. (1937). Ostracoda from the Kolchugino Series of the coal-bearing strata of the Kuznetsk Basin]: Trudy Vserossiiskii Neftianoi Nauchno-Issledovatelskii Geologorazvedochnyi Institut (VNIGRI), 97, 139–171.

Treerotchananon, A. (2012). Lithostratigraphy of Huai Hin Lat Formation. Technical report (3/2555). Division of Geological Survey. Department of Mineral Resources. 63 p. (in Thai)

Van Doninck, K., Schön, I., Maes, F., De Bruyn, L., & Martens, K., 2003. Ecological strategies in the ancient asexual animal group Darwinulidae (Crustacea, Ostracoda). *Freshwater Biology*,48, 1285-1294.

Ward, D. E. & Bunnag, D. (1964). Stratigraphpy of the Mesozoic Khorat Group in Northeastern Thailand. Department of Mineral Resources, Report of Investigation No. 6, 95.

Weems, R. & Lucas, S. (2015). A revision of the Norian conchostracan zonation in North America and its implications for Late Triassic North American tectonic history. In: Sullivan P.R. and Lucas, S. G., Fossil Record 4. *New Mexico Museum Natural History and Science Bulletin*, 67, 303-317.

Williams, M., Leng, M. L., Stephenson, M., Andrews, J. E., Wilkinson, I. P., Siveter, D. J., Horne, D. J., & Vannier, J. M. C. (2006). Evidence that Early Carboniferous ostracods colonised coastal flood plain brackish water environments. *Palaeogeography, Palaeoclimatology, Palaeoecology*, 230, 299–318.

Wongprayoon, T. & Saengsrichan, W. (2004). Geology of Mapsheets Amphoe Kaset Somboon 5341I, Tung Lui Lai 5341IIV, Amphoe Konsarn 5342II and Chulabhorn Dam 5342III. Technical Report 6/2551. Division of Geological survey. Department of Mineral Resource. 141 p.

Xu, M.Y. (1988). Ostracods from the Mesozoic coal-bearing strata of Northern Shaanxi, China. *Developments in Palaeontology and Stratigraphy*, 11, 1283-1291.

Yamaguchi, S. and Endo, K. (2003). Molecular phylogeny of Ostracoda (Crustacea) inferred from 18S ribosomal DNA sequences: implication for its origin and diversification. *Marine Biology*, 143, 23-38.

Thai Geoscience Journal 3(3), 2022, p. 51-58

ISSN-2730-2695; DOI-10.14456/tgj.2022.5

Cycle performance investigation in compressed air energy storage in aquifers

Lichao Yang, Cai Li, Chaobin Guo, Kai Liu, Qingcheng He*

Chinese Academy of Geological Sciences, Beijing 100037, China

***Corresponding author: 479400160@qq.com*

Received 17 March 2021; Accepted 4 July 2021.

Abstract

Compressed air energy storage (CAES) is one of the promising technologies to store the renewable energies such as surplus solar and wind energy in a grid scale. Due to the widespread of aquifers in the world, the compressed air energy storage in aquifers (CAESA) has advantages compared to the conventional CAES technologies, which store the compressed air in caverns. In this study, numerical modeling by TOUGH3/EOS3 was conducted to simulate a field-scale application of a novel CAES by storing the compressed air in an aquifer. Four types of cycles, namely daily cycle, weekly cycle, monthly cycle and seasonal cycle, were designed to study their performances. The simulation results demonstrated that the air temperature in CAESA system increases as the cycle continues. The seasonal cycle can be achieved under appropriate conditions. The air recharge should be taken to continue the seasonal cycle. The simulation results can provide references for engineering application in future.

Keywords: aquifers**,** compressed air energy storage, cycles, numerical model

1. Introduction

Renewable energies hold a lot of promise when it comes to replace the conventional energy sources such as fossil fuels. However, the intermittent feature of the power generated by renewable energies, such as wind and solar energy, will greatly constrain the utilization efficiency. Therefore, grid-scale energy storage technologies are required to improve the stability and utilization rate of the renewable energies. Among other energy storage technologies (e.g., battery and flywheel energy storage), compressed air energy storage (CAES) has been demonstrated as a promising technology for its large storage scale, economic feasibility, high reliability and low environmental influence (Oldenburg & Pan, 2013; Luo et al., 2015).

The feasibility and requirements of CAES have been proved by energy storage in air tanks, underground caverns and aquifers (Eakes et al., 1983). The Huntorf CAES project and the McIntosh CAES project are two commercial grid-scale CAES facilities with caverns operated successfully in Germany and USA, respectively (Succar & Williams, 2008; Raju et al., 2012). The compressed air energy storage in aquifers (CAESA) has advantage against compressed air energy storage in cavern due to the wide availability of aquifers as well as lower economic costs (Allen et al., 1983).

An aquifer field experiment at Pittsfield, Illinois, USA was carried out in 1981(Wiles & Mccann, 1983). The aim of this project was a feasibility demonstration of cyclical air injection and withdrawal at ambient and elevated temperatures in an aquifer reservoir (Kannberg et al., 1980; Istvan et al., 1990). The cycle of the injection and withdrawal of the air at the Pittsfield project was a daily cycle. However, the investigation on different cycle modes and their performance to CAESA system is still limited. It is therefore necessary to conduct research on different cycle modes of CAESA system to achieve the maximum utilization rate of renewable energies and meet various demands of users.

2. Model design

2.1 Conceptual model and numerical model

Compressed air was injected into an aquifer with dome-shaped anticline structure in the Pittsfield CAESA test (Wiles & McCann,

1981; Allen et al., 1983; Istvan et al., 1983). Fig. 1 shows the structure of the Pittsfield dome indicated by the contours of the uppermost Silurian formation and the well-defined closure indicated by the contours of the upper stratum. The reservoir used to store the compressed air is the highly permeable quartz-dominated St. Peter sandstone, which is beneath the impervious Gelena-Platteville-Joachim carbonate cap rock complex. The core tests showed that the cap rock formations are sufficiently impervious to hold the compressed air during the lifetime of the field test (Allen et al., 1983).

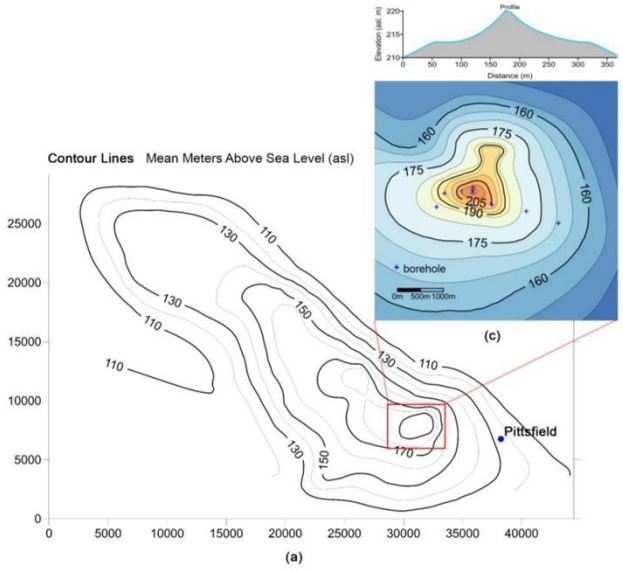

Fig. 1: The structure of the Pittsfield dome; (a) elevation contours of the uppermost Silurian formation and (b) elevation contours of the upper stratum (Allen et al., 1985).

In this study, a conceptual model was set up based on the stratigraphy of the Pittsfield site (Fig. 2). The CAESA system included two stages; the initial bubble stage and the working cycle stage. In the first stage, a large amount of compressed air was injected into an aquifer to form a large initial gas bubble (cushion gas), which was used to provide sufficient pressure and avoid water coning. In the second stage, a certain amount of compressed air was injected into the aquifer for the working cycle.

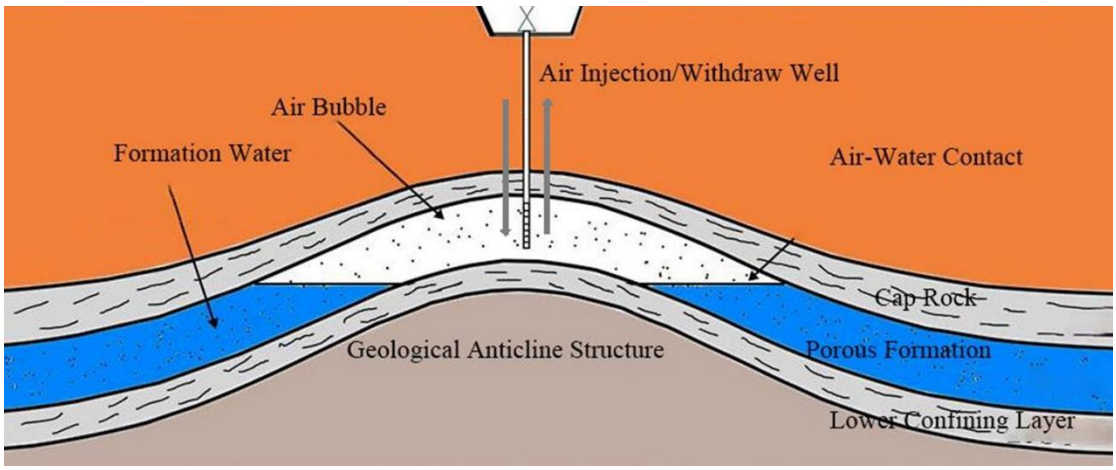

Fig. 2: Conceptual model for Pittsfield CAESA model (Wang et al., 2017).

The TOUGH3/EOS3 simulator, developed by Lawrence Berkeley National Laboratory (LBNL) in USA, was used to conduct the numerical simulations. TOUGH3 is a general-purpose numerical simulation program for multi-dimensional fluid and heat flows of multiphase, multicomponent fluid mixtures in porous and fractured media. The EOS3 module is developed to describe the system consisting of H_2O-Air-Heat components in a porous medium (Jung et al., 2021).

In the numerical modeling, the model scale is set to 3 km×3 km in the horizontal direction and 172 m in the vertical direction. Horizontally, the grids are refined gradually from the boundary to the injection/withdrawal well, which is located in the center of the model with diameter of 0.2 m (Fig. 3a and 3b). Vertically, the model includes four lithologies, which are limestone (upper layer), impervious dolomite rocks (cap rock), St. Peter sandstone (porous formation), and impervious dolomite rocks (lower confined layer), respectively (Fig. 3c). The model is divided into 35 layers vertically and the thickness for each type of lithology is 32 m, 50 m, 70 m and 20 m, respectively. In particular, the St. Peter sandstone is composed of three sub-layers, which are green layer (3 m), white layer (6 m) and grey layer (61 m), respectively (Table 1).

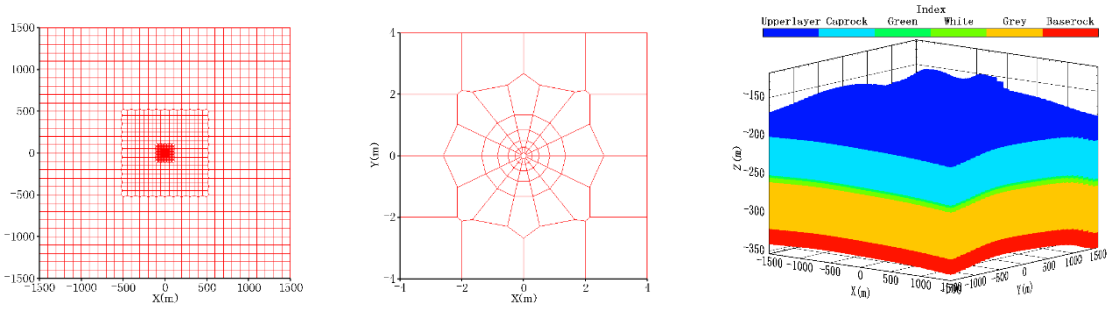

(a) (b) (c)

Fig. 3: (a) Domain discretization from boundary to wellbore in plain view, (b) wellbore refinement with wellbore diameter of 0.2 m in center, and (c) the lithologies distribution vertically in 3D view.

Table 1: Vertical layer refinement of the Pittsfield model.

Lithology	Thickness (m)		Sublayers	Thickness per layer (m)
Limestone (Upper layer)	172	32	1	2
			2	15
Dolomite rocks (Cap rock)		50	2	20
			1	6
			2	2
Sandstone (Green layer)		3	3	1
Sandstone (White layer)		6	6	1
Sandstone (Grey layer)		61	6	1
			5	2
			4	5
			1	25
Dolomite rocks (Base rock)		20	2	10

The upper and bottom boundaries were set up as constant pressure boundary. The lateral boundaries were set up as no flux boundary. In this model, the surface is set to the surface ground, where the temperature is set to 20°C and the geothermal gradient is 0.03°C/m. The initial pressure and initial temperature of this model are shown in Fig. 4. The initial pressure distribution is in hydrostatic equilibrium with atmospheric pressure at the water level, where the pressure is set as 1.01×10^5 Pa, and the hydrostatic gradient is 9.8×10^3 Pa/m.

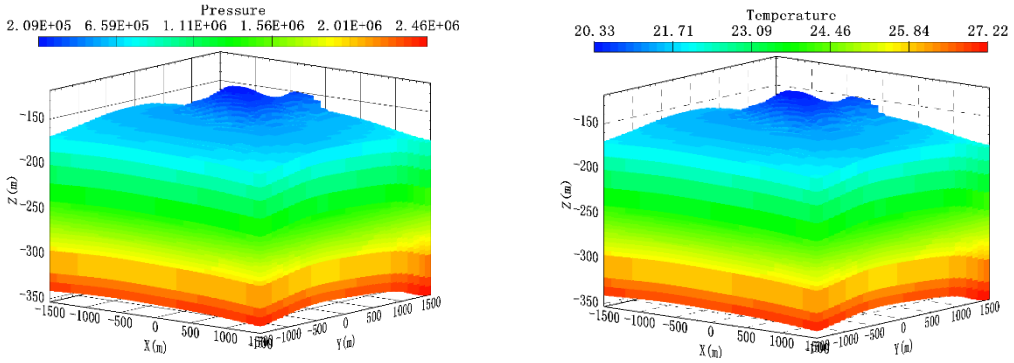

(a) (b)

Fig. 4: Initial pressure (a) and initial temperature (b) of the Pittsfield model.

2.2 Input parameters

The typical parameters for the aquifer and the injection/withdrawal (I/W) well are shown in Table 1, including permeabilities and porosities, which come from the experimental test conducted by Electric Power Research Institute (EPRI), California in the Pittsfield site (Kannberg et al., 1980; Bui et al., 1990).

Table 2: Parameters of the aquifer and wellbore.

Aquifer		**Value**		**Unit**
Grain density		2600		kg/m^3
Heat conductivity		2.16		W/m°C
Grain specific heat		920		J/kg°C
Relative permeability function		Van Genuchten-Mualem model		
Capillary pressure function		Van Genuchten function		
Residual liquid saturation (S_{lr})		0.10		
Minimal capillary pressure (P_0)		675.68		Pa
Maximal capillary pressure (P_{max})		5.0×10^5		Pa
Saturated liquid saturation (S_{ls})		1.00		
Lithology		**Porosity**	**k_h (m^2)**	**k_v (m^2)**
Sandstone	Green layer	0.17	9.05×10^{-13}	7.60×10^{-13}
	White layer	0.16	8.06×10^{-13}	6.62×10^{-13}
	Grey layer	0.16	8.70×10^{-13}	7.27×10^{-13}
Limestone	Upper layer	0.13	6.00×10^{-15}	6.00×10^{-16}
Dolomite	Cap rock & Base rock	0.13	6.00×10^{-15}	6.00×10^{-16}

3. Results and discussion

3.1 Initial bubble development

Before carrying out the working cycle, initial air bubbles need to be developed in the reservoir as cushion gas for insuring sufficient pressure and avoiding water coning (Wiles & McCann, 1981). In this model, the initial bubbles were developed with a mass flow rate of compressed air 2 kg/s and injection time of 165 days. The temperature of injection air was set to 20°C with a fixed specified enthalpy. Fig. 5 shows the gas saturation of the initial bubbles after 165 days injection. The injection point is located at the bottom of the I/W well, where the red dot corresponds to in Fig. 5. It states that the plume of bubbles, where the gas saturation is 0.3, can reach up to 650 m in the horizontal direction, and the biggest thickness of the bubble is about 70 m in the vertical direction.

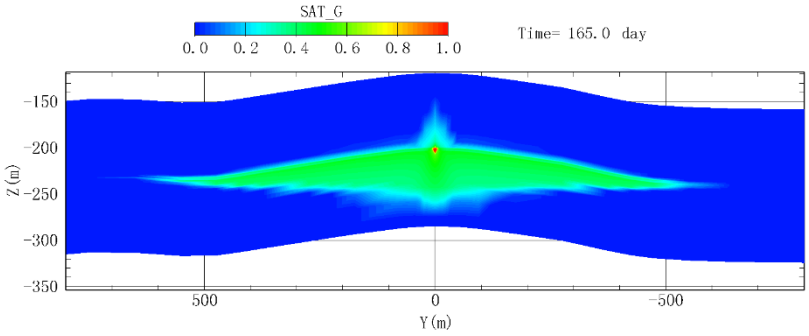

Fig. 5: Gas saturation at the initial bubble development after 165 days air injection.

3.2 Mass flow rates of designed cycles

The daily cycle was designed to 12 hours injection and 12 hours production (Fig. 6a), the weekly cycle was 3.5 days injection and 3.5 days production (Fig. 6b), the monthly cycle was 14 days injection and 14 days production (Fig. 6c), and the seasonal cycle was 90 days injection, 90 days shut-in, 90 days production and 90 days shut-in (Fig. 6d). The mass flow rates of the daily cycle, weekly cycle and monthly cycle were all 2 kg/s, and 1 kg/s for seasonal cycle.

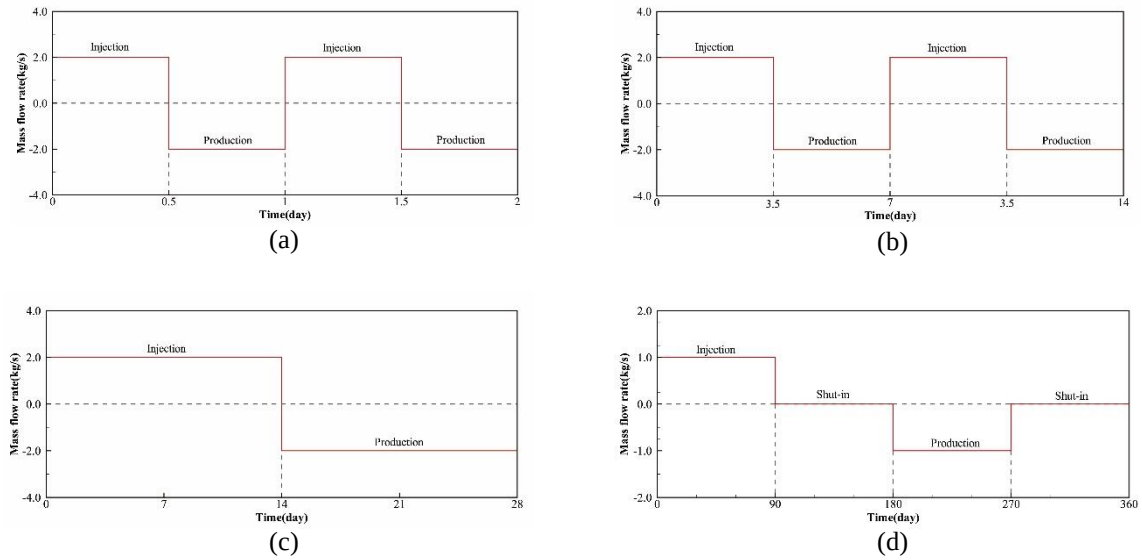

Fig. 6: The mass flow rate of four designed cycles. Minus values stand for production process.

3.3 Pressure and temperature performance of three designed cycles

Before the working cycle, the pressure in the aquifer at point r_1 (0.2 m away from the bottom of the I/W well) was 4.17 MPa, and the temperature is 22.78°C. After one month's simulation, the pressure at r_1 became 1.49 MPa, 1.44 MPa and 1.43 MPa for daily cycle, weekly cycle and monthly cycle, respectively (Fig. 7). It indicates that the energy loss in daily cycle is the smallest because the daily cycle has the shortest period.

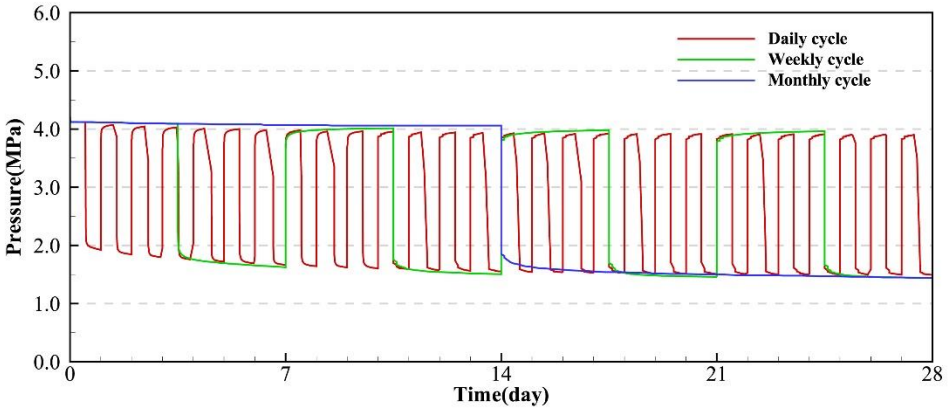

Fig. 7: Pressure variations in daily cycle, weekly cycle and monthly cycle in the aquifer at point r_1 (0.2 m away from the bottom of the I/W well).

The temperature of the air injected into the I/W well was 50°C with a fixed enthalpy. Fig. 8 shows the temperature variation of three types of cycles. When the cycles of 28 days were finished, the air temperature at r_1 was 39°C, 33.6°C and 28.2°C for daily cycle, weekly cycle and monthly cycle, respectively. It indicates that during the same working cycle, the temperature in the aquifer increases as the cycle continues.

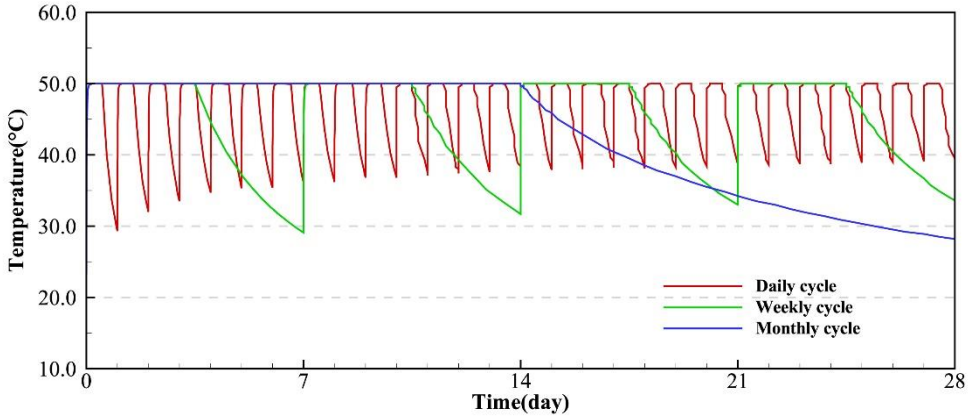

Fig. 8: Temperature variations in daily cycle, weekly cycle and monthly cycle at point r_1 in the aquifer.

3.4 Pressure and temperature performance of seasonal cycle

Fig. 9 shows the pressure variation at points r_1, r_2 and r_3, which were in the aquifer and 0.2 m, 1 m and 100 m, respectively, away from the bottom of the I/W well.

Before the air injection, the pressure at r_1 is 4.17 MPa (overlapped with Y-axis). During the injection stage (A to B), the energy spreads to surroundings gradually, so the pressure decreases in the early stage. As the air injection continued, the rates of energy loss decreased, then the pressures increased to 3.7 MPa, 3.48 Mpa, and 3.19 Mpa at r_1, r_2 and r_3, respectively. During the shut-in stage (B to C), the pressure decreased suddenly because the injection rate decreased to zero, and then the pressure basically became stable in the shut-in stage. During the production stage (C to D), firstly the

pressure decreased because of the sudden air withdrawal, and then kept decreasing as the production continued. When the air production finished, the pressure at r_1, r_2 and r_3 were 1.93 MPa, 2.51 MPa and 2.85 MPa, respectively. During the second shut-in stage (D to E), the pressure recovered firstly, and then basically kept stable. It can be seen that the pressure loss in the I/W well at the end of one cycle was too large to continue the cycle, so in this study, the recharge of compressed air was needed to continue the cycles.

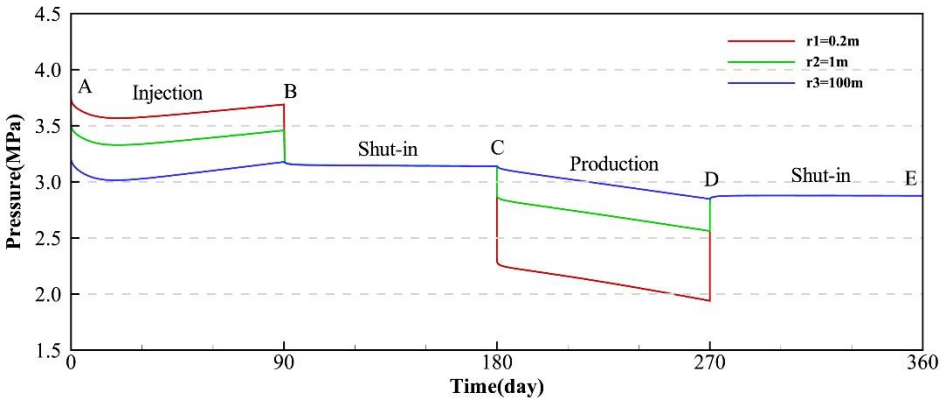

Fig. 9: Pressure variation of seasonal cycle at different sites.

Fig. 10 shows the temperature variation at r_1, r_2 and r_3. The injection air temperature was 50°C. During the injection stage (A to B), the temperature at r_1 was 50°C due to the small distance from the bottom of I/W well. The temperature at r_2 increased from 30°C to 49°C, while the temperature at r_3 kept 22.8°C during the whole cycle because of the long distance from the I/W well. During the shut-in stage (B to C), the temperature at r_1 and r_2 decreased to 38 °C and 35.9°C because of the temperature transfer from high to low. During the production stage (C to D), the temperature decreased gradually, and the temperature at r_1 and r_2 decreased to 25.1°C and 24.9°C when the air production finished. During the second shut-in stage, the high temperature air had been withdrawn, so the temperature in the aquifer had no big difference, with 25.5°C both at r_1 and r_2.

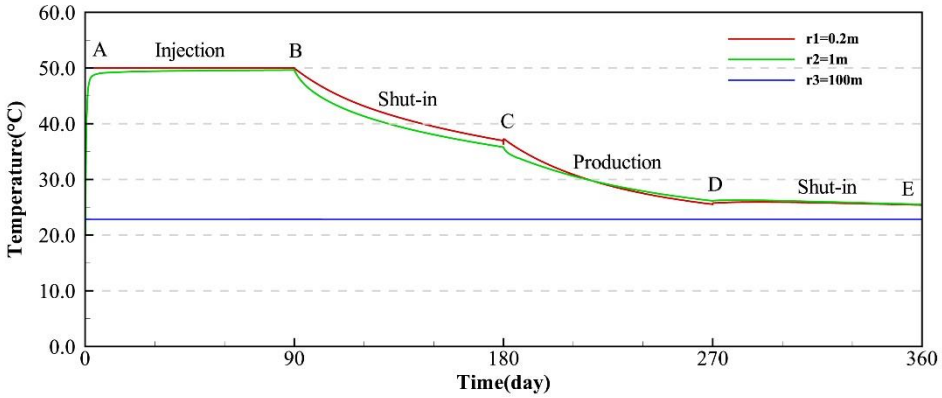

Fig. 10: Temperature variation of seasonal cycle at different sites.

4. Conclusions

In this study, a numerical model was built to investigate the performance of various injection and withdrawal cycles of CAESA: daily, weekly, monthly and seasonal cycles. The modelling results show that during the same working cycle, the temperature of the aquifer increases as the cycle repeats. In addition, the seasonal cycle can be achieved with appropriate conditions, but recharge of the compressed air is needed to continue the cycle due to the large pressure loss. In a practical CAESA project in future, the working cycle

should be designed according to specific characteristics of renewable energy and the actual power demands of users. A comprehensive consideration should be placed to choose the most cost-efficient CAESA system. There are still many fundamental issues for the CAESA system research. With regard to the study and field operation in future, more attention should be paid to the characterization of the reservoir structure. The CAESA system performance largely depends on the aquifers' properties, especially the permeability and porosity.

Acknowledgments

The authors gratefully acknowledge the funding support from the Chinese Academy of Geological Sciences, China (Grant No. DD20201165 and No. JKY202004). The authors also gratefully thank to all the reviewers of their thorough comments.

References

Allen, R. D., Doherty, T. J., Erikson, R. L., & Wiles, L. E. (1983). Factors affecting storage of compressed air in porous-rock reservoirs. technical report.

Allen, R. D., Doherty, T. J., & Kannberg, L. D. (1985). Summary of selected compressed air energy storage studies. technical report.

Eakes, R. G., Kempka, S. N., & Lamoreaux G. H. (1983). Review of environmental studies and issues on compressed air energy storage. technical report.

Wang, B., & Bauer, S. (2017). Pressure response of large-scale compressed air energy storage in porous formations. *Energy Procedia*, 125, 588-595.

Bui, H. V., Herzog, R. A., Jacewicz, D. M., Lange, G. R., Scarpace, E. R., & Thomas, H. H. (1990). Compressed-air energy storage: Pittsfield aquifer field test. technical report.

Istvan, J. A., Crow, C. V., Pereira, J. C., & Bakhtiari, H. (1983). Compressed Air Energy Storage (CAES) in an Aquifer - A Case History. Soc.pet.eng.aime Pap; (United States).

Istvan, J. A., Pereira, J. C., Roark, P., & Bakhtiari, H. (1990). Compressed-air energy storage field test using the aquifer at Pittsfield, Illinois. technical report.

Jung, Y., Pau, G., Finsterle, S., & Doughty, C. (2021). TOUGH3 User's Guide, Version 1.0. Lawrence Berkeley National Laboratory.

Kannberg, L. D., Doherty, T. J., & Allen, R. D. (1980). Aquifer field test for compressed air energy storage. Proc., Intersoc. Energy Convers. Eng. Conf.; (United States).

Luo, X., Wang, J., Dooner, M., & Clarke, J. (2015). Overview of current development in electrical energy storage technologies and the application potential in power system operation. *Applied Energy*, 137, 511-536.

Oldenburg, C. M., & Pan, L. (2013). Porous Media Compressed-Air Energy Storage (PM-CAES): Theory and Simulation of the Coupled Wellbore–Reservoir System. *Transport in Porous Media*, 97(2), 201-221.

Raju, M., & Khaitan, S. K. (2012). Modeling and simulation of compressed air storage in caverns: A case study of the Huntorf plant. *Applied Energy*, 2012,89(1), 474-481.

Succar, S., & Williams, R. H. (2008). Compressed air energy storage: theory, resources, and applications for wind power, Princeton Environmental Institute.

Wiles, L. E., & McCann, R. A. (1981). Water coning in porous media reservoirs for compressed air energy storage. technical report.

Wiles, L. E., & Mccann, R. A. (1983). Reservoir characterization and final pre-test analysis in support of the compressed-air-energy-storage Pittsfield aquifer field test in Pike County, Illinois. technical report.

THAI GEOSCIENCE JOURNAL

If you are interested in earth sciences
Support geoscience with a subscription to

Thai Geoscience Journal

The **Thai Geoscience Journal** publishes original research
And review articles from the international community in all
Fields of geological sciences such as

- Engineering Geology
- Petrology
- Paleontology
- Economic Geology
- Geophysics
- Tectonics
- Structural Geology
- Geochemistry

All articles published by the **Thai Geoscience Journal**
are made freely and permanently accessible online
Immediately upon publication, **without subscription charges or registration barriers.**

Please scan for

VISIT US

ARTICLES SUBMISSION

SUBSCRIPTION TO TGJ

AND MORE INFORMATION

Contact
Mineral Resources Research and Development Center
Department of Mineral Resources 75/10 RAMA VI Road,
Ratchatewee, Bangkok 10400 Phone: +66 2-6219731
Website : https://www.dmr.go.th/tgjdmr/
E-mail : tgj.2020@gmail.com

Published by

CONCEPT DESIGN

This logo composes of Abbreviations of Thai Geoscience Journal

T = THAI G = GEOSCIENCE J = JOURNAL

Coexistence of 3 abbreviations design in a concept of modernity blend with a Thainess
Modification of G alphabet in a shape of ammonoid shows relevance to geology
and infinite development of Thai Geoscience Journal

- **SCOPE AND AIM OF THAI GEOSCIENCE JOURNAL (TGJ):** TGJ is an international (Thai and English) journal publishing original research articles dealing with the geological sciences. It focuses, mainly but not exclusively, on: Sedimentology and Geomorphology, Palaeontology, Quaternary, Geology and Environment Change, Geological Hazards, Environmental Geosciences, Geophysics, Mineral and Petroleum Geology, Tectonics and Structural Geology, Geochemistry and Geochronology, Metamorphic Geology and Volcanic and Igneous Geology. Two types of articles are published in the Journal: Research Articles and Reviews. Research Articles are new original articles, normally not exceeding 25 pages. Review Articles are those papers that summarize the current state of knowledge on specific fields or topics of geosciences. They analyze and discuss previously published research results, rather than report new results. TGJ Aim is to provide valuable geoscience knowledge and information and push more inspiration for readers and researchers to produce treasure research in the future.
- **FEEDBACK AND CONTACT:** We welcome your feedback, comments and suggestions for the development of TGJ

Please contact: Dr. Apsorn Sardsud (Editor-in-Chief, TGJ)
Department of Mineral Resources
75/10 RamaVI Road Ratchathewee Bangkok 10400, Thailand

Phone: +66 (0)2 6219731

Email: tgj.2020@gmail.com

Website: http://www.dmr.go.th/tgjdmr

TGJ Contributors

Assoc. Prof. Dr. Apichet Boonsoong	Chiang Mai University, Thailand
Dr. Apsorn Sardsud	Department of Mineral Resources, Thailand
Prof. Dr. Che Aziz bin Ali	Universiti Kebangsaan Malaysia, Malaysia
Prof. Dr. Clive Burrett	Mahasarakham University, Thailand
Assoc. Prof. Dr. Danupon Tonnayopas	Prince of Songkla University, Thailand
Dr. Dhiti Tulyatid	Coordinating Committee for Geoscience Programmes in East and Southeast Asia, Thailand (CCOP)
Dr. Ian Watkinson	University of London, England
Mr. Jittisak Premmanee	Department of Mineral Resources, Thailand
Prof. Dr. Katsumi Ueno	Fukuoka University, Japan
Prof. Dr. Katsuo Sashida	Mahidol University, Kanchanaburi campus, Thailand
Prof. Dr. Ken-Ichiro Hisada	University of Tsukuba, Japan
Assoc. Prof. Dr. Kieren Howard	Kingsborough Community College, City University of New York, USA
Prof. Dr. Koji Wakita	Yamaguchi University, Japan
Assoc. Prof. Dr. Kriengsak Srisuk	Khon Kaen University, Thailand
Assoc. Prof. Dr. Lindsay Zanno	North Carolina State University, USA
Dr. Mallika Nillorm	Department of Mineral Resources, Thailand
Dr. Martin Smith	Global Geoscience, British Geological Survey, UK
Adj. Prof. Dr. Michael Ryan King	Western Colorado University, Thailand
Prof. Dr. Montri Choowong	Chulalongkorn University, Thailand
Assoc. Prof. Dr. Mongkol Udchachon	Mahasarakham University, Thailand
Prof. Dr. Nigel C. Hughes	University of California, Riverside, USA
Mr. Niwat Boonnop	Department of Mineral Resources, Thailand
Asst. Prof. Nussara Surakotra	Khon Kaen University, Thailand
Asst. Prof. Dr. Passkorn Pananont	Kasetsart University, Thailand
Dr. Phumee Srisuwan	Department of Mineral Fuels, Thailand
Prof. Dr. Pitsanupong Kanjanapayont	Chulalongkorn University, Thailand
Dr. Pol Chaodumrong	Geological Society of Thailand, Thailand
Dr. Pradit Nulay	Department of Mineral Resources, Thailand
Dr. Prinya Putthapiban	Mahidol University Kanchanaburi Campus, Thailand
Prof. Dr. Punya Charusiri	Department of Mineral Resources, Thailand
Asst. Prof. Dr. Rattanaporn Hanta	Suranaree University of Technology, Thailand
Assoc.Prof. Rungruang Lertsirivorakul	Khon Kaen University, Thailand
Assoc. Prof. Dr. Sachiko Agematsu-Watanabe	University of Tsukuba, Japan
Dr. Sasiwimol Nawawitphisit	Department of Mineral Resources, Thailand
Dr. Seung-bae Lee	Korea Institute of Geoscience and Mineral Resources, Republic of Korea
Dr. Siriporn Soonpankhao	Department of Mineral Resources, Thailand
Asst. Prof. Dr. Sombat Yumuang	Geo-Informatics and Space technology Development Agency, Ministry of Science and Technology (GISTDA), Thailand
Mr. Somchai Chaisen	Department of Mineral Resources, Thailand
Dr. Surin Intayos	Burapha University, Chanthaburi Campus, Thailand
Mr. Sutee Chongautchariyakul	Department of Mineral Resources, Thailand
Dr. Tawatchai Chualaowanich	Department of Mineral Resources, Thailand
Mr. Thananchai Mahatthanachai	Department of Mineral Fuels, Thailand
Assoc. Prof. Dr.Thasinee Charoentitirat	Chulalongkorn University, Thailand
Dr. Toshihiro Uchida	Retired geophysicist, Japan
Mr.Tritip Suppasoonthornkul	Department of Mineral Fuels, Thailand
Dr. Weerachat Wiwegwin	Department of Mineral Resources, Thailand
Assoc. Prof. Dr. Yoshihito Kamata	University of Tsukuba, Japan

Thai Geoscience Journal
Vol. 3 No. 3
January 2022
ISSN 2730-2695

CONTENTS

Published by
Department of Mineral Resources
Geological Society of Thailand
Coordinating Committee for Geoscience Programmes in East And Southeast Asia (CCOP)